

Spring 5-31-2015

## **New screening methodology for selection of polymeric materials for transdermal drug delivery devices**

Roberto P. Falcone  
*New Jersey Institute of Technology*

Follow this and additional works at: <https://digitalcommons.njit.edu/dissertations>



Part of the [Materials Science and Engineering Commons](#)

---

### **Recommended Citation**

Falcone, Roberto P., "New screening methodology for selection of polymeric materials for transdermal drug delivery devices" (2015). *Dissertations*. 116.  
<https://digitalcommons.njit.edu/dissertations/116>

This Dissertation is brought to you for free and open access by the Electronic Theses and Dissertations at Digital Commons @ NJIT. It has been accepted for inclusion in Dissertations by an authorized administrator of Digital Commons @ NJIT. For more information, please contact [digitalcommons@njit.edu](mailto:digitalcommons@njit.edu).

## Copyright Warning & Restrictions

The copyright law of the United States (Title 17, United States Code) governs the making of photocopies or other reproductions of copyrighted material.

Under certain conditions specified in the law, libraries and archives are authorized to furnish a photocopy or other reproduction. One of these specified conditions is that the photocopy or reproduction is not to be “used for any purpose other than private study, scholarship, or research.” If a user makes a request for, or later uses, a photocopy or reproduction for purposes in excess of “fair use” that user may be liable for copyright infringement,

This institution reserves the right to refuse to accept a copying order if, in its judgment, fulfillment of the order would involve violation of copyright law.

**Please Note: The author retains the copyright while the New Jersey Institute of Technology reserves the right to distribute this thesis or dissertation**

Printing note: If you do not wish to print this page, then select “Pages from: first page # to: last page #” on the print dialog screen

The Van Houten library has removed some of the personal information and all signatures from the approval page and biographical sketches of theses and dissertations in order to protect the identity of NJIT graduates and faculty.

## **ABSTRACT**

### **NEW SCREENING METHODOLOGY FOR SELECTION OF POLYMERIC MATERIALS FOR TRANSDERMAL DRUG DELIVERY DEVICES**

**by**  
**Roberto P. Falcone**

As medical advances extend the human lifespan, the level of chronic illnesses will increase and thus straining the needs of the health care system that, as a result, governments will need to balance expenses without upsetting national budgets.

Therefore, the selection of a precise and affordable drug delivery technology is seen as the most practical solution for governments, health care professionals, and consumers.

Transdermal drug delivery patches (TDDP) are one of the best economical technologies that are favored by pharmaceutical companies and physicians alike because it offers fewer complications when compared to other delivery technologies. TDDP provides increased efficiency, safety and convenience for the patient. The TDDP segment within the US and Global drug delivery markets were valued at \$5.6 and \$12.7 billion respectively in 2009. TDDP is forecasted to reach \$31.5 billion in 2015.

The present TDDP technology involves the fabrication of a patch that consists of a drug embedded in a polymeric matrix. The diffusion coefficient is determined from the slope of the cumulative drug release versus time. It is a trial and error method that is time and labor consuming. With all the advantages that TDDPs can offer, the methodology used to achieve the so-called optimum design has resulted in several incidents where the safety and design have been put to question in recent times (e.g. Fentanyl).

A more logical screening methodology is needed. This work shows the use of a modified Duda Zielinsky equation (DZE). Experimental release curves from commercial

are evaluated. The experimental and theoretical Diffusion Coefficient values are found to be within the limits specified in the patent literature. One interesting finding is that the accuracy of the DZE is closer to experimental values when the type of Molecular Shape and Radius are used.

This work shows that the modified DZE could be used as an excellent screening tool to determine the optimal polymeric matrices that will yield the desired Diffusion Coefficient and thus effectively decreasing the amount of time and labor when developing TDDPs.

**NEW SCREENING METHODOLOGY FOR SELECTION OF POLYMERIC  
MATERIALS FOR TRANSDERMAL DRUG DELIVERY DEVICES**

**by  
Roberto P. Falcone**

**A Dissertation  
Submitted to the Faculty of  
New Jersey Institute of Technology  
In Partial Fulfillment of the Requirements for the Degree of  
Doctor of Philosophy in Material Science and Engineering  
Interdisciplinary Program in Materials Science and Engineering**

**May 2015**

Copyright © 2015 by Roberto P. Falcone

ALL RIGHTS RESERVED

**APPROVAL PAGE**

**NEW SCREENING METHODOLOGY FOR SELECTION OF POLYMERIC  
MATERIALS FOR TRANSDERMAL DRUG DELIVERY DEVICES**

**Roberto P. Falcone**

---

Dr. N.M. Ravindra, Co-Dissertation Advisor Date  
Professor, Physics, NJIT

---

Dr. Michael Jaffe, Co- Dissertation Advisor Date  
Research Professor, Biomedical Materials Engineering, NJIT

---

Dr. Bozena Michniak Kohn, Committee Member Date  
Professor, Department of Pharmaceutics, EM School of Pharmacy, Rutgers – The State  
University of New Jersey

---

Dr. Treena Arinzeh, Committee Member Date  
Professor, Biomedical Materials Engineering, NJIT

---

Dr. Kamallesh K. Sirkar, Committee Member Date  
Distinguished Professor, Chemical Engineering, NJIT

---

Dr. Laurent Simon, Committee Member Date  
Assistant Professor, Chemical Biological and Pharmaceutical Engineering, NJIT



## BIOGRAPHICAL SKETCH

**Author:** Roberto P. Falcone  
**Degree:** Doctor of Philosophy  
**Date:** May 2015

### **Undergraduate and Graduate Education:**

- Doctor of Philosophy in Materials Science and Engineering, New Jersey Institute of Technology, Newark, NJ, 2015
- Master of Science in Chemical Engineering, Manhattan College, Riverdale, NY, 1981
- Bachelor of Science in Physical Chemistry, Fairleigh Dickinson University, Teaneck, NJ, 1979

**Major:** Material Science and Engineering

### **Presentations and Publications:**

Falcone, R., Jaffe, M. and Ravindra, N.M., New screening methodology for selection of polymeric matrices for transdermal drug delivery devices, [Bioinspired, Biomimetic and Nanobiomaterials, Volume 2, Issue 2](#), February 2013.

This Dissertation is dedicated to the two people who have been quite influential and supportive even if one of them is no longer physically around but always in mind, my Dad, Adelmo and my wife, Pamela

## ACKNOWLEDGMENT

Over the past eight years, I have received support and encouragement from a great number of individuals. My doctoral co-advisors, Drs. N.M. Ravindra and M. Jaffe have been superb mentors, great colleagues, and unwavering friends. Their guidance has made this a thoughtful and highly rewarding journey. My thanks to Dr. Bozena Michniak Kohn not only for giving timely and insightful feedback but also providing several opportunities for presenting parts of this work.

I would like to thank the remaining dissertation committee members, Drs. Treena Arinzeh, Kamelesh Sirkar and Laurent Simon for their support and patience over the past four years as I moved from an idea to a complete study. In addition, I want to express my gratitude to Dr. David T. Stanton for providing the molecular shape simulation values without which this work would not have been completed.

Finally, thanks to my wife Pamela for spending time in proofreading and helping editing this dissertation throughout the writing and along with mother in believing (and the occasional proverbial kick in the pants) and keeping the faith in me.

## TABLE OF CONTENTS

Chapter	Page
1 INTRODUCTION .....	1
1.1 Objective .....	1
1.2 Transdermal Drug Delivery.....	1
1.3 Scope of the Study .....	11
1.4 Specific Objectives of the Study .....	12
1.5 Thesis Organization .....	13
2 BACKGROUND .....	14
2.1 ADME Mechanism .....	14
2.2 First Pass Effect .....	15
2.3 Routes of Administration.....	18
2.4 Therapeutic Index .....	19
2.5 Structure of the Skin .....	31
2.5.1 Hypodermis .....	37
2.5.2 Adipose Tissue .....	38
2.5.3 Areolar Tissue .....	39
2.5.4 Dermis .....	40
2.6 Epidermis .....	45
2.6.1 Stratum Corneum. ....	47
2.6.2 Stratum Lucidum.....	47
2.6.3 Stratum Granosolum.....	47
2.6.4 Stratum Spinosum.....	48

**TABLE OF CONTENTS**  
(Continued)

<b>Chapter</b>	<b>Page</b>
2.6.6 Merkel Cells.....	49
2.6.7 Langerhans Cells.....	50
2.6.8 Keratinocytes.....	50
2.6.9 Melanocytes.....	51
2.6.10 Macrophages.....	52
2.7 Routes of Drug Entry into the Skin.....	53
2.8 TDD Techniques .....	55
2.9 Transdermal Patch Design .....	57
<b>3 DIFFUSION CONCEPT .....</b>	<b>61</b>
3.1 Definition.....	61
3.2 Definition of Molecular Models .....	62
3.3 Free Volume.....	68
3.4 Free Volume Models.....	72
3.5 Effect of Various Conditions. ....	77
3.5.1 Effect of Molecular Radius.....	77
3.5.2 Effect of Molecular Shape.....	81
3.6 Theoretical Background.....	82
<b>4 EXPERIMENTAL RESULTS .....</b>	<b>84</b>
4.1 Experimental Method .....	84
4.2 Theoretical Approach / Calculation of Diffusion Coefficient D.....	89

**TABLE OF CONTENTS**  
**(Continued)**

<b>Chapter</b>	<b>Page</b>
4.3 Nicotine Values Estimation .....	90
4.4 Estimation of the Values of Polymeric Matrix Components. ....	94
4.5 Energy Calculations. ....	95
4.6 Effect of Molecular Radius of Gyration .....	98
4.7 Effect of Molecular Shape. ....	100
4.8 Effect of Combining Molecular Radius of Gyration and Shape factors. ....	102
5 DISCUSSION.....	107
6 CONCLUSIONS.....	112
7 FUTURE WORK .....	115
APPENDIX A .....	116
APPENDIX B .....	120
APPENDIX C .....	122
APPENDIX D .....	125
APPENDIX E .....	137
REFERENCES .....	142

## LIST OF FIGURES

<b>Figure</b>	<b>Page</b>
1.1 TDD Global Sales (2007 – 2014).....	4
1.2 Manufacturer’s Revenue from TDD Technologies (2010 – 2017)) .....	5
1.3 Timeline showing transdermal patches date of approval by the FDA .....	6
1.4 Global Percent sales for Different TDD .....	8
1.5 Cumulative number of transdermal drugs approved by the FDA.....	9
1.6 In vitro release of Nitrendipine from transdermal patches.....	10
2.1 First pass effect .....	15
2.2 Different routes for therapeutic actives to enter the body .....	17
2.3 Typical plot of Cp versus time after oral administration fast and slow .....	17
2.4 Typical plot of Cp versus time after sublingual administration .....	18
2.5 Typical plot of Cp versus time after buccal administration.....	18
2.6 Typical plot of Cp versus time after rectal administration.....	19
2.7 Typical plot of Cp versus time during an IV infusion administration.....	25
2.8 Typical plot of Cp versus time after intramuscular administration.....	26
2.9 Typical plot of Cp versus time after subcutaneous administration .....	27
2.10 Various routes of drug administration through injections.....	28
2.11 Plot of drug blood concentration versus time of different parenteral systems.....	29
2.12 Typical plot of Cp versus time after inhalation administration.....	30
2.13 Plot of drug plasma concentration versus time topical administration.....	31
2.14 Plot of drug plasma concentration versus time between IV and oral systems.....	32

**LIST OF FIGURES**  
**(Continued)**

<b>Figure</b>	<b>Page</b>
2.15 Skin structure .....	36
2.16 Hypodermis structure .....	37
2.17 Adipose tissue/cells .....	38
2.18 Areolar tissue .....	39
2.19 Dermis .....	40
2.20 Papillary and Reticular layers .....	42
2.21 Fibroblasts .....	43
2.22 Tropocollagen structure .....	44
2.24 Layers of the epidermis.....	45
2.25 Schematic image showing a section of epidermis with epidermal layers labeled...	46
2.26 Types of cells present in the epidermis layers .....	48
2.27 Merkel cells .....	50
2.28 Langerhans cells .....	51
2.29 Keratinocytes as seen under a microscope .....	52
2.30 Melanocytes .....	52
2.31 Macrophages .....	53
2.32 Delivery Skin Routes .....	54
2.33 Brick and Mortar .....	55
2.34 Hypothetical blood level pattern .....	57
2.35 Types of transdermal patches .....	58



**LIST OF FIGURES**  
(Continued)

<b>Figure</b>	<b>Page</b>
2.36 TDDP release mechanism .....	59
3.1 Fick's self-diffusion .....	61
3.2 Molecular mobility through voids / oscillating cavities .....	63
3.3 Diffusion motion .....	63
3.4 Mechanism steps and activation energies .....	65
3.5 Free Volume Model .....	68
3.6 Eyring Molecular Model .....	69
3.7 Free volume 3D representation .....	70
3.8 Representation of volume disposition in a rubbery matrix as function of T .....	71
3.9 Cohen and Turnbull graphical representation .....	74
3.10 Comparison between radiuses of rotation, hydrodynamic, gyration and mass .....	79
3.11 3D nicotine model .....	81
4.1 Nicotine ultraviolet absorption chart .....	85
4.2 Diagram of a typical commercial nicotine patch.....	87
4.3 Franz static cell components .....	88
4.4 Fully assembled typical Franz static cell .....	89
4.5 Cumulative nicotine release .....	90
4.6 Nicotine molecular structure .....	92
4.7 Cumulative release comparison between $D_{\text{dep}}$ and $D_{\text{ecal}}$ .....	99
4.8 Diffusion coefficient comparisons between $R_g$ and $R_h$ .....	100

**LIST OF FIGURES  
(Continued)**

<b>Figure</b>	<b>Page</b>
4.9 Diffusion coefficient comparison between $\xi$ , $\xi_L$ and experimental values .....	102
4.10 Fully Comparison between $D_{CL}$ and $D_{Rh}$ .....	103
4.11 Diffusion coefficient comparison between experimental and $D_{Rg(0.77)+\xi+\xi_l(IIa)}$ .....	104
4.12 Comparison of Diffusion coefficient of experimental and $D_{Rg(1.732)+\xi+\xi_l(IIb)}$ .....	105
4.13 Comparison of Diffusion coefficient of experimental and $D_{Rg(0.77)+\xi_L+\xi(IIIa)}$ .....	106
4.14 Comparison of Diffusion coefficient of experimental and $D_{Rg(1.732)+\xi_L+\xi(IIIb)}$ .....	107
5.1 Comparison of Diffusion Coefficient using shape factors.....	108
5.2 Comparison of Diffusion Coefficients .....	109
5.3 Comparison of Diffusion Coefficient using different molecular shape and radius	110
5.4 Overall Comparison of Diffusion Coefficients .....	111
6.1 De Gennes Molecular Representation.....	114
6.2 De Gennes Molecular Reptation Pattern .....	115

## LIST OF SYMBOLS

$M_t$	Amount of drug available at time t
$M_{in}$	Initial amount of drug introduced into the body
$C_t$	Initial drug concentration
$C_{\infty}$	Drug concentration at time t
$V_p$	Plasma volume
TI	Therapeutic Index
D	Diffusion Coefficient
$V_f$	Free Volume
Tg	Glass Transition Temperature
$V_I^*$	Critical molar free volume needed for any displaced singularity of species 1 to move
$V_{FH}$	Free volume per mole of all individual moving solute units in the matrix
$D_{01}$	Temperature – independent constant
$M_{ij}$	Molecular weight diffusing units

# CHAPTER 1

## INTRODUCTION

### 1.1 Objective

The objective of this dissertation is to present a screening methodology for trans-dermal patches (TDDP) that will simplify and expedite the design implementation of new passive drug delivery systems. These patches can be used to increase the number of therapeutic devices in the market, thus, helping to improve the quality of life.

The screening methodology uses physical parameters that comprise free volume, thermodynamic estimators and material—solute (active) interactions. This methodology has been compared with commercially available TDDP to determine the validity of such an approach.

### 1.2 Transdermal Drug Delivery

As medical technology continues to improve human lifespan, it will increase the number of chronic illnesses and consequently strain the needs of the health care system. Having 74% of 65- to 69-year-olds in the US, stricken with one or more chronic conditions, creates an increasing burden on health care providers, patients, and their caregivers. This situation will place a greater emphasis on the selection of a more precise drug delivery technology for the patient and the caregiver. <sup>(1)</sup>

Statistics:

1. It is projected that US health care spending will reach \$4.3 trillion in 2018.
2. Of the US population, 43% will be older than 55 years old.

3. It is estimated that 25% of elderly people will take a minimum of three medications.
4. The daily average number of pills ingested per patient in a nursing home is 13.
5. The number of elderly people who have swallowing difficulties (dysphagia) is 65%.
6. Twenty-three percent of caregivers indicate challenges with managing medications.
7. Forty percent of elderly people must be admitted into nursing homes because of their inability for self-medication.

In this context, transdermal drug delivery patches (TDDP) are considered to be the best alternative drug delivery technology that is highly sought by pharmaceutical companies and physicians alike<sup>(2)</sup>. TDDP offer fewer complications when compared to other delivery technologies. Additional benefits include increased efficiency, safety, and convenience for the patient.<sup>(3, 4)</sup>

The TDD market within the US, in 2009, was valued at \$5.6 billion,<sup>(4)</sup> The size of the global market was estimated by Jain Pharma Biotech to be \$12.7 billion in 2005 with expected increases to \$21.5 billion and \$31.5 billion in 2010 and 2015 respectively<sup>(5)</sup>.

However, on a global perspective, drug delivery systems have shown a dramatic sales growth from \$42B in 2007 to \$80B in 2014 as shown in Figure 1.1. Moreover, TDDs contributed 75 % of these sales in 2007 (\$30B). Although their contribution in 2014 is estimated to be 57 % (\$45B) and smaller when compared with 2007 figures. This category still contributes to a lion's share when compared with other global drug deliveries as seen in Figure 1.1<sup>(3)</sup>

**SUMMARY FIGURE  
GLOBAL SALES FOR DRUG DELIVERY PRODUCTS, 2007-2014  
(\$ BILLIONS)**

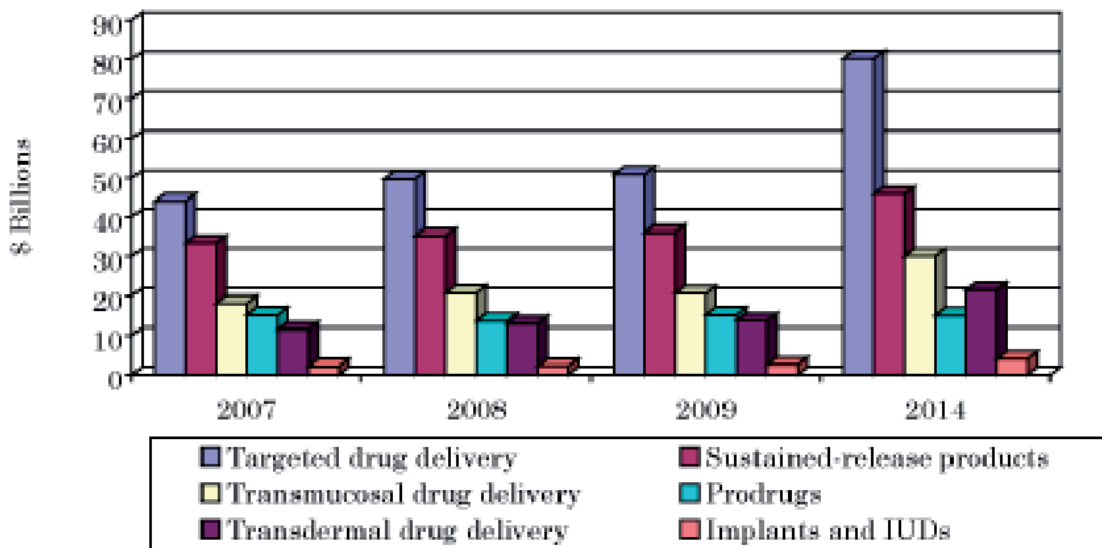


**Figure 1.1** TDD Global Sales (2007-2014)

Source: Advanced Drug Delivery Systems: New Developments, New Technologies, (<http://www.bccresearch.com/market-research/pharmaceuticals/drug-delivery-systems-phm006g.html>), Accessed on October 28, 2014

Another advantage that TDD devices offer is the revenues that drug manufacturers get from leveraging this technology. It is expected that revenues will grow from \$628.6M in 2010 to an estimated \$902.1M in 2017. This represents an approximate 50% growth as seen in Figure 1.2<sup>(4)</sup>.

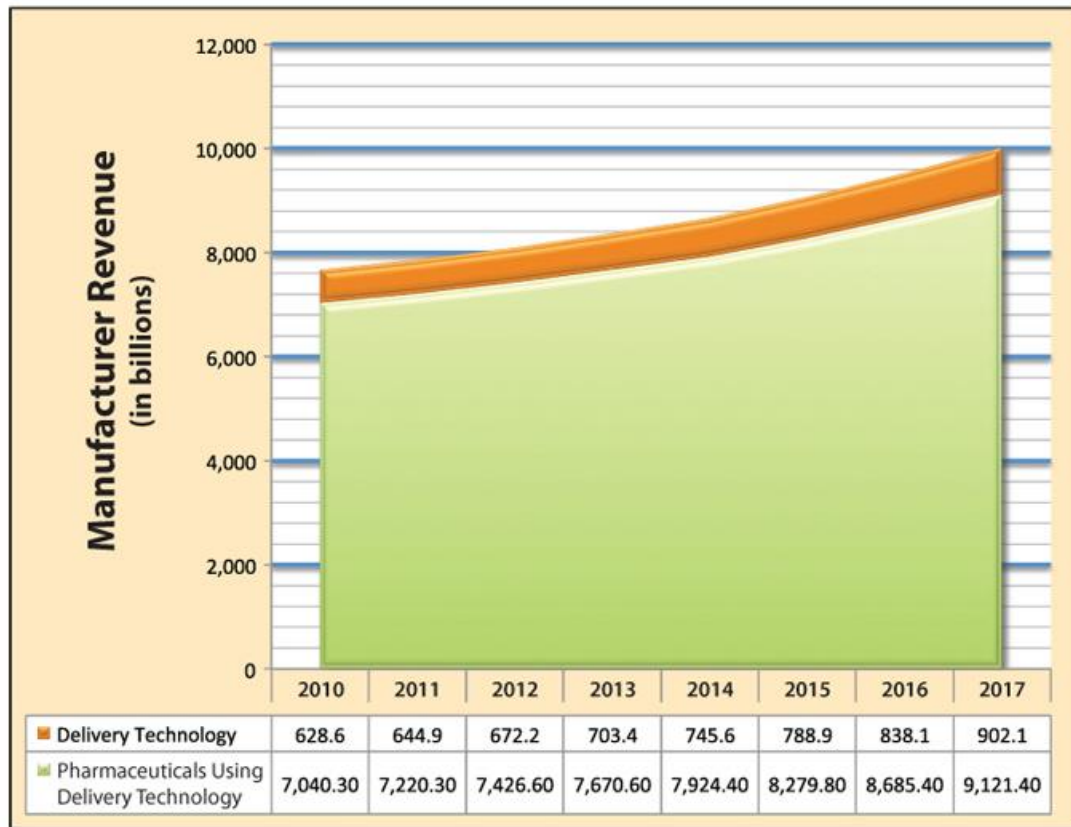


**Figure 1.2** Manufacturer’s Revenue from TDD Technologies (2010-2017)

Source: Wright, P., Transdermal drug delivery looks for new frontiers, ([http://pharmaceuticalcommerce.com/manufacturing\\_and\\_packaging?articleid=2677](http://pharmaceuticalcommerce.com/manufacturing_and_packaging?articleid=2677)). Accessed on October 28, 2014.

Because of the advantages offered by TDDs, research and patents using them have substantially increased since the FDA approved the first TDD patch in 1981. The active drug was scopolamine used for the treatment of motion sickness. Figure 1.3 shows the timeline of transdermal patches since their introduction in 1979<sup>(5)</sup>.

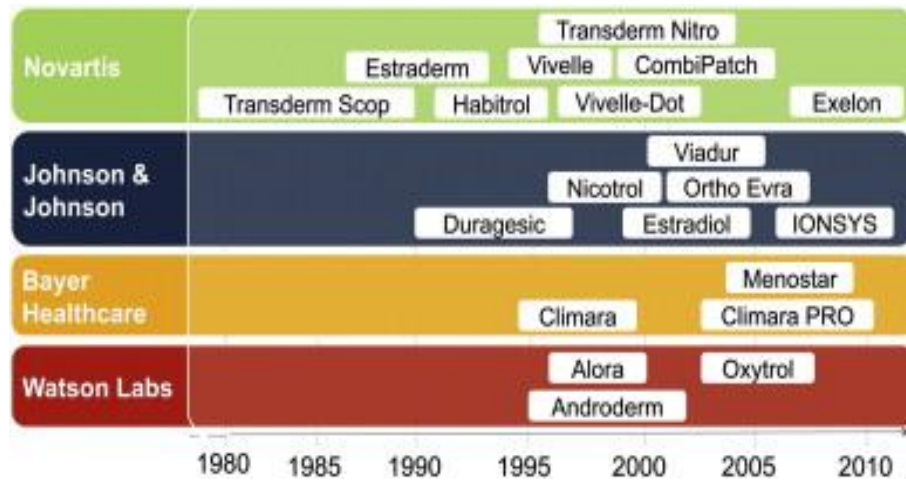


**Figure 1.3** Timeline showing transdermal patches since their date of approval by FDA

Source: Zielinski, B., Controlled Drug Delivery, Transdermal Drug Delivery System (TDDS), Brown University Lecture, <https://canvas.brown.edu/courses/773684/.../download> Accessed on November 29, 2014.

Table 1.1 provides a summary of the most popular TDDs approved by the FDA along with their commercial trade names and intended treatment purpose from 1979 to the present.



**Table 1. 1** Commercially Available Drugs in the Form of Transdermal Patches

Approval Year	Drug/Product Name	Purpose	Marketing Company
1979	Scopolamine/Transderm-Scop	Motion sickness	Novartis Consumer Health (Parsippany, NJ, USA)
1981	Nitroglycerin/Transderm-Nitro	Angina pectoris	Novartis
1984	Clonidine/Catapres-TTS	Hypertension	Boehringer Ingelheim (Ridgefield, CT, USA)
1986	Estradiol/Estraderm	Menopausal symptoms	Novartis
1990	Fentanyl/Duragesic	Chronic pain	Janssen Pharmaceutica (Titusville, NJ, USA)
1991	Nicotine/Nicoderm, Habitrol, ProStep	Smoking cessation	GlaxoSmithKline (Philadelphia), Novartis, Elan (Gainesville, GA, USA)
1993	Testosterone/Testoderm	Testosterone deficiency	Alza (Mountain View, CA, USA)
1995	Lidocaine with epinephrine (iontophoresis)/Iontocaine	Local dermal analgesia	Iomed (Salt Lake City, UT, USA)
1998	Estradiol with norethidrone/Combipatch	Menopausal symptoms	Novartis
1999	Lidocaine/Lidoderm	Post-herpetic neuralgia pain	Endo Pharmaceuticals (Chadds Ford, PA, USA)
2001	Ethinyl estradiol with norelgestromin/Ortho Evra	Contraception	Ortho-McNeil Pharmaceutical (Raritan, NJ, USA)
2003	Estradiol with levonorgestrel/Climara Pro	Menopausal symptoms	Bayer Healthcare Pharmaceuticals (Wayne, NJ, USA)
2003	Oxybutynin/Oxytrol	Overactive bladder	Watson Pharma (Corona, CA, USA)
2004	Lidocaine (ultrasound)/SonoPrep	Local dermal anesthesia	Echo Therapeutics (Franklin, MA, USA)
2005	Lidocaine with tetracaine/Synera	Local dermal analgesia	Endo Pharmaceuticals
2006	Fentanyl HCl (iontophoresis)/Ionsys	Acute postoperative pain	Alza
2006	Methylphenidate/Daytrana	Attention deficit hyperactivity disorder	Shire (Wayne, PA, USA)
2006	Selegiline/Emsam	Major depressive disorder	Bristol-Myers Squibb (Princeton, NJ, USA)

**Table 1.2** Commercially Available Drugs in the Form of Transdermal Patches  
(Continued)

2007	Rotigotine/Neupro	Parkinson's disease	Pharma (Mequon, WI, USA)
2007	Rivastigmine/Exelon	Dementia	Novartis

Source: VIJAY KRISHNA RACHAKONDA, EFFECTIVE SCREENING OF CHEMICAL PENETRATION ENHANCERS FOR TRANSDERMAL DRUG DELIVERY  
[https://shareok.org/bitstream/handle/11244/9658/Rachakonda\\_okstate\\_0664M\\_2865.pdf?sequence=1](https://shareok.org/bitstream/handle/11244/9658/Rachakonda_okstate_0664M_2865.pdf?sequence=1),  
 Accessed on May 10, 2015

Figure 1.4 shows the percent of global sales for different transdermal patch use segments.

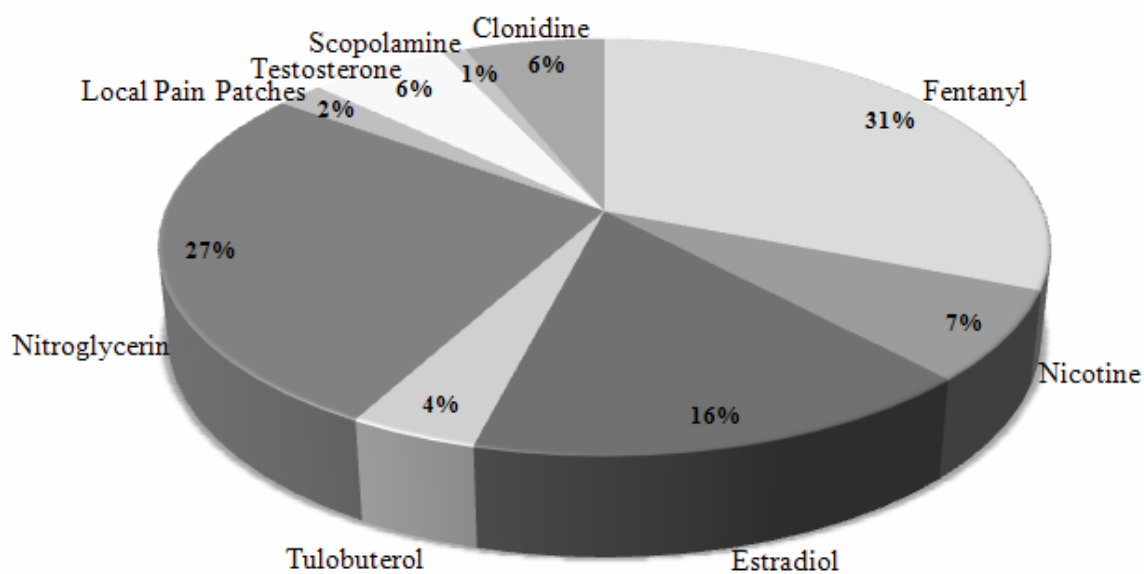


**Figure 1.4** Global Percent sales for Different TDD Segments

Source: Rachakonda, V.K., Effective Screening of Chemical Penetration Enhancers for Drug Delivery, Master Thesis, Oklahoma State University, p. 2, 2006.

The cumulative number of TDDs approved by the FDA is shown in Figure 1.5. This cumulative number of TDDs has steadily been increasing since their introduction in 1979.

There are currently 19 drugs and drug combinations administered by various delivery methods that are approved in the United States as shown in Figure 1.5<sup>(6)</sup>.

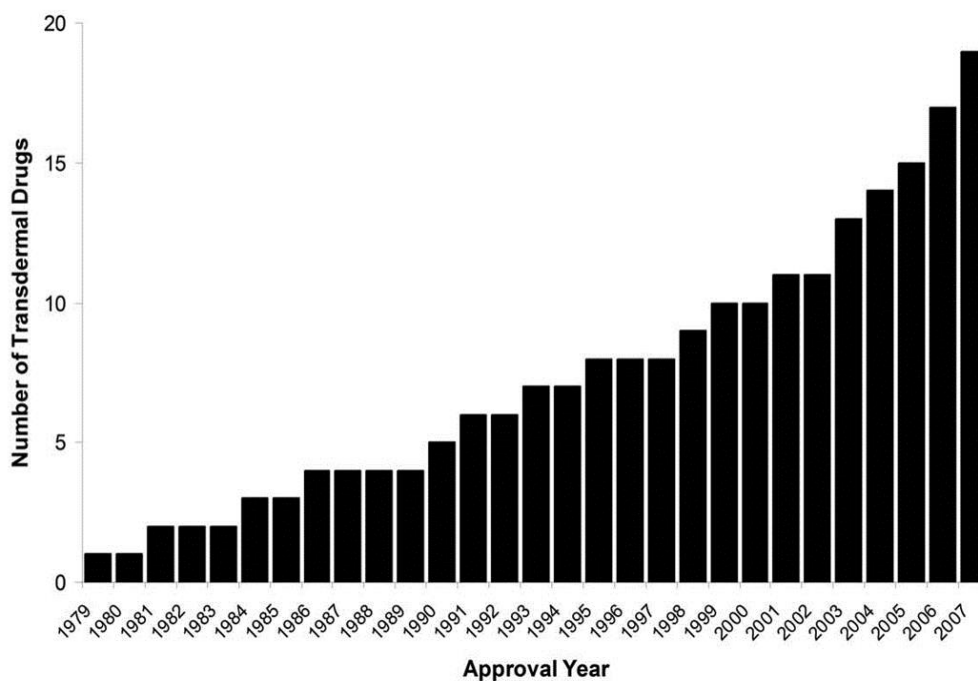


**Figure 1.5** Cumulative number of transdermal drugs approved by the FDA

Source: Prausnitz, M.R., Mitragotri, S. and Langer, R., Current status and future potential of transdermal drug delivery, *Nature Reviews Drug Discovery*, **3**, 115-124, 2004

There are several TDDs in the market today <sup>(4)</sup> and the development trend continues as described in appendices A, B, and C.

The present TDDP methodology involves the fabrication and testing of the in-vitro release of drug embedded within a polymeric matrix in which the cumulative drug release is plotted against time as shown in Figure 1.6<sup>(5)</sup>. This permits an estimation of the Diffusion Coefficient for the system in question which in turn is used to calculate the optimal usage to be expected when used by the patient as well as establishing safety factors for maximum time usage.

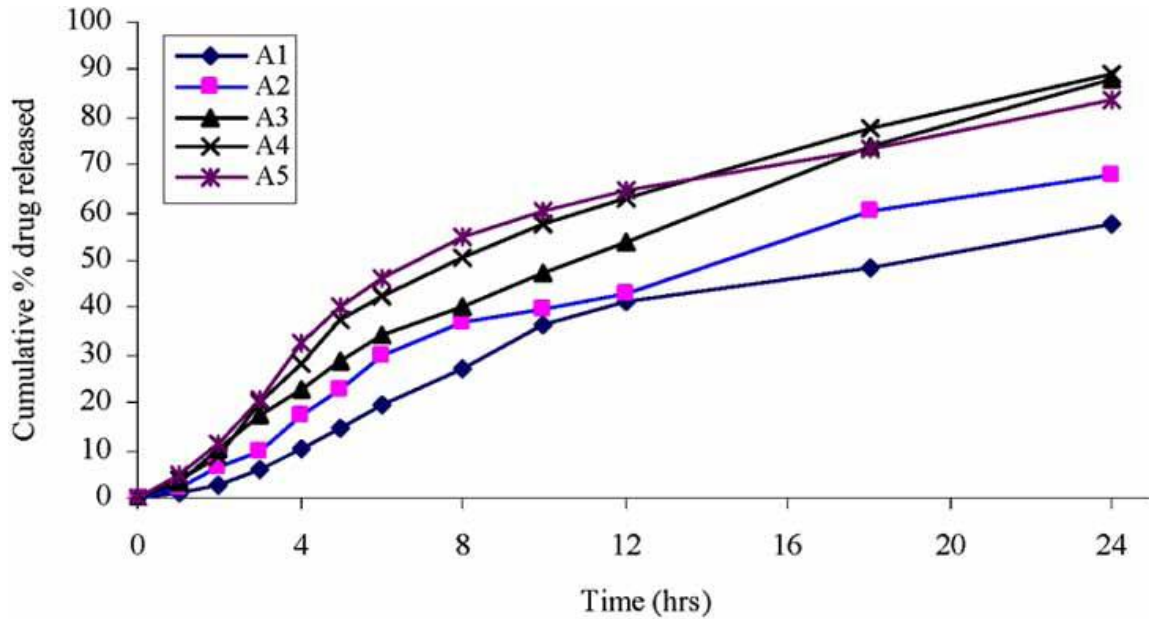


**Figure 1.6** In vitro release of Nitrendipine from transdermal patches

Source: Gannu, R., Vishnu, Y. V. Kishan, V., and Rao, M., Development of nitrendipine transdermal patches: In vitro and ex vivo characterization, *Current Drug Delivery*, 4, 69-76, 2007.

This is obtained via a trial and error method, which is time and labor consuming. Although, with all the advantages that TDDs can offer, the methodology that is used to achieve the so-called optimum design has created several incidents in which the safety and design have been put to question as in the case of Fentanyl in Table 1.2.<sup>(6-8, 10)</sup>

**Table 1.3** Transdermal fentanyl patch medication incidents classified by medication system stage involved

Stage involved	All incidents (n=3271) Number	Percent*	Incidents resulting in harm or death (n=271) Number	Percent **
Physician ordering (prescribing)	419	12.8%	38	14.0%
Order entry and transcription	417	12.8%	16	5.9%
Preparation, dispensing and delivery of drugs	397	12.1%	17	6.3%
Administration and supply of a drug from a clinical area	1692	51.7%	180	66.4%
Monitoring/follow-up of drug use	185	5.7%	22	8.1%
N/A	168	5.1%	1	0.4%
Other	41	1.3%	6	2.2%
Total selections:	3319	101.5%	280	103.3%
Total incidents:	3271	100.00%	271	100.00%

\* Percentage is calculated based on the total number of medication incidents (n = 3271). Since a medication incident may involve more than one stage selection, the total percentage is greater than 100%.

\*\* Percentage is calculated based on the total number of medication incidents with outcome of harm or death (n = 271). Since a medication incident may involve more than one stage selection, the total percentage is greater than 100%.

Source: Cheng, R., Samples, C., Ho, C., Lee, C., Cohen, M., U. D., Cousins, D., and Kirke, C., Medication incidents related to the use of fentanyl transdermal systems: An international aggregate analysis, International Medication Safety Network (IMSN), 2008 <http://www.intmedsafe.net/wp-content/uploads/2013/12/FentanylPatchesReport.pdf> accessed on November 29, 2014

This has prompted the redesign of several TDDPs since the approval of the first patch in 1981<sup>(10)</sup>. There are 675 patents and patent applications, relating to this technology in the US alone<sup>(6,7)</sup>. The majority of these submissions have taken place since the late 1990s.

Therefore, alternate drug delivery technologies are highly sought by pharmaceutical companies and physicians alike, thus, increasing efficiency, safety, and convenience for the patient.

### **1.3 Scope of the Study**

The purpose of this work is to show a new approach for setting a more robust screening method when considering redesigning or designing new TDD patches, especially for the ones where the drug is embedded within the body of the matrix.

The diffusion coefficient is determined by measuring the cumulative release against time. These experiments are usually done using in-vitro techniques where the cumulative amount is quantified by analytical techniques such as high performance liquid chromatography (HPLC), infrared spectroscopy (IR), and ultraviolet spectroscopy (UV) among others. Along with the selection and fabrication techniques described in section 1.2, this can be resource (i.e., labor and equipment) and time consuming, cost prohibitive, and have limited throughput. Moreover, these protocols provide an indirect assessment on how effective the TDD will be when applied unto the skin.

Models to predict the diffusion coefficient have been used to measure the permeation of solutes through polymeric membranes. This suggests that these models can be used to predict the diffusion coefficient of drug actives through the polymeric films that are used in TDDs. Vrentas and Vrentas (2003) proposed the idea of using such models for the

diffusion of drug actives. No research to date has demonstrated how the model compares with the experimental techniques that are presently in use.

#### **1.4 Specific Objectives of the Study**

**Objective 1:** Comparison between experimentally obtained and calculated diffusion coefficients.

In this study, the diffusion coefficient of nicotine was experimentally obtained and compared with the calculated value using the Dudas Zielinski equation (DZE).

This is because most of the physical parameters of nicotine were not readily available in the open literature that is required by the DZE, to calculate the diffusion coefficient, they had to be estimated from group contribution methods. The results show a good agreement between the experimental and calculated values, thus, confirming the usefulness of DZE for predicting meaningful diffusion coefficient values.

**Objective 2:** Comparison between radius of gyration ( $R_g$ ) and hydrodynamic radius ( $R_h$ ).

The solute/diffusant is always assumed to have a spherical shape ( $R_h$ ). However, since most molecules could be rotating around their center axis ( $R_g$ ) while diffusing through the polymeric membrane, calculated  $R_g$  values of nicotine were estimated and incorporated into the DZE and the diffusion coefficient values were compared with the experimental results.

**Objective 3:** The effects of molecular shape on the diffusion coefficient.

Another parameter included in the DZE is the molecular shape. The molecular shape of nicotine was calculated using the Vrentas ( $\xi_L$ ) and Nobrega ( $\xi$ ) approximations that were incorporated into the DZE.

### **1.5 Thesis Organization**

The thesis consists of six chapters. Chapters one and two introduce the topic and provide a literature review and background for this work. Chapter 3 shows the theoretical foundations while chapter 4 describes the experimental and theoretical determination of the diffusion coefficient. The Discussion and Conclusions details the results from this work along with future outlook which are summarized in chapters 5, 6 and 7, respectively.



## CHAPTER 2

### BACKGROUND

#### 2.1 ADME Mechanism

For any treatment to be effective, the active ingredients must undergo the physiological process known as *Absorption Distribution Metabolism Excretion* (ADME)<sup>(11)</sup>.

These are the steps that any ingredient that the body is exposed to must undergo in order to be assimilated. Vergnaud and Rosca defined ADME as follows, “Absorption is the drug assimilation from the gastrointestinal tract (GIT) into the bloodstream or the lymphatic system. These molecules must go through several complex membranes made of lipid barriers, thus, involving different steps.”<sup>(12)</sup>

The steps are as follows:

1. Drug dissolution into the membrane,
2. Transcellular passive diffusion or active transport through the membrane walls, and
3. Luminal and epithelial metabolism.

This can be considered as a first order kinetics. The drug concentration in the GIT will decrease as shown in equation (2.1):

$$M_t = M_{in} \exp (-k_a t) \quad (2.1)$$

where,

$k_a$  is the rate absorption constant,

$M_{in}$  is the initial amount of drug introduced into the body,

$M_t$  is the amount of drug available at time  $t$ ,

and  $t$  is time after drug introduction into the body.

This will lead to a concurrent drug concentration increase in the blood:

$$C_t = C_\infty [1 - \exp(-k_a t)] \quad (2.2)$$

where,

$C_t$  is the initial drug concentration,

$C_\infty$  is the drug concentration at time  $t$ ,

The unbound/free drug concentration in the plasma is:

$$C_\infty = M_{in} / V_p \quad (2.3)$$

and  $V_p$  is the plasma volume.

Then  $k_a$  is estimated from the drug profile in the bloodstream at time  $t$ . The change in maximum drug concentration with time is described in equation (2.4):

$$T_{max} = 1 / (k_a - k_e) \ln (k_a / k_e) \quad (2.4)$$

Distribution is the step where the unbound drug molecule, present in the bloodstream, passes into the tissues and organs. The human organism consists of cells and fluids. The fluid can be divided into three distinctive compartments: intravascular, interstitial or extracellular, and intracellular.

Metabolism can be defined as the sum of all the chemical reactions involved in the biotransformation of endogenous and exogenous substances that can occur in the cells. Although several processes are part of the biotransformation processes, catabolic and anabolic are the most predominant. Catabolic is the breakdown of the drug into simpler entities. Anabolic is the synthesis of new compounds from simpler entities.

## 2.2 First Pass Effect

The first pass effect is defined for the hepatic metabolism of a drug when it is absorbed from the gastrointestinal tract and delivered to the liver via the bloodstream as seen in Figure 2.1. The greater the first pass effect, the lesser will be the amount of drug to reach the systemic circulation. This is the case for orally delivered drugs.

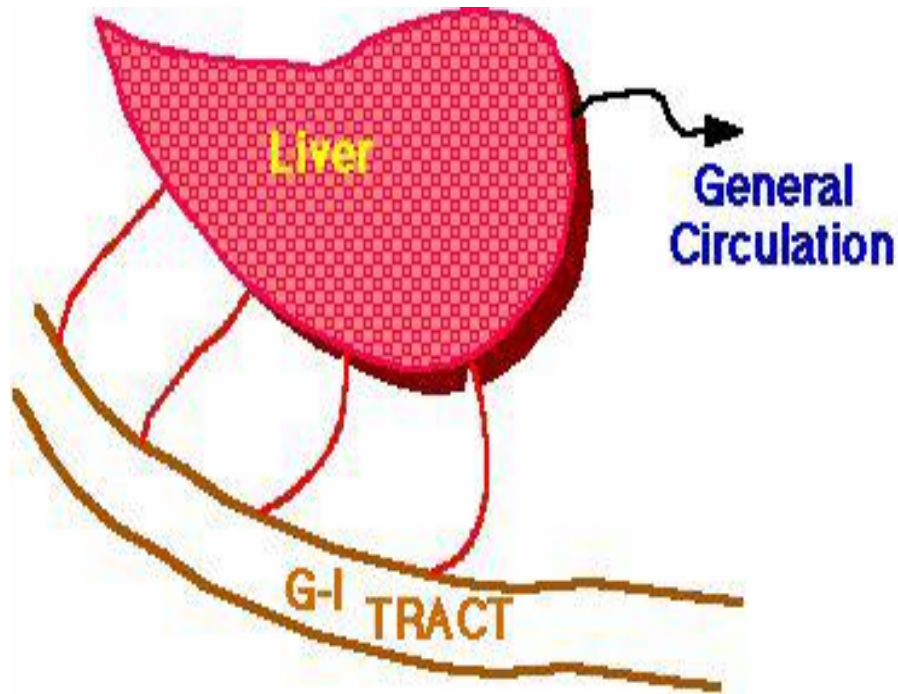


**Figure 2.1** First pass effect

Source: Boomer, D., PHAR 7633 Chapter 7, Routes of Drug Administration  
<http://www.boomer.org/c/p4/c07/c07.pdf>

The effect of the first pass effect or extraction ratio (ER) is given by equation (2.5):

$$ER = CL_{\text{liver}} / Q \quad (2.5)$$

where, Q is the hepatic blood flow (usually, approximately 90 L per hour).

Systemic drug bioavailability (F) may be determined from the extent of absorption (f) and the extraction ratio (ER) as described in equation (2.6):

$$F = f_x (1 - ER) \quad (2.6)$$

The greater the first pass effect, the lower is the rate and extent of the drug reaching cells and target organs. This is also known as drug bioavailability.

Excretion or clearance of the active drug usually takes place in the kidney and intestinal tract with the exception of gaseous deliveries such as anesthetics and inhalers, which are secreted through the lungs. The main excretion route is via the kidneys where the rate and extent is regulated by glomerular filtration, tubular reabsorption, and secretion. Clearance (Cl) happens by blood perfusion through the extraction organs. Extraction (E) is directly related to the drug that is excreted or metabolized. The following relationship is found:

$$Cl = QE \quad (2.7)$$

where, Q is the blood flow through the organ where secretion is taking place. Since the secretion organs are mostly the liver and kidneys, with hepatic clearance  $Cl_h$  and renal clearance  $Cl_r$ , the overall mass systemic balance Cl is:

$$Cl = Cl_h + Cl_r \quad (2.8)$$

Thus, clearance is a function of the necessary blood volume passing through the excretion organ to discharge the drug in a certain period of time:

$$RE = Cl * C \quad (2.9)$$

RE is the rate of excretion of drug discharged per unit time.

## 2.3 Therapeutic Index (TI)

Ehrlich defined the Therapeutic Index (TI) as the relationship between the minimum curative and maximum tolerated dose. In pharmacological terms, TI is the ratio associating the median lethal dose (drug concentration in the bloodstream that promotes the deaths of 50% of the test population,  $LD_{50}$ ) to the median effective dose (drug concentration in the bloodstream that is effective for 50% of the test population,  $ED_{50}$ ):

$$TI = (LD_{50}) / (ED_{50}) \quad (2.10)$$

TI is a derivation of the threshold model that assumes an exposure concentration, or threshold, for the drug to be effective.

## 2.4 Routes of Administration

There are several approaches or routes that drugs can be delivered as shown in Figure 2.2.

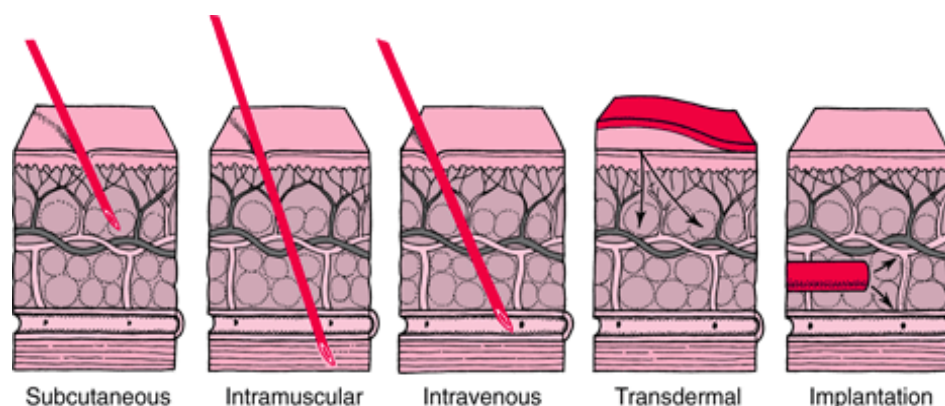


**Figure 2.2** Different routes for therapeutic actives to enter the body

Source: Administration, Merck Manual,  
[http://www.merckmanuals.com/home/drugs/administration\\_and\\_kinetics\\_of\\_drugs/drug\\_administration.html](http://www.merckmanuals.com/home/drugs/administration_and_kinetics_of_drugs/drug_administration.html).  
Accessed on November 28, 2014

For the subcutaneous route, a needle is inserted into the fatty tissue just beneath the skin. After a drug is injected, it then moves into small blood vessels (capillaries) and is

carried away by the bloodstream. Alternatively, a drug reaches the bloodstream through the lymphatic vessels. Protein drugs that are large in size usually reach the bloodstream through the lymphatic vessels because these drugs move slowly from the tissues into capillaries. The subcutaneous route is used for many protein drugs because such drugs would be destroyed in the digestive tract if they were taken orally.

Certain drugs (such as progestins used for birth control) may be given by inserting plastic capsules under the skin (implantation). Although this route of administration is rarely used, its main advantage is to provide a long-term therapeutic effect (for example, etonogestrel that is implanted for contraception may last up to 3 years).

The **intramuscular route** is preferred to the subcutaneous route when larger volumes of a drug product are needed. Because the muscles lie below the skin and fatty tissues, a longer needle is used. Drugs are usually injected into the muscle of the upper arm, thigh, or buttock. The rate of absorption of the drug into the bloodstream depends, in part, on the blood supply to the muscle. The sparser the blood supply, the longer it takes for the drug to be absorbed.

For the **intravenous route**, a needle is inserted directly into a vein. A solution containing the drug may be given in a single dose or by continuous infusion. For infusion, the solution is moved by gravity (from a collapsible plastic bag) or, more commonly, by an infusion pump through a thin flexible tubing to a tube (catheter) inserted in a vein, usually in the forearm. Intravenous administration is the best way to deliver a precise dose quickly and in a well-controlled manner throughout the body. It is also used for irritating solutions, which would cause pain and damage tissues if given by subcutaneous or intramuscular injection.

When given intravenously, a drug is delivered immediately to the bloodstream and tends to take effect more quickly than when given by any other route. Consequently, healthcare practitioners closely monitor people who receive an intravenous injection for signs that the drug is working or is causing undesired side effects.

Also, the effect of a drug given by this route tends to last for a shorter time. Therefore, some drugs must be given by continuous infusion to keep their effect constant.

These routes can be divided into two potential avenues of entry into the human body. They are categorized as:

- Enteral,
- Parenteral,
- inhalation, and
- Topical and local application.

Enteral is when the drug is placed directly in the GIT. The enteral path could be subdivided as:

Oral – this is when the drug is swallowed. The efficacy and delivery can vary depending on the rate of how the active can dissolve and be quickly absorbed by the lower intestine as seen in Figure 2.3.

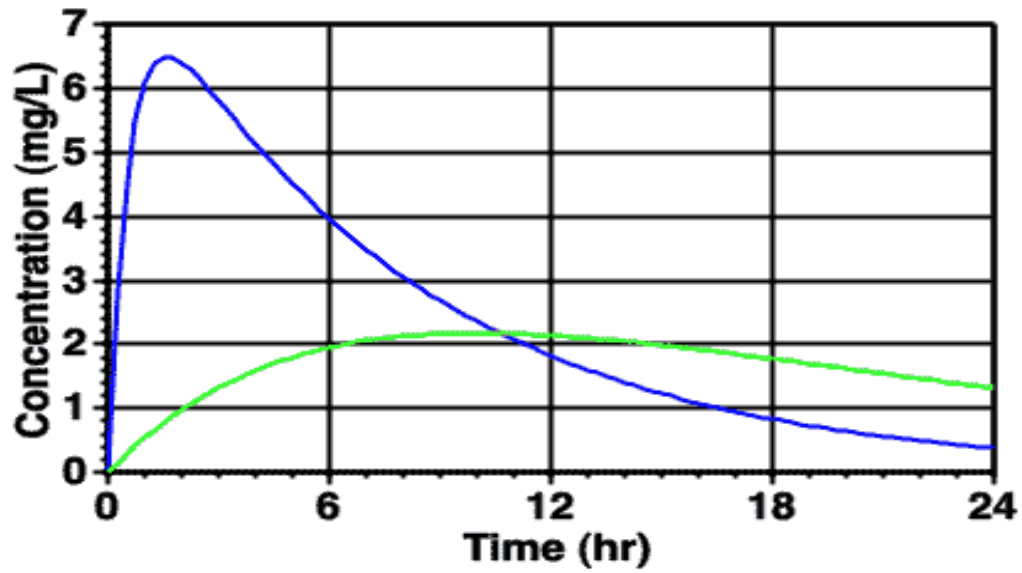


**Figure 2.3** Typical plot of  $C_p$  versus time after oral administration fast and slow

Source: Boomer, D., PHAR 7633 Chapter 7, Routes of Drug Administration  
<http://www.boomer.org/c/p4/c07/c07.pdf>. Accessed on November 28, 2014

Sublingual is when the drug is placed under the tongue. The drug release is fast and short-lived as shown in Figure 2.4.



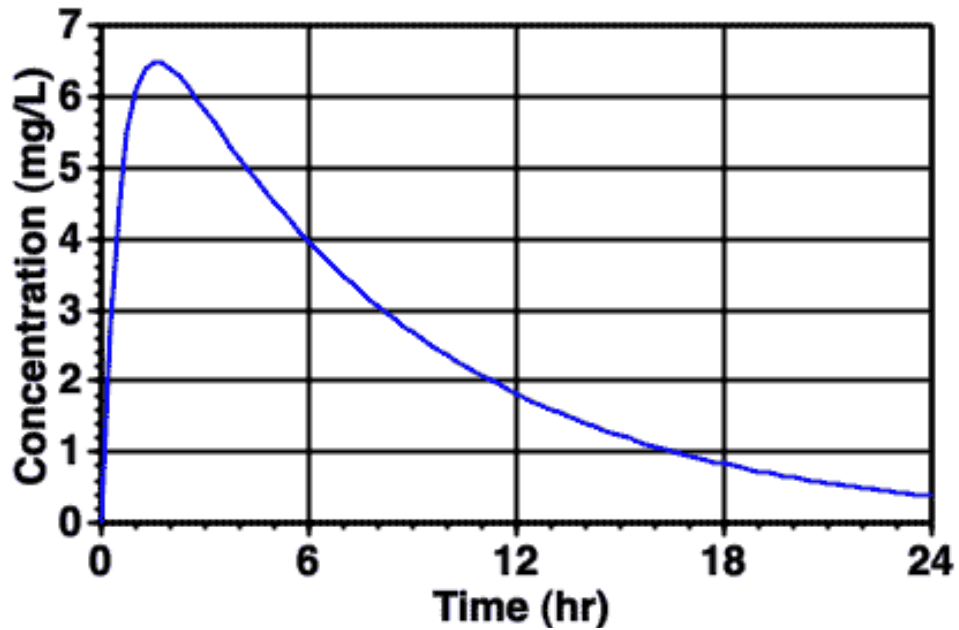


**Figure 2.4** Typical plot of  $C_p$  versus time after sublingual administration

Source: Boomer, D., PHAR 7633 Chapter 7, Routes of Drug Administration  
<http://www.boomer.org/c/p4/c07/c07.pdf> Accessed on November 28, 2014

Buccal is when the active drug is placed in the buccal cavity where it dissolves / is transported through the mucous membrane. The drug release is slow and more consistent when compared to the oral and sublingual methodologies as seen in Figure 2.5.

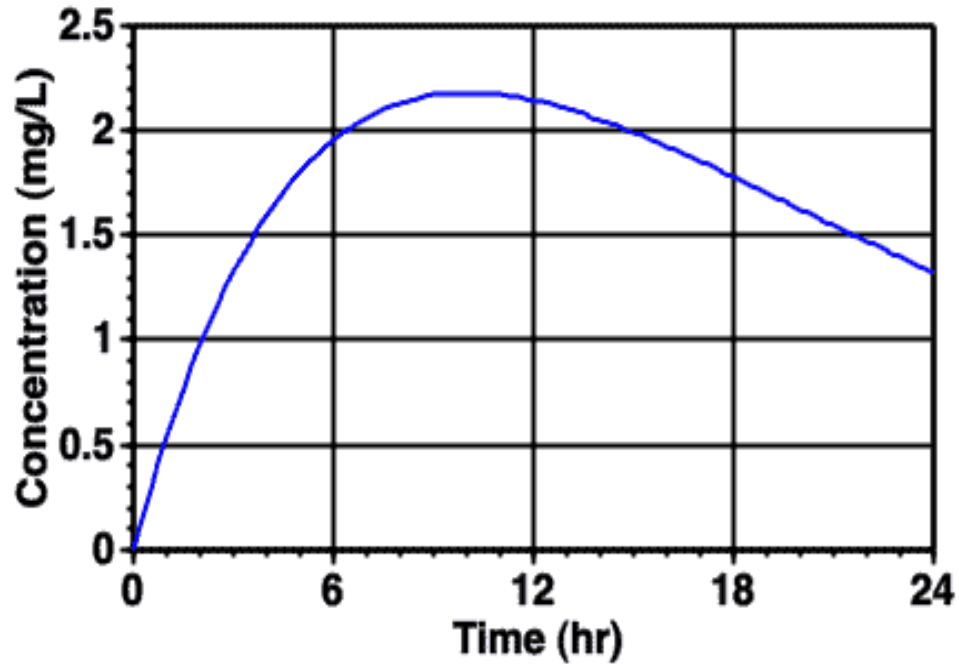


**Figure 2.5** Typical plot of  $C_p$  versus time after buccal administration

Source: Boomer, D., PHAR 7633 Chapter 7, Routes of Drug Administration  
<http://www.boomer.org/c/p4/c07/c07.pdf>. Accessed on November 28, 2014

Rectal is when the drug is directly absorbed through the rectum. It shows a drug release pattern similar to sublingual delivery systems. This is because both technologies must go through the mucosa in order to enter the bloodstream as seen in Figure 2.6.

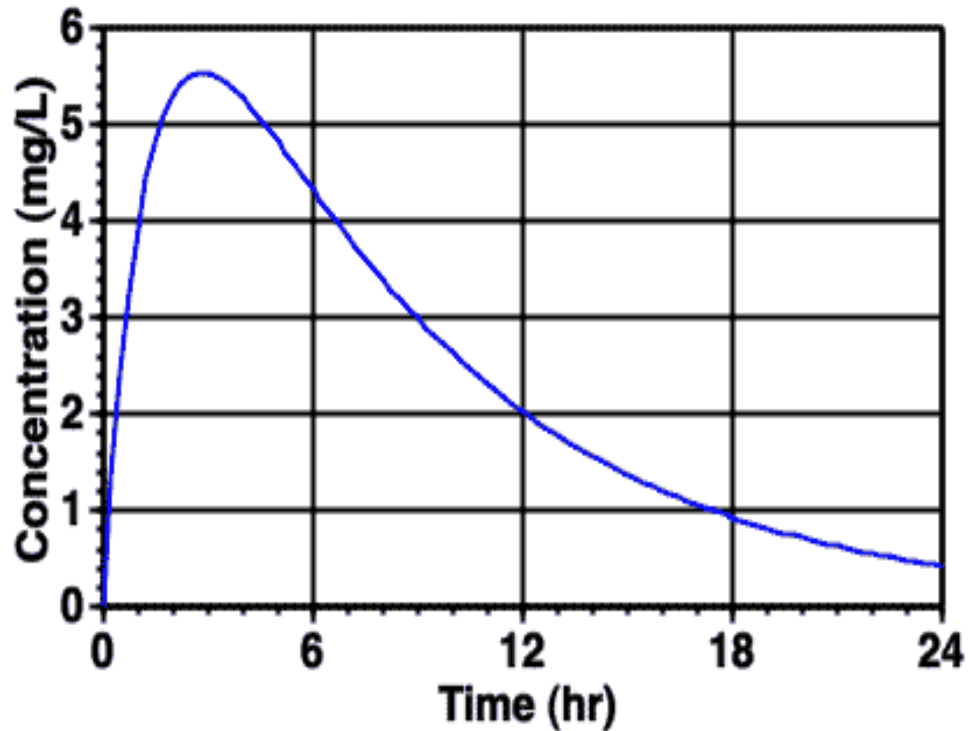


**Figure 2.6** Typical plot of  $C_p$  versus time after rectal administration

Source: Boomer, D., PHAR 7633 Chapter 7, Routes of Drug Administration  
<http://www.boomer.org/c/p4/c07/c07.pdf>. Accessed on November 28, 2014

Parenteral is when the drug is not placed directly in the GIT. The parenteral path could be subdivided as:

Intravenous (IV, IA)—placing a drug directly into the bloodstream. The absorption phase is bypassed (100% bioavailability). It is precise, accurate and almost immediate onset of action where large quantities can be given, fairly pain-free as seen in Figure 2.7.

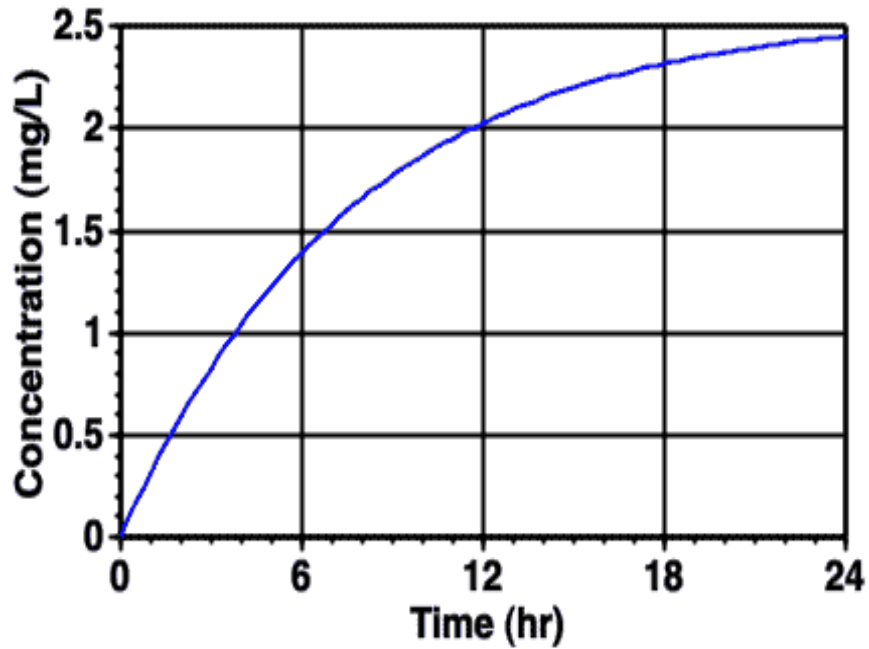


**Figure 2.7** Typical plot of  $C_p$  versus time during an IV infusion administration

Source: Boomer, D., PHAR 7633 Chapter 7, Routes of Drug Administration  
<http://www.boomer.org/c/p4/c07/c07.pdf>. Accessed on November 28, 2014

Intramuscular is similar to Intravenous in which a very rapid absorption of drugs in aqueous solution is typically used as a repository and requires slow release preparations.

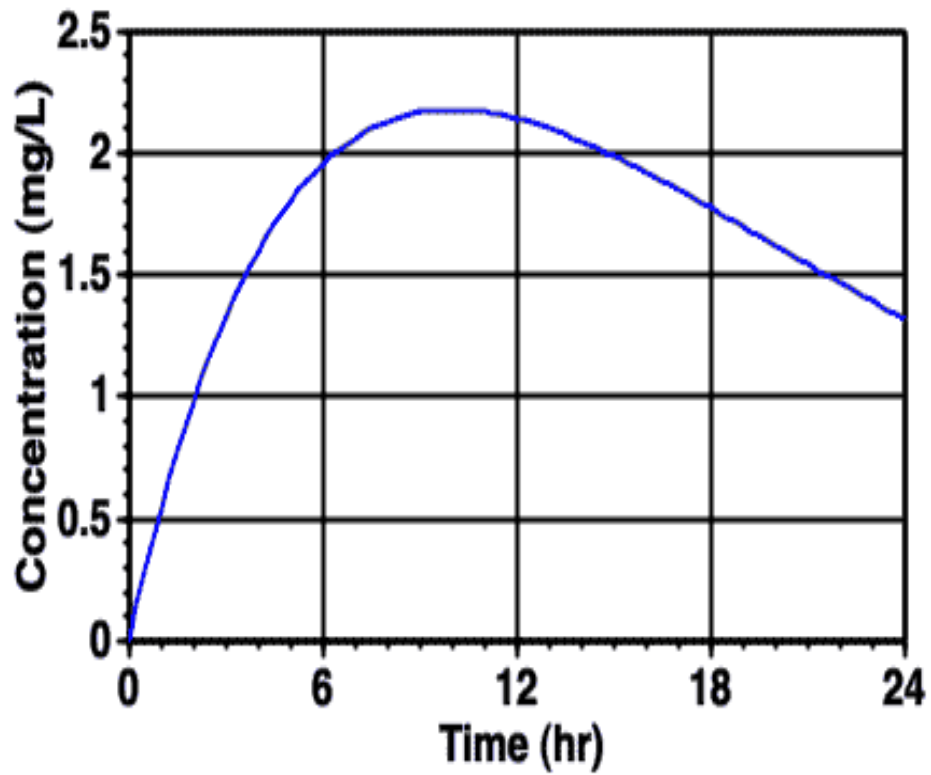


**Figure 2.8** Typical plot of  $C_p$  versus time after intramuscular administration

Source: Boomer, D., PHAR 7633 Chapter 7, Routes of Drug Administration  
<http://www.boomer.org/c/p4/c07/c07.pdf>

Subcutaneous is absorption of drugs from the subcutaneous tissues.

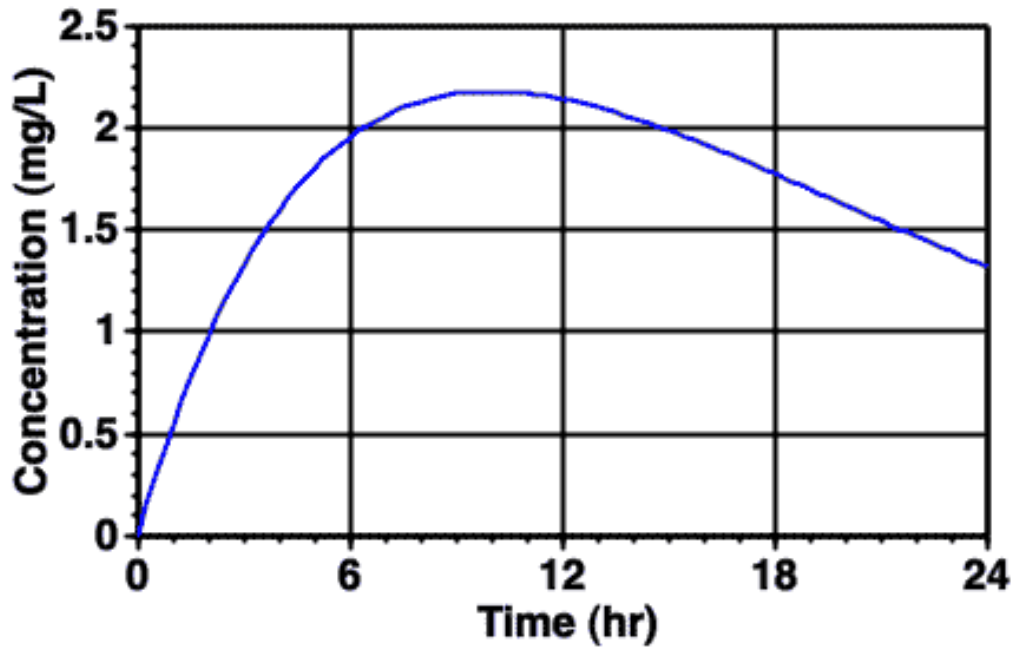


**Figure 2.9** Typical plot of  $C_p$  versus time after subcutaneous administration

Source: Boomer, D., PHAR 7633 Chapter 7, Routes of Drug Administration  
<http://www.boomer.org/c/p4/c07/c07.pdf>

Figures 2.8 and 2.9 show plot of  $C_p$  versus time after intramuscular administration and  $C_p$  versus time after subcutaneous administration slow and constant absorption, respectively.

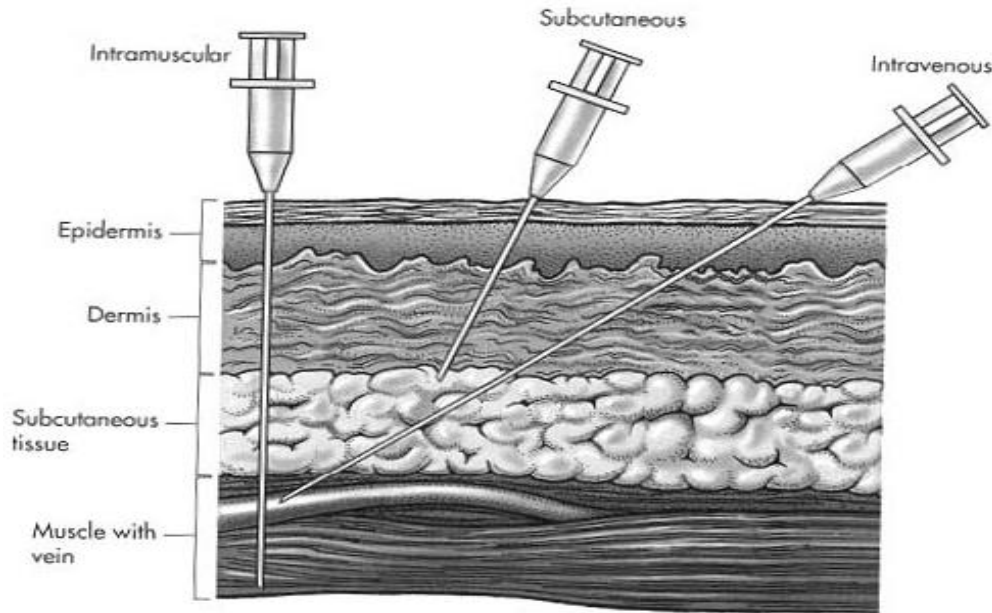


**Figure 2.10** Various routes of drug administration through injections

Source: Rachakonda, V.K., Effective Screening of Chemical Penetration Enhancers for Drug Delivery, Master Thesis, Oklahoma State University, p. 17, 2006.

Figure 2.10 shows the various routes for drug administration. These include:

- intra-arterial
- intra-articular, and
- Intra-dermal.

Inhalation is when the active drug is delivered directly from the lungs. Topical and local application is when the drug is delivered upon and through the skin. Parenteral is an intramuscular (IM) drug injected into skeletal muscle. Figures 2.11 – 2.14 show various case studies of concentration versus time after administration of the drug.

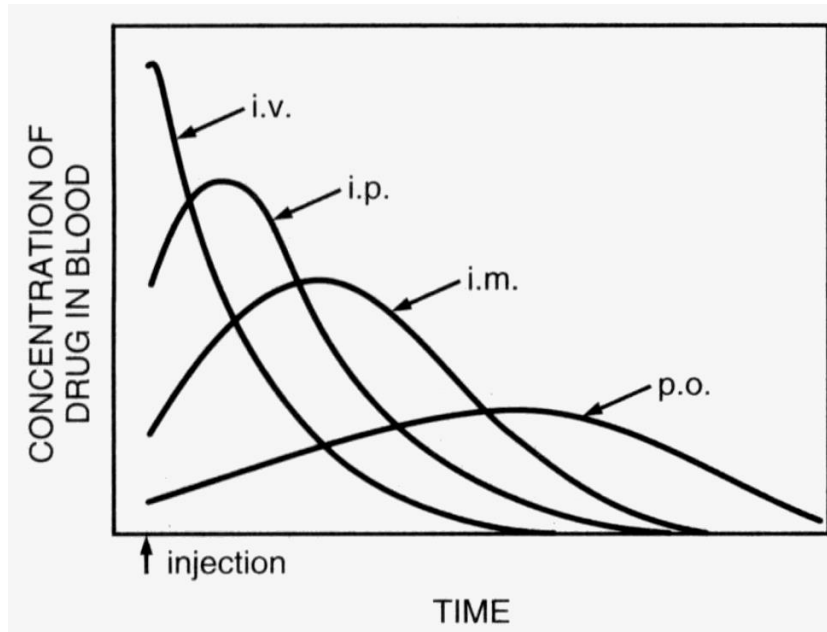


**Figure 2.11** Plot of drug blood concentration versus time comparison of different parenteral delivery systems

Source: Pharmacokinetics Presentation,  
<http://web.calstatela.edu/faculty/mchen/454L%lectures/pharmacokinetics.ppt>  
 Accessed on November 29, 2014

Inhalation is absorption through the lungs by means of gaseous, volatile agents and aerosols. This creates a rapid onset of action due to rapid access to circulation, because of the following factors

- a. large surface area,
- b. thin membranes separates alveoli from circulation, and
- c. high blood flow.

The effect versus time is shown in Figure 2.12.



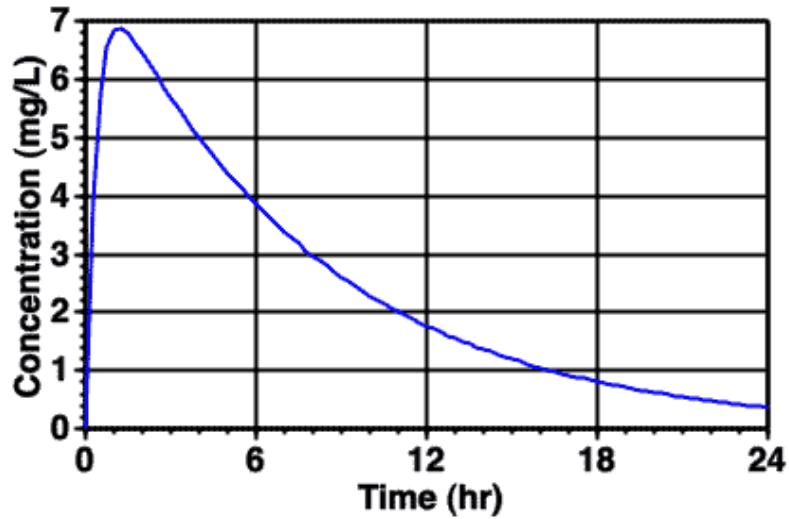


**Figure 2.12** Typical plot of  $C_p$  versus time after inhalation administration

Source: Boomer, D., PHAR 7633 Chapter 7, Routes of Drug Administration  
<http://www.boomer.org/c/p4/c07/c07.pdf>. Accessed on November 29, 2014

Topical administrations leverage the *mucosal membranes* (e.g., eye drops, antiseptic, sunscreen, and callous removal, nasal) and *skin* to deliver drug actives by means of

- a. dermal - rubbing in of oil or ointment (local action) and
- b. transdermal - absorption of drug through skin (systemic action).

providing a longer time which increases effectiveness. Topicals can be considered as the best Chronopharmacokinetic systems as seen in Figure 2.13.

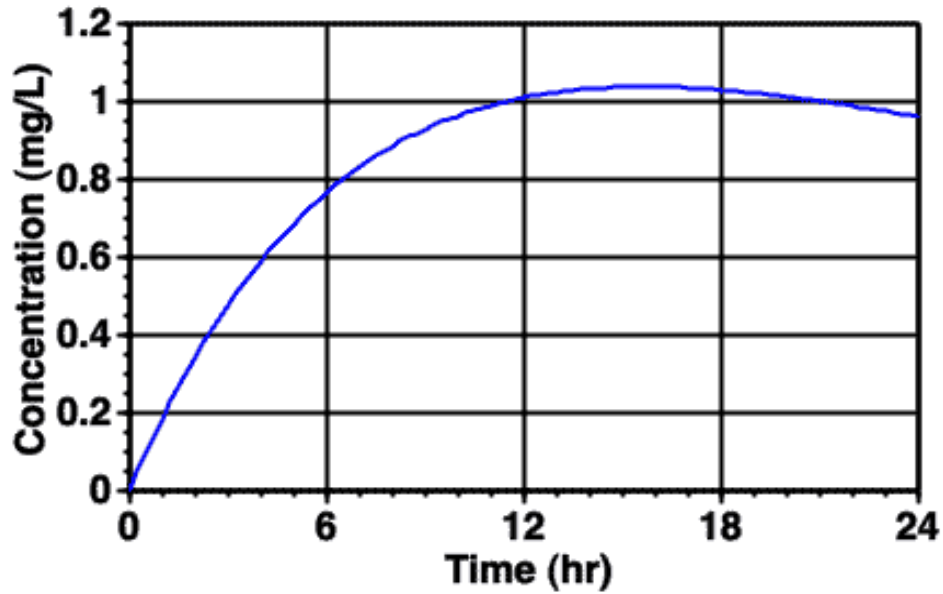


**Figure 2.13** Typical plot of  $C_p$  versus time after topical administration

Source: Boomer, D., PHAR 7633 Chapter 7, Routes of Drug Administration  
<http://www.boomer.org/c/p4/c07/c07.pdf>. Accessed on November 29, 2014

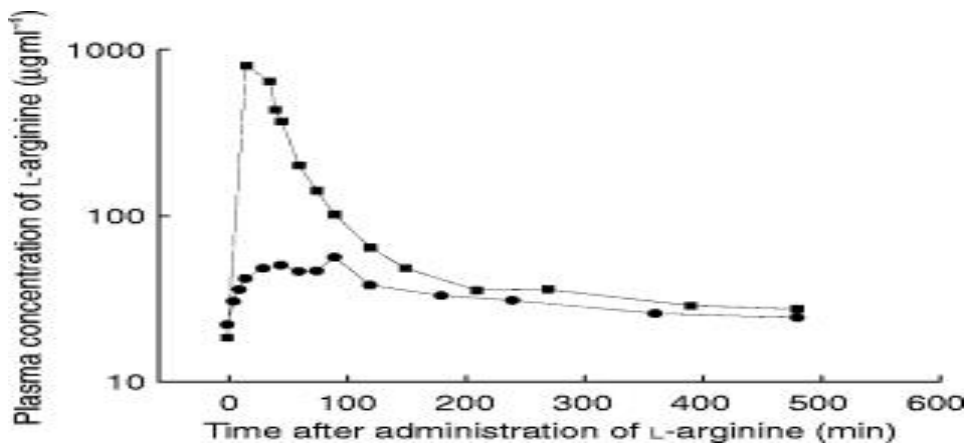


**Figure 2.14** Plot of drug plasma concentration versus time comparison between IV and oral administration.

Source: [Tangphao](#), O., [Grossmann](#), M., [Chalon](#), S., [Hoffman](#), B.B., and [Blaschke](#), T.F.,  
 Pharmacokinetics of intravenous and oral L-arginine in normal volunteers,  
 Br J Clin Pharmacol. 47(3): 261–266, 1999

Tables 2.1 and 2.2 summarize the routes of administration of drugs and their associated advantages and disadvantages, respectively. Table 2.1 shows the effective time by the different routes of administration.

**Table 2.1** Routes of Administrations and Effective Times

Route of Administration	Effective Time
Intravenous	30-60 seconds
Inhalation	2-3 minutes
Sublingual	3-5 minutes
Intramuscular	10-20 minutes
Subcutaneous	15-30 minutes
Rectal	5-30 minutes
Ingestion	30-90 minutes

Source: Manitoba Health, ROUTES for DRUG ADMINISTRATION, EMERGENCY TREATMENT GUIDELINES, APPENDIX A2, <http://www.gov.mb.ca/health/ems/guidelines/docs/A2.08.03.pdf>. Accessed on November 30, 2014.

Table 2.2 shows the advantages and disadvantages of the different types of administration routes.

**Table 2.2** Advantages and Disadvantages of different Types of Administration

Type of Administration	Advantages	Disadvantages
Oral	<p>Convenient - portable, safe, no pain, easy to take.</p> <p>Cheap - no need to sterilize (but must be hygienic of course), compact, multi-dose bottles, automated machines produce tablets in large quantities.</p> <p>Variety of dosage forms available - fast release tablets, capsules, enteric coated, layered tablets, slow release, suspensions, mixtures</p>	<p>Sometimes inefficient - high dose or low solubility drugs may suffer poor availability, only part of the dose may be absorbed.</p> <p>First pass effect - drugs absorbed orally are transported to the general circulation via the liver. Thus drugs which are extensively metabolized will be metabolized in the liver during absorption.</p> <p>Food - Food and GI motility can affect drug absorption. Often, patient instructions include a direction to take with food or take on an empty stomach. Absorption is slower with food for tetracycline and penicillin, etc.</p> <p>Local effect - Antibiotics may kill normal gut flora and allow overgrowth of fungal varieties. Thus, antifungal agent may be included with an antibiotic.</p> <p>Unconscious patient - Patient must be able to swallow solid dosage forms. Liquids may be given by tube.</p>
Buccal and Sublingual	<p>First pass - The liver is bypassed, thus, there is no loss of drug by first pass effect for buccal or sublingual administration</p> <p>Bioavailability is higher. Rapid absorption - Because of the good blood supply to the area of absorption is usually quite rapid, especially for drugs with good lipid solubility.</p> <p>Drug stability - pH in mouth relatively neutral (cf. stomach - acidic). Thus, a drug may be more stable.</p>	<p>Holding the dose in the mouth is inconvenient. If any part of the dose is swallowed, that portion must be treated as an oral dose and subject to first pass metabolism.</p> <p>Usually, more suitable for drugs with small doses.</p> <p>Drug taste may need to be masked.</p>

**Table 2.3** Advantages and Disadvantages of different Types of Administration  
(Continued)

Rectal	<p>By-pass liver - Some (but not all) of the veins draining the rectum lead directly to the general circulation, thus, bypassing the liver. Therefore, there may be a reduced first pass effect.</p> <p>Useful - This route may be most useful for patients unable to take drugs orally or with younger children.</p>	<p>Erratic absorption - Drug absorption from a suppository is often incomplete and erratic. However, for some drugs it is quite useful. There is research being conducted to look at methods of improving the extent and variability of rectal administration. Absorption from solutions used as an enema may be more reliable. Not well accepted. May be some discomfort.</p>
Intravenous (IV)	<p>Rapid - A quick response is possible. Plasma concentration can be precisely controlled using IV infusion administration.</p> <p>Total dose - The whole dose is delivered to the bloodstream. That is the bioavailability is generally considered 100% after IV administration. Larger doses may be given by IV infusion over an extended time.</p> <p>Poorly soluble drugs may be given in a larger volume over an extended time period.</p> <p>Veins relatively insensitive - to irritation by irritant drugs at higher concentration in dosage forms.</p>	<p>Suitable vein - It may be difficult to find a suitable vein. There may be some tissue damage at the site of injection.</p> <p>May be toxic - Because of the rapid response, toxicity can be a problem with rapid drug administrations. For drugs where this is a particular problem the dose should be given as an infusion, monitoring for toxicity.</p> <p>Requires trained personnel - Trained personnel are required to give intravenous injections.</p> <p>Expensive - Sterility, pyrogen testing and larger volume of solvent means greater cost for preparation, transport, and storage.</p>
Subcutaneous	<p>Can be given by patient (e.g. in the case of insulin).</p> <p>Absorption can be fast from aqueous solution but slower with depot formulations.</p> <p>Absorption is usually complete.</p> <p>Improved by massage or heat.</p> <p>Vasoconstrictor may be added to reduce the absorption of a local anesthetic agent, thereby prolonging its effect at the site of interest.</p>	<p>Can be painful. Finding suitable sites for repeat injection can be a problem.</p> <p>Irritant drugs can cause local tissue damage.</p> <p>Maximum of two ml injection, thus, often small doses limit use.</p>

**Table 2.4** Advantages and Disadvantages of different Types of Administration  
(Continued)

Intramuscular	Larger volume than SC can be given by IM. They may be easier to administer than IV injections. A depot or sustained release effect is possible with IM injections (e.g. procaine penicillin). Absorption can be rapid from aqueous solution.	Trained personnel required for injections. The site of injection will influence the absorption; generally, the deltoid muscle provides faster and more complete absorption. Absorption is sometimes erratic, especially for poorly soluble drugs (e.g. diazepam, phenytoin). The solvent may be absorbed faster than the drug causing precipitation of the drug at the site of injection. Irritating drug may be painful.
Inhalation	May be used for a local effect, e.g. bronchodilators. Can be used for systemic effect (e.g. general anesthesia). Rapid absorption by-passing the liver.	Absorption of gases is relatively efficient; however, solids and liquids are excluded if larger than 20 micron and even then only 10% of the dose may be absorbed. Larger than 20 micron and the particles impact in the mouth and throat. Smaller than 0.5 micron and they are not retained. Some portion of the dose may be swallowed.
Topical or Transdermal	The local effect (e.g., ear drops, eye drops or ointment, antiseptic creams and ointments, sunscreens). The systemic effect (e.g., nitroglycerin ointment). Absorption is quite slow. Transdermal patches can provide prolonged or controlled drug delivery.	There may be some skin irritation. Drug absorption will vary by site of administration, skin condition, age, and gender. Absorption is better with low dose, low MW, lipid soluble drugs.

Source: Understanding Pharmacology for Health Professionals, Fourth Edition, by Susan M. Turley, 2010. [http://wps.pearsoncustom.com/wps/media/objects/10490/10742713/HC115\\_Ch04.pdf](http://wps.pearsoncustom.com/wps/media/objects/10490/10742713/HC115_Ch04.pdf)  
Accessed on November 29, 2014

## 2.5 Structure of the Skin

The skin is the largest organ in the human body. The best approximation that a material scientist could make of the skin is of a multi-component/compartmental membrane.

This membrane consists of three separate and distinct components; the superficial, thinner portion is the epidermis. The subsequent thicker part is the dermis, and the deeper part, which connects to the blood vessels, muscles, and bones, is the hypodermis as seen in Figure 2.15.

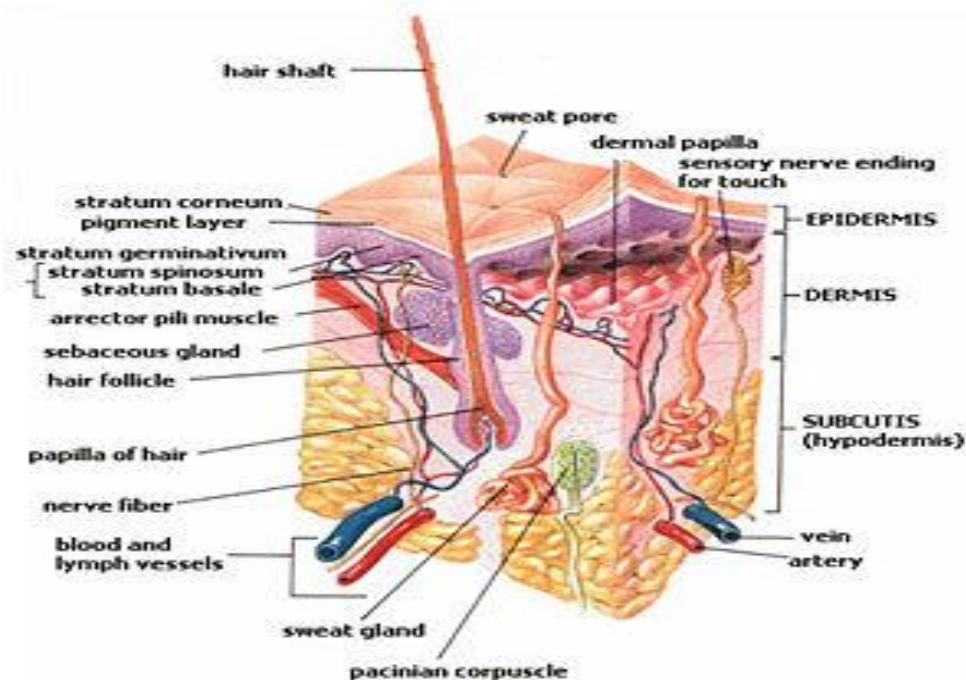


**Figure 2.15** Skin structure

Source: Subcutaneous tissue, [http://en.wikipedia.org/wiki/Subcutaneous\\_tissue](http://en.wikipedia.org/wiki/Subcutaneous_tissue). Accessed on November 30, 2014

### 2.4.1 Hypodermis

The hypodermis, shown in Figure 2.16, is the skin's innermost/deepest component that consists of adipose and areolar tissue along with nerves, blood, and lymph vessels. It is the component that surrounds muscles and bones.



**Figure 2.16** Hypodermis structure (200X Magnification)

Source: Human Skin Tissues. PPT

<http://www.google.com/url?sa=t&rct=j&q=&esrc=s&source=web&cd=11&ved=0CB0QFjAAOAO&url=http%3A%2F%2Fwww.tamdistrict.org%2Fsite%2Fhandlers%2Ffiledownload.ashx%3Fmoduleinstanceid%3D7776%26dataid%3D14305%26FileName%3DHumanSkinTissuesLecture.ppt&ei=ysF7VJ3NIobesAT-jIH4AQ&usg=AFQjCNE66ihbnqoftxh5XtVXRul3ywueDg&bvm=bv.80642063.d.cWc>

Accessed on November 30, 2014.



### 2.4.2 Adipose Tissue

Adipose tissue consists of cells designed to store fat that could be released as fuel to the skin and surrounding tissues as required. Their structure consists of lipids surrounded by a cytoplasmic membrane as seen in Figure 2.17.



**Figure 2.17** Adipose tissue/cells (320 x 240 enlargement)

Source: Adipose Tissue, *Tissues of the Human Body*, McGraw Hill.

[http://www.mhhe.com/biosci/ap/histology\\_mh/adiposfs.html](http://www.mhhe.com/biosci/ap/histology_mh/adiposfs.html). Accessed on November 30, 2014.

The cytoplasmic membrane releases the lipids upon mechanical stress, thus, enabling the skin to leverage the lipids as a fuel when additional energy is required to fulfill immediate needs.

### **2.4.3 Areolar Tissue**

Areolar tissue, also known as loose connective tissue, is a randomly arranged series of fibers that creates a mesh surrounding blood, lymph vessels, and organs, thus, making it the ideal cushioning agent providing a greater degree of protection as seen in Figure 2.18.

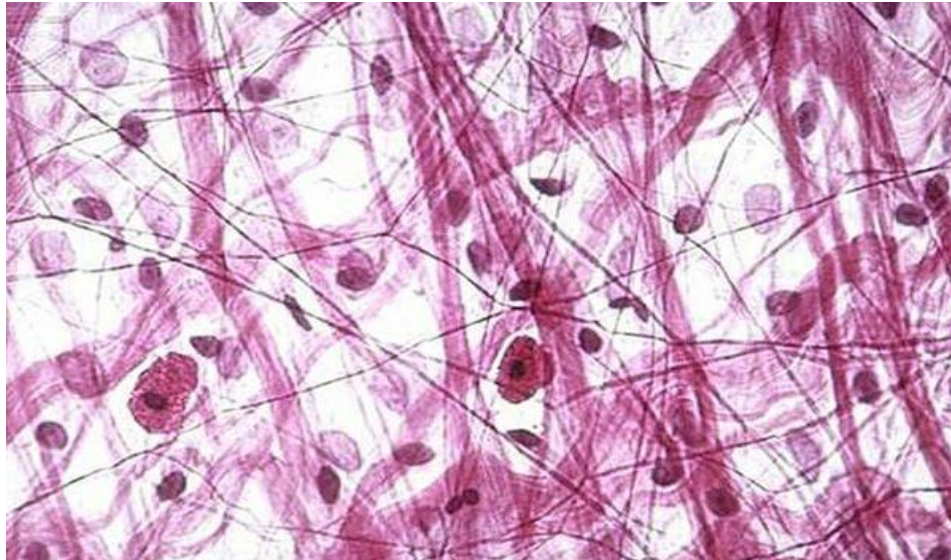


**Figure 2.18** Areolar tissue (600 x 381 magnification)

Source: <http://www.anatomybox.com/wpcontent/uploads/2012/01/AreolarConnectiveTissueSkin.jpg>.  
Accessed on November 30, 2014

### **2.4.4 Dermis**

The dermis is a layer of skin that is between the epidermis and the hypodermis as shown in Figure 2.19.

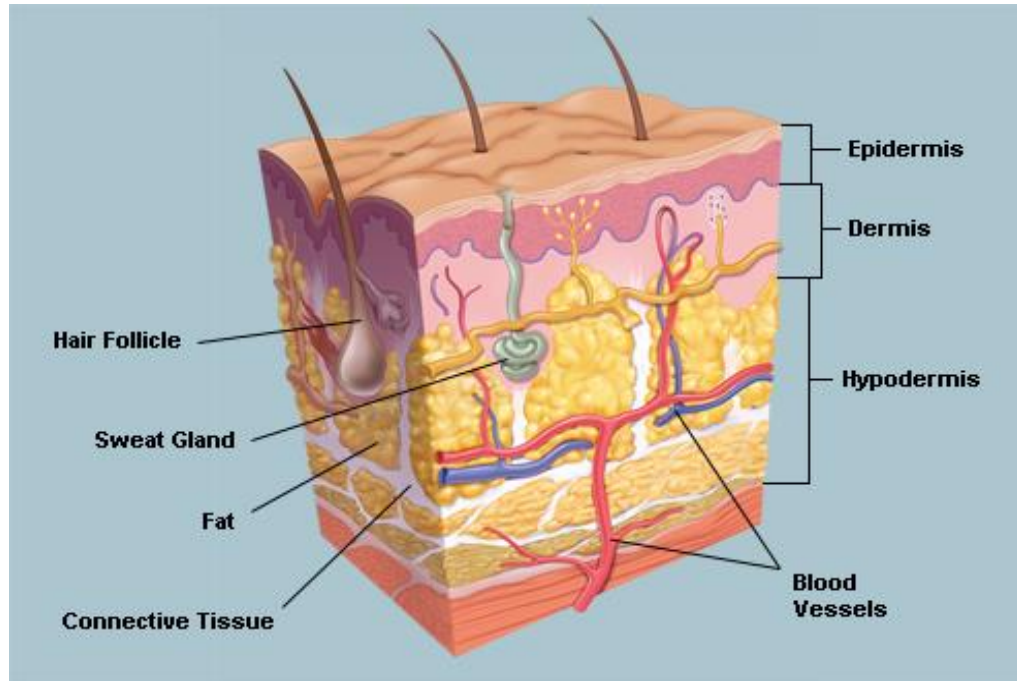


**Figure 2. 19** Dermis

Source: <http://www.webmd.com/skin-problems-and-treatments/picture-of-the-skin>  
Accessed on November 30, 2014.

It is divided into two adjacent substrates or layers. The one next to the epidermis is called the papillary region and the deeper thicker layer, known as the reticular dermis, is shown in Figure 2.20.

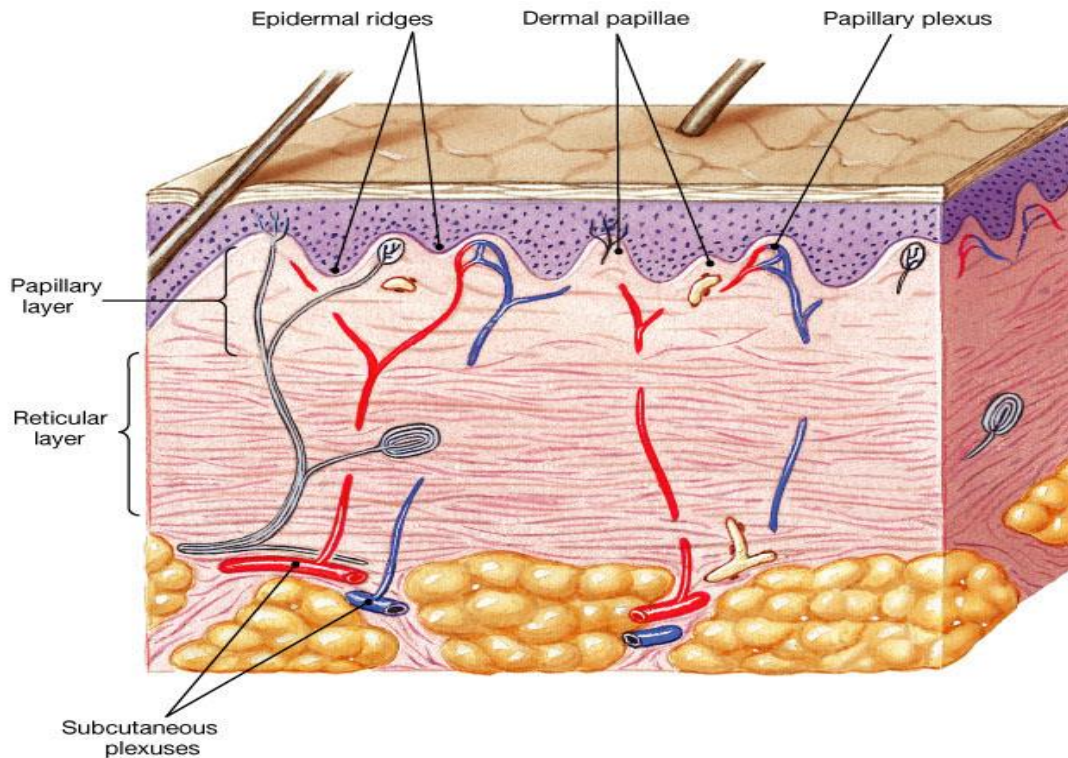


**Figure 2. 20** Dermis layers

Source: [http://droualb.faculty.mjc.edu/Lecture%20Notes/Unit%201/FG04\\_07.jpg](http://droualb.faculty.mjc.edu/Lecture%20Notes/Unit%201/FG04_07.jpg). Accessed on November 30, 2014.

The papillary layer lies directly beneath the epidermis and connects to it via papillae (i.e., finger-like projections). The reticular layer of the dermis contains crisscrossing collagen fibers that form a strong elastic network. Both the layers are depicted in Figure 2.21.

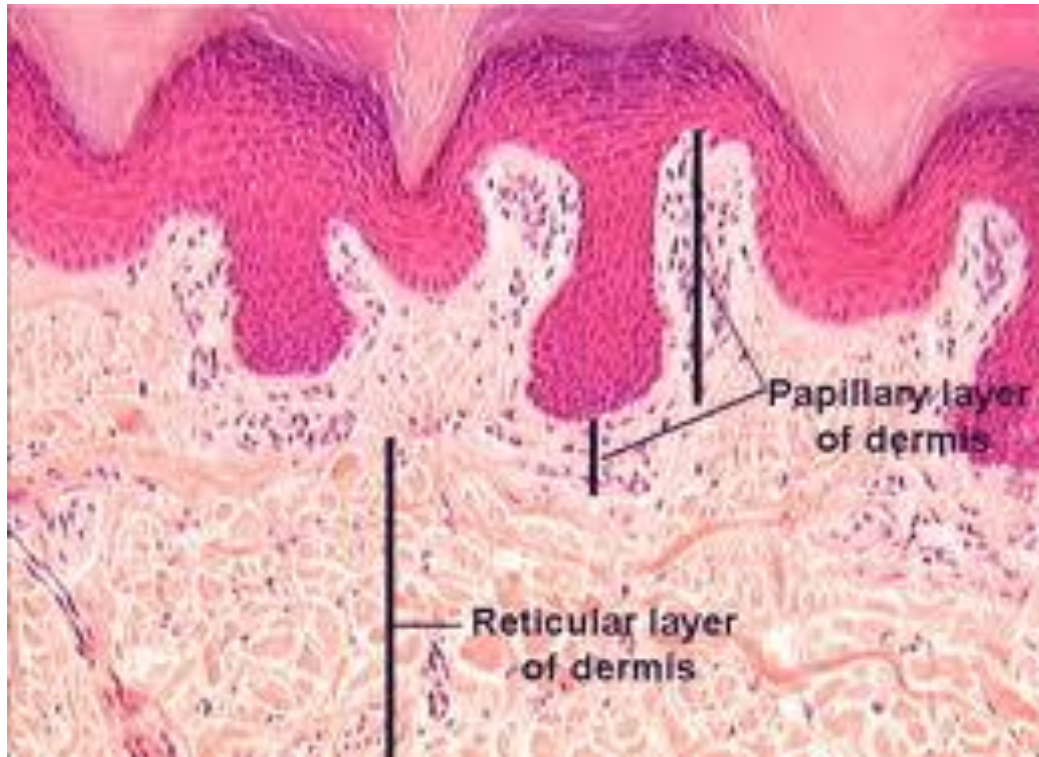


**Figure 2. 21** Papillary and Reticular layers (384 x 288 magnification)

Source: [http://rubred.files.wordpress.com/2013/05/161\\_dermis.gif](http://rubred.files.wordpress.com/2013/05/161_dermis.gif). Accessed on November 30, 2014.

Papillary region (i.e., the upper layer immediately beneath epidermis) consists of areolar connective tissue containing thin collagen and elastic fibers, dermal papillae (including capillary loops), corpuscles of touch and free nerve endings. The papillary region is the superficial part of the dermis. The surface area of the papillary region is greatly increased by small fingerlike projections called dermal papillae. Some dermal papillae contain tactile receptors called corpuscles of touch or Meissner corpuscles. These are nerve endings that are sensitive to touch. Also present in dermal papillae are free nerve endings, which initiate a signal that gives rise to sensations of warmth, coolness, pain, tickling, and itching.

The reticular region is the deeper part of the dermis. In this region, bundles of collagen fibers are interlaced in a net-like manner. Adipose cells, hair follicles, nerves, sebaceous glands, and sweat glands occupy the space between the fibers. A combination of collagen and elastic fibers in the reticular region is responsible for providing the skin with strength, extensibility, and elasticity.

Fibroblasts provide the structural framework for many tissues and have a critical role in wound healing. They are also responsible for synthesizing the dermal proteins as seen in Figure 2.22.

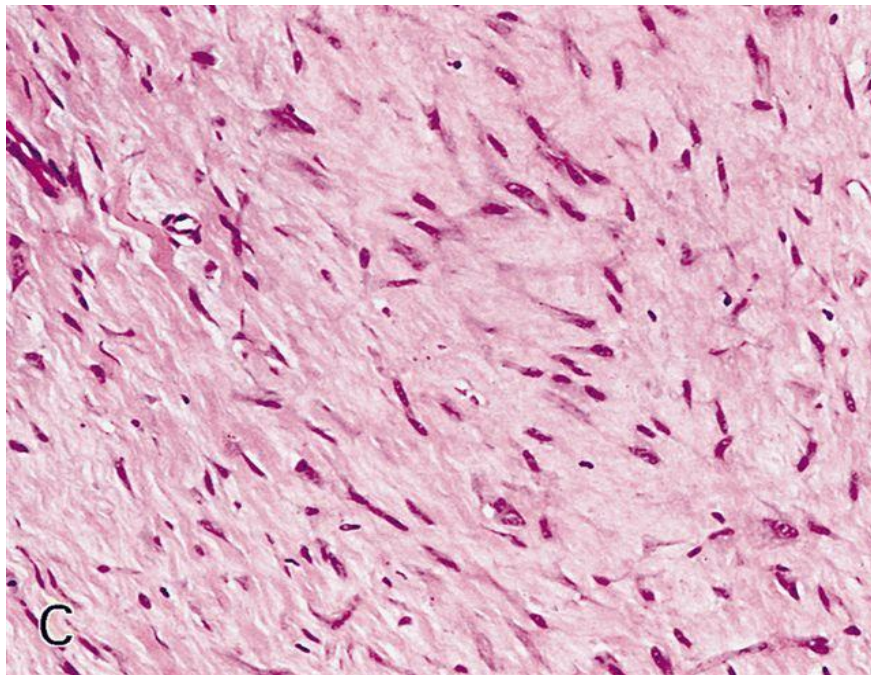


**Figure 2. 22** Fibroblasts (640 x 530 magnification)

Source: [http://www.pathologyoutlines.com/images/softtissue/02\\_28C.jpg](http://www.pathologyoutlines.com/images/softtissue/02_28C.jpg). Accessed on November 30, 2014

Collagen is composed of a triple helix, which generally consists of two identical chains ( $\alpha 1$ ) and an additional chain that differs slightly in its chemical composition ( $\alpha 2$ ) (Figure 2.23).<sup>(15)</sup> The amino acid composition of collagen is atypical for proteins, particularly with respect to its high hydroxyproline content.

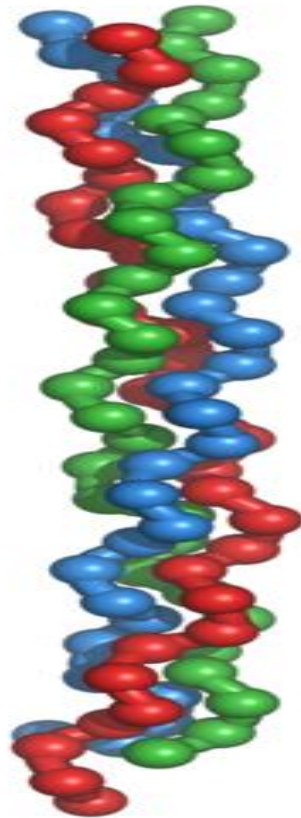


**Figure 2. 23** Tropocollagen structure

Source: <http://en.wikipedia.org/wiki/Collagen>. Accessed on November 30, 2014.

### 2.4.5 Epidermis

The epidermis encompasses different stages of cellular differentiation, gradual loss of nuclear material, and accumulation of keratin proteins. These stages are physically four layers:

- Stratum Basale
- Stratum Spinosum
- Stratum Granulosum
- Stratum Corneum

but there are a few areas where exposure to friction is greatest (e.g. fingertips, palms, and soles have five layers - Figure 2.24).



**Figure 2. 24** Layers of the epidermis: (B) Stratum Basale, (S) Stratum Spinosum, (G) Stratum Granulosum, and (C) Stratum Corneum (497 x 311 magnification)

Source: <http://pharmaxchange.info/press/wp-content/uploads/2011/03/Figure-6-Layers-of-epidermis.jpg>. Accessed on November 30, 2014



These layers are stratified in a sequential order as shown in Figure 2.25.

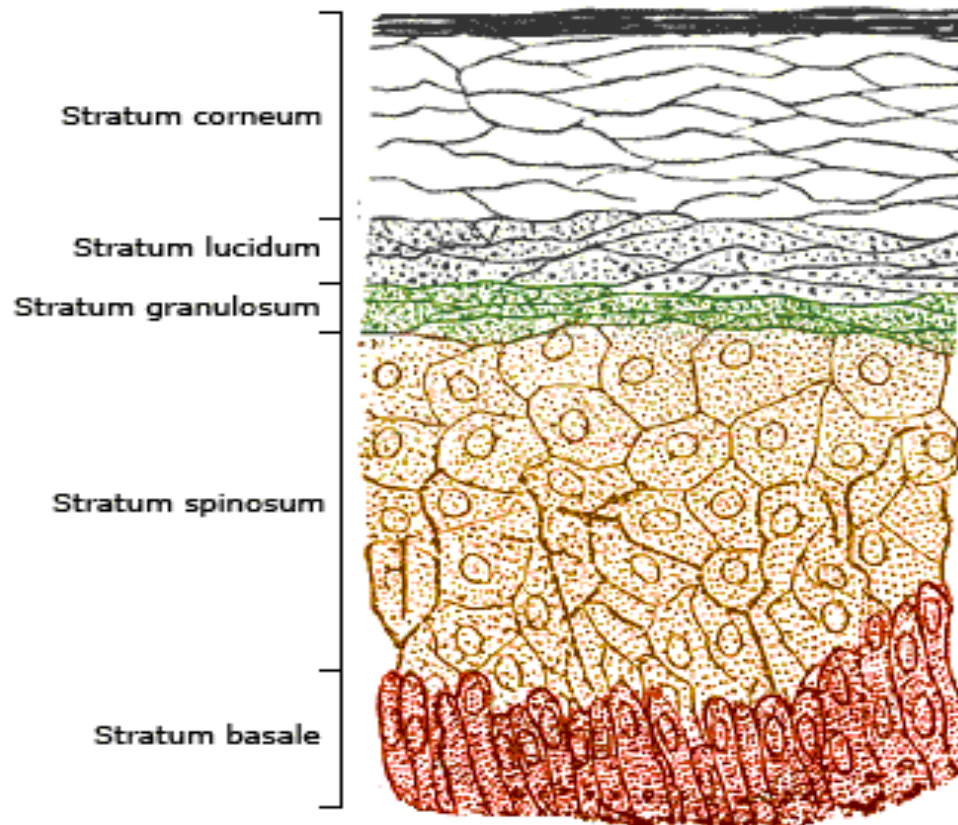


**Figure 2. 25** Schematic image showing a section of epidermis with labelled layers

Source: [http://wikidraft.referata.com/wiki/Epidermis\\_\(skin\)](http://wikidraft.referata.com/wiki/Epidermis_(skin)). Accessed on November 30, 2014

### **2.6.1 Stratum Corneum**

This layer is composed of 10 to 30 polyhedral, anucleated corneocytes, which is the final phase of keratinocytes differentiation. Palm and soles have most of these layers.

Corneocytes are surrounded by a protein sheath (cornified proteins) filled with water-retaining with keratinized proteins, attached together through corneodesmosomes and surrounded in the extracellular space by stacked layers of lipids.<sup>[10]</sup> Most of the barrier functions of the epidermis localize within this layer.<sup>[11]</sup>

### **2.6.2 Stratum Lucidum**

This is a clear/translucent layer that is only present in palms and soles. This layer is present only in those areas that are prone to friction (i.e. in thick skin). It consists of a large amount of keratin and thickened plasma membrane. The layer is made of three to five layers of flattened dead keratinocytes.

### **2.6.3 Stratum Granulosum**

This is the middle layer of the epidermis. It consists of a protein called keratohyalin, which converts to no filaments into keratin. This layer consists of three to five layers of flattened keratinocytes. Also present in the keratinocytes are membrane enclosed lamellar granules, which release a lipid-rich secretion. This secretion fills the space between cells of stratum granulosum, stratum lucidum, and stratum corneum. They act as a water repellent sealant that helps retard loss of body fluids and entry of foreign materials.

#### **2.6.4 Stratum Spinosum**

This is the layer above the stratum basale. It provides both strength and flexibility to the skin. This layer consists of 8 to 10 layers of keratinocytes. The Keratinocytes become connected through desmosomes and start to produce lamellar bodies, from within the Golgi, enriched in polar lipids, glycosphingolipids, free sterols, phospholipids and catabolic enzymes.<sup>[4]</sup> Langerhans cells, immunologically active cells, are located in the middle of this layer.

#### **2.6.5 Stratum basale**

This layer is mainly composed of disseminating and non-disseminating keratinocytes, attached to the basement membrane by hemidesmosomes. Melanocytes are present, connected to numerous keratinocytes in this and other strata through dendrites.

Within these layers, different types of cells with specific functionality are present as seen in Figure 2.26 and the key cells are known as Langerhans.

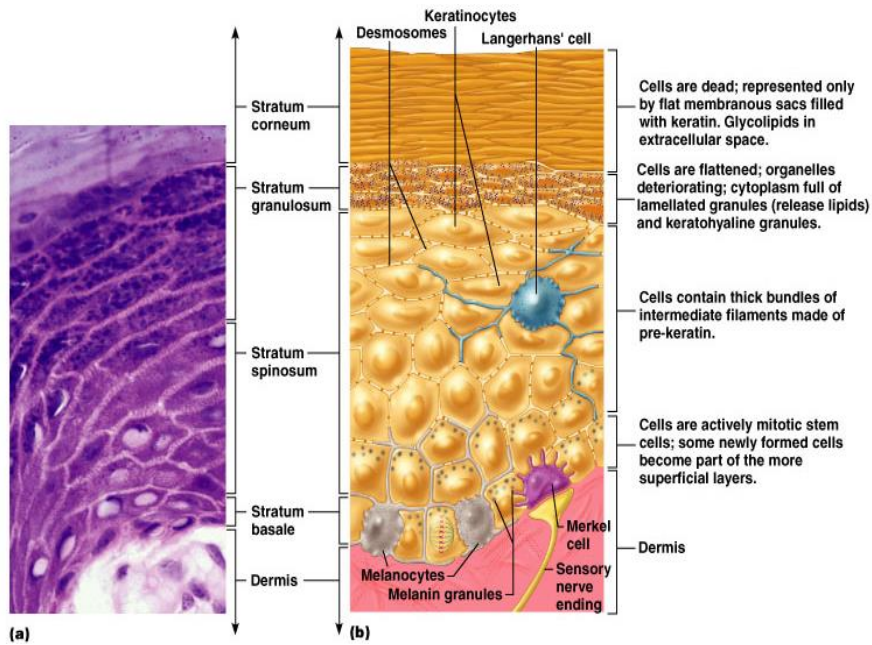


**Figure 2.26** Types of cells present within the epidermis layers

Source: [https://bohone09.wikispaces.com/file/view/Picture\\_3.jpg/87308785/619x422/Picture\\_3.jpg](https://bohone09.wikispaces.com/file/view/Picture_3.jpg/87308785/619x422/Picture_3.jpg). Accessed on November 30, 2014

### 2.6.6 Merkel Cells

Merkel cells are also found in the stratum basale with large numbers in touch-sensitive sites such as the fingertips and lips. They are closely associated with cutaneous nerves and seem to be involved in light touch sensation.<sup>[10]</sup>

Merkel cells are used as sensory receptors for light touch. They are usually located in the deepest layer of the epidermis. These cells are in contact with the flattened process of a sensory neuron structure called a tactile disc. Merkel cells and tactile discs together detect different aspects of touch sensation. Figure 2.27 shows the schematic representation of a Merkel cell-neurite complex as observed ultra-structurally. This diagram depicts (1) a dendritic Merkel cell (Mc) with its desmosomal attachments to adjacent keratocytes (K),

intranuclear “rodlet,” and membrane-bound dense core granules (G) and (2) a mitochondria-rich myelinated axon (A) with postsynaptic thickening of its terminal membrane.



**Figure 2. 27** Merkel cells

Source: <http://www.derm101.com/wp-content/uploads/ac01g069.jpg>. Accessed on November 30, 2014

### **2.6.7 Langerhans Cells**

Langerhans cells arise from red bone marrow and migrate to the epidermis. They participate in immune response against microbes that invade the skin and these cells are easily damaged by ultraviolet light (Figure 2.28).

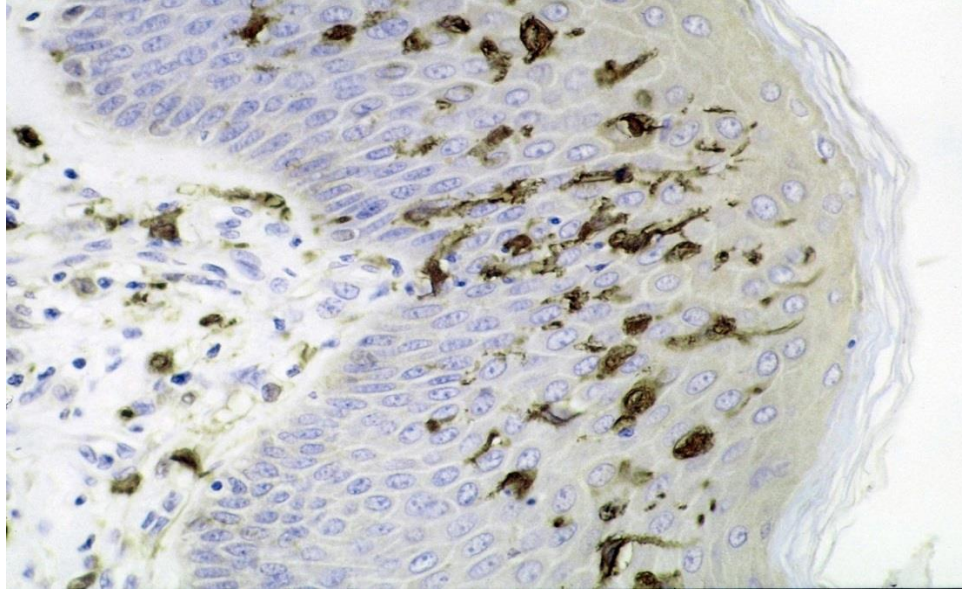


**Figure 2. 28** Langerhans cells (1818 x 1228 magnification)

Source: [http://upload.wikimedia.org/wikipedia/commons/2/2e/Dendritic\\_cells.jpg](http://upload.wikimedia.org/wikipedia/commons/2/2e/Dendritic_cells.jpg). Accessed on November 30, 2014.

### **2.6.8 Keratinocyte**

They make up 90% of the epidermal layer of the skin and they produce the protein keratin. The protein protects the skin and underlying tissues from heat, microbes, and chemicals. It also produces lamellar granules, which release a water repellent sealant. This is shown in Figure 2.29.

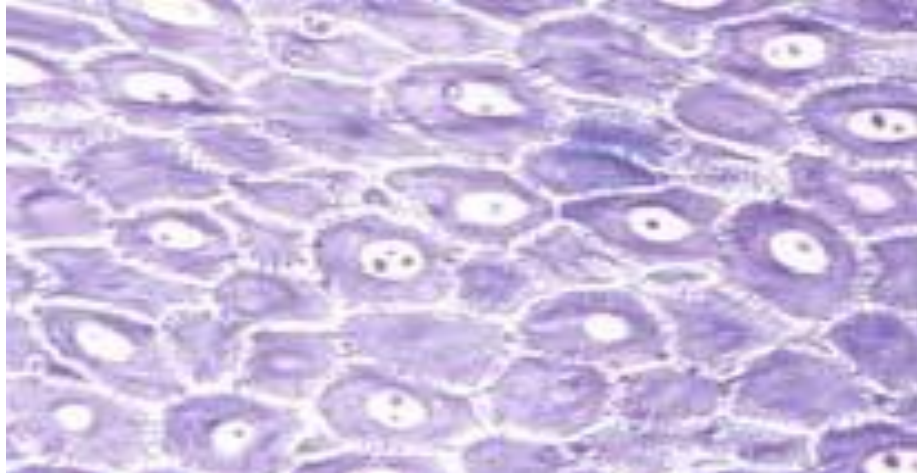


**Figure 2. 29** Keratinocytes as seen under a microscope

Source: <http://pharmaxchange.info/press/wp-content/uploads/2011/03/Figure-2-keratinocytes- as-seen-under-a-microscope.jpg>. Accessed on November 30, 2014.

### 2.6.9 Melanocytes

Melanocytes make up 8% of the epidermis. It produces the pigment melanin, which contributes to the color of the skin and absorbs the damaging ultraviolet light. Figure 2.30 shows the structure of Melanocytes.

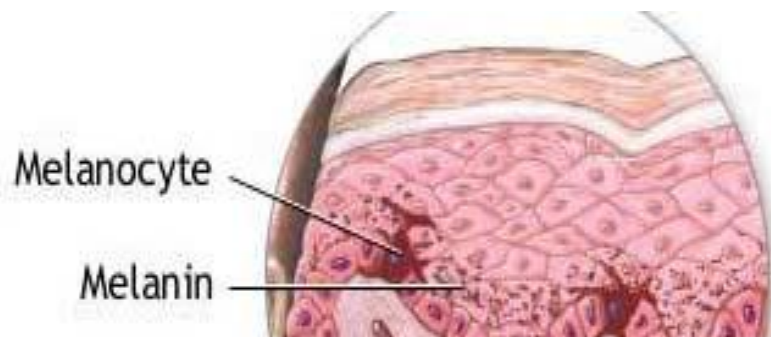


**Figure 2.30** Melanocytes

Source: [http://upload.wikimedia.org/wikipedia/commons/d/dd/Illu\\_skin02.jpg](http://upload.wikimedia.org/wikipedia/commons/d/dd/Illu_skin02.jpg). Accessed on November 30, 2014

### 2.6.10 Macrophages

Macrophages are white blood cells, also called big eaters, as their role is to digest and eat (phagocytosis) cellular debris and pathogens. They are about 21 micrometers (0.00083 in) in diameter and are produced by the differentiation of [monocytes](#) in tissues. This is shown in Figure 2.31.

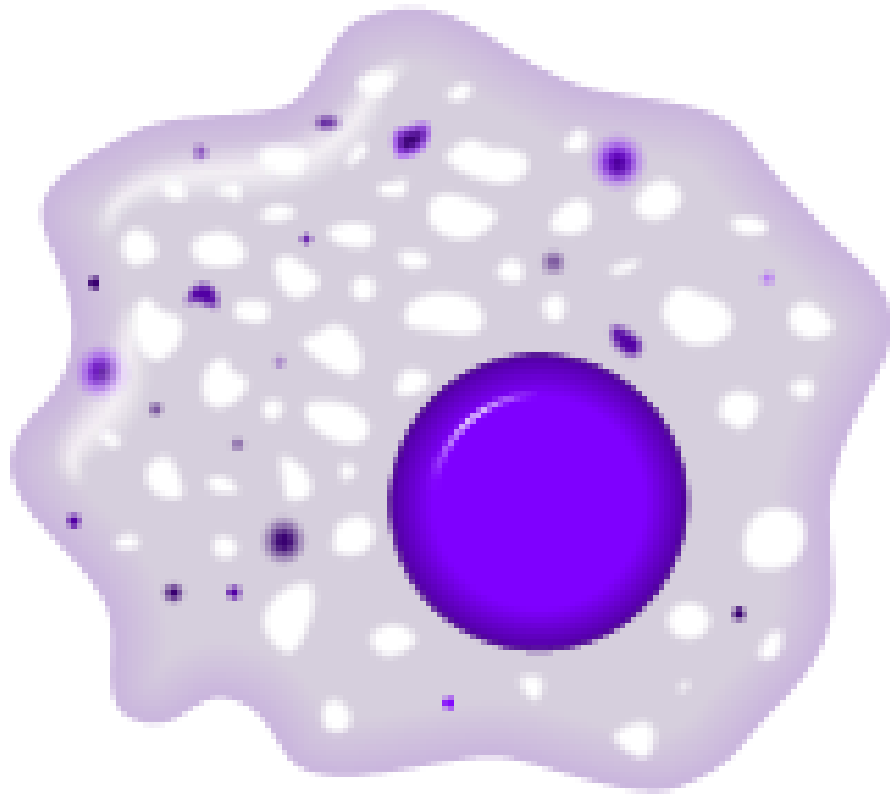


**Figure 2.31** Macrophage

Source: [http://www.phartoonz.com/wp-content/uploads/2010/11/leukocyte\\_immunity\\_Macrophage.png](http://www.phartoonz.com/wp-content/uploads/2010/11/leukocyte_immunity_Macrophage.png).  
Accessed on November 30, 2014



## 2.7 Routes of Drug Entry unto the Skin

There are three paths that drug actives can penetrate the skin. These paths are known as the intercellular, transcellular, and follicular routes<sup>(17)</sup>. This is shown in Figure 2.32.

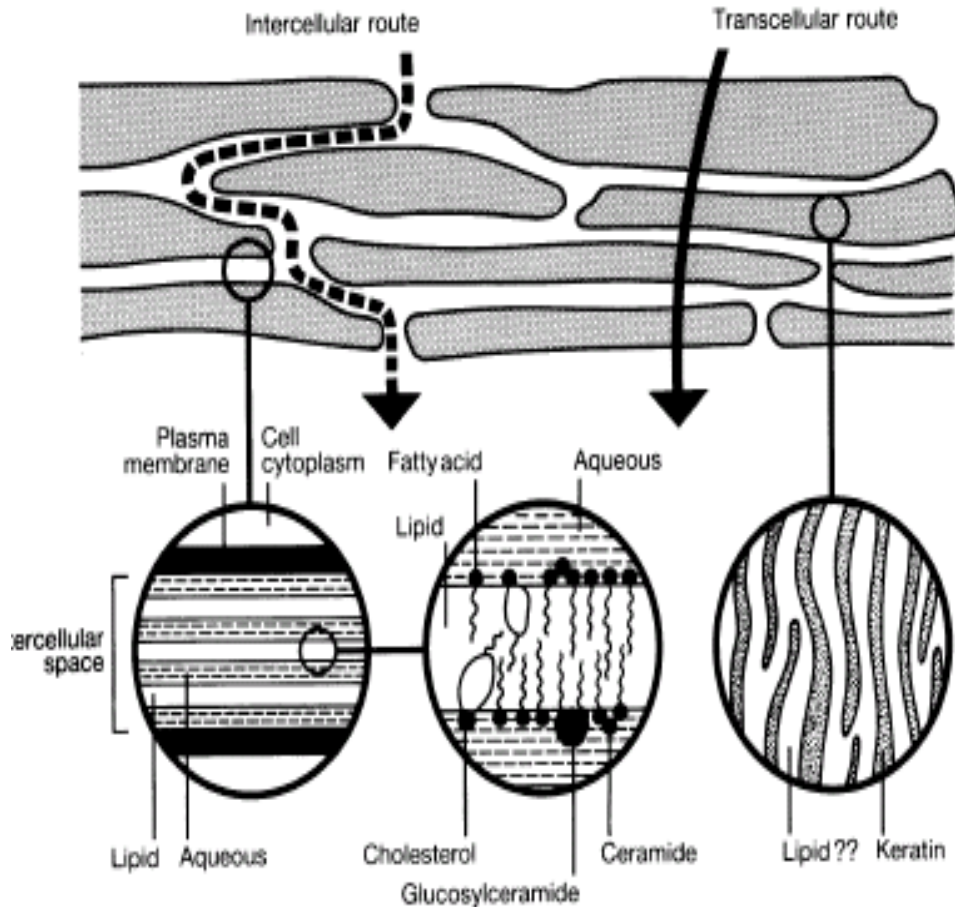


**Figure 2.32** Delivery Skin Routes

Source: [http://biomed.brown.edu/Courses/BI108/BI108\\_2003\\_Groups/Transdermal/Skin/SkinPerm.htm](http://biomed.brown.edu/Courses/BI108/BI108_2003_Groups/Transdermal/Skin/SkinPerm.htm)  
Accessed on December 1, 2014.

This is also well known as the “brick and mortar” model. The brick is the protein where trans-cellular penetration occurs whilst the lipid is the mortar in which the intercellular diffusion takes place. This is shown in Figure 2.33.

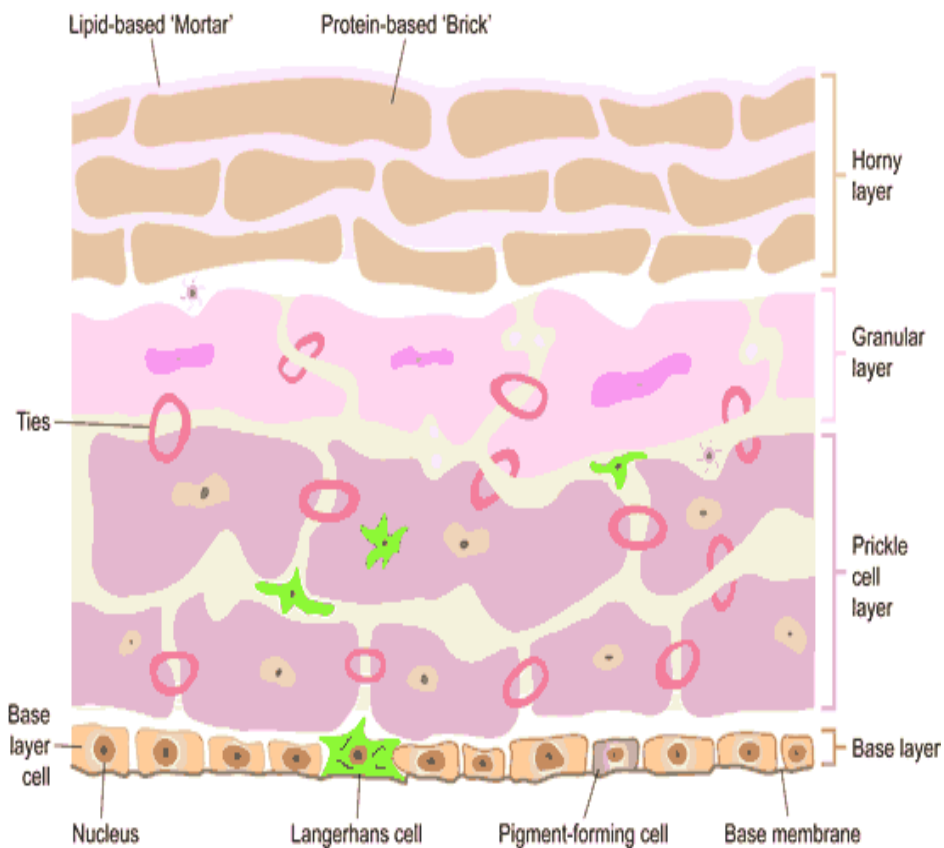


**Figure 2. 33** Brick and Mortar

Source: Understanding the causes of skin disease, Health and Safety Executive, <http://www.hse.gov.uk/skin/professional/causes/understand.htm>. Accessed on December 1, 2014.

## 2.8 TDD Techniques

The delivery of drugs is the basis for the improvement in patient health. The usual route is to develop such deliveries to be administered orally for improved patient compliance.

However, using the oral route can cause issues such as the following:

1. Irritation of the GIT. GIT is the chemical interaction between the active drug and mucosa membranes of the gastrointestinal track comprised of the region from the upper esophagus to the duodenum region of the intestine that can create discomfort and potential chemical erosion of the membranes. In turn, this can make the patient either skip or discontinue the use of the treatment, thus, making the patient no longer abide by the therapeutic regime set by the physician, thus, effectively delaying the sought after benefits. This is perhaps one of the major issues encountered by physicians when prescribing orally delivered therapies.
2. First pass metabolism, or pre-systemic metabolism, is defined as the condition in which the bio-available concentration of the drug is significantly reduced when passing through the liver before it is in contact with the bloodstream. <sup>[1, 2]</sup> Therefore, in order to overcome this, the concentration of the drug must be substantially increased in order to be effective, thus, ensuring that the patient receives the correct amount. However, as seen in Figure 2.34<sup>(14)</sup> this can create situations during which the drug is rarely at the desired therapeutic level (TL). This can be either fully below or above the TL, thus, practically rendering the treatment inadequate or dangerous.
3. Low patient compliance - For any treatment to be effective, the patient must adhere to the regime prescribed by the physician. Aside from the influence of GIT along with busy schedules, people very often skip doses, thus, rendering the designed procedure to be therapeutically ineffective.

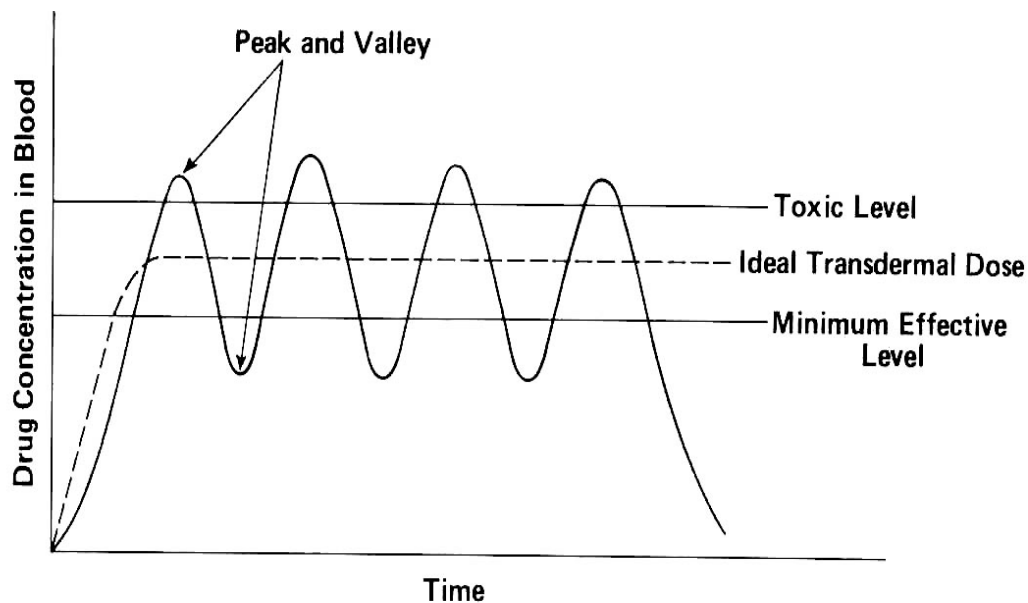


**Figure 2.34** Hypothetical blood level pattern from a conventional multiple dosing schedule and the idealized pattern from a transdermal controlled release system.

Source: Falcone, R., Jaffe, M. and Ravindra, N.M., New screening methodology for selection of polymeric matrices for transdermal drug delivery devices, *Bioinspired, Biomimetic and Nanobiomaterials*, Volume 2 Issue BBN2, p. 65 – 75, 2013

TDDs are passive drug delivery systems that provide a constant active drug flow to the patient through the skin.

The advantages of leveraging TDD against any other non-oral delivery (NOD) can be summarized as follows:

- complete avoidance of the first pass metabolism through the liver,
- non-GIT incompatibility,
- lower side effects or better plasma – concentration time profiles,
- greater predictability and long period of drug activity,
- increased patient compliance,
- enhanced therapeutic efficacy,
- dose frequency is reduced,

- increased flexibility in ending protocol by simply removing the source, and
- Non-invasive and ease of implementation/use.

## 2.9 Transdermal Patch Design

Transdermal patches (TDDP) are systems consisting of several components that are specifically designed for different applications as shown in Figure 2.35<sup>(18)</sup>.

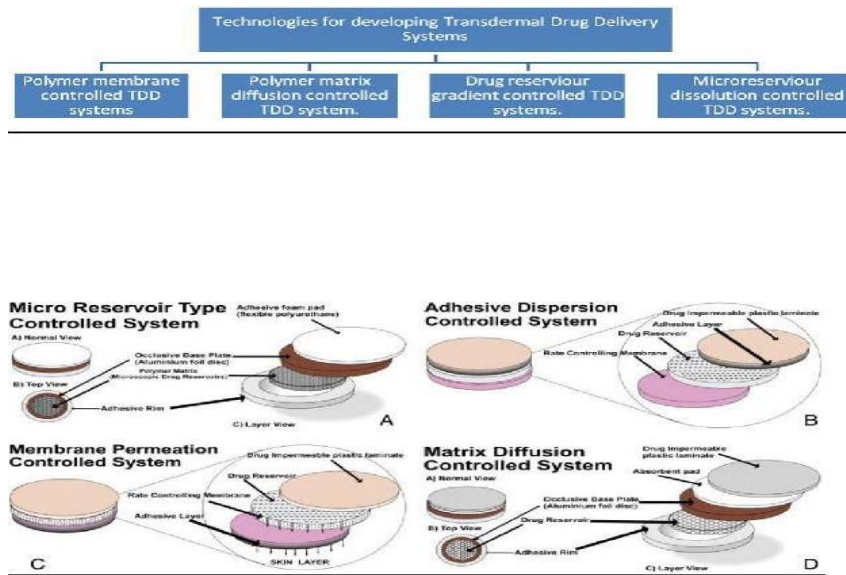


**Figure 2.35** Types of transdermal patches

Source: Sachan, R. and Bajpai, M., TRANSDERMAL DRUG DELIVERY SYSTEM: A REVIEW, International Journal of Research and Development in Pharmacy and Life Sciences, Vol.3, No.1, pp 748-765, 2013 Accessed on December 2, 2014

The basic TDDP working release mechanism is shown in Figure 2.36.

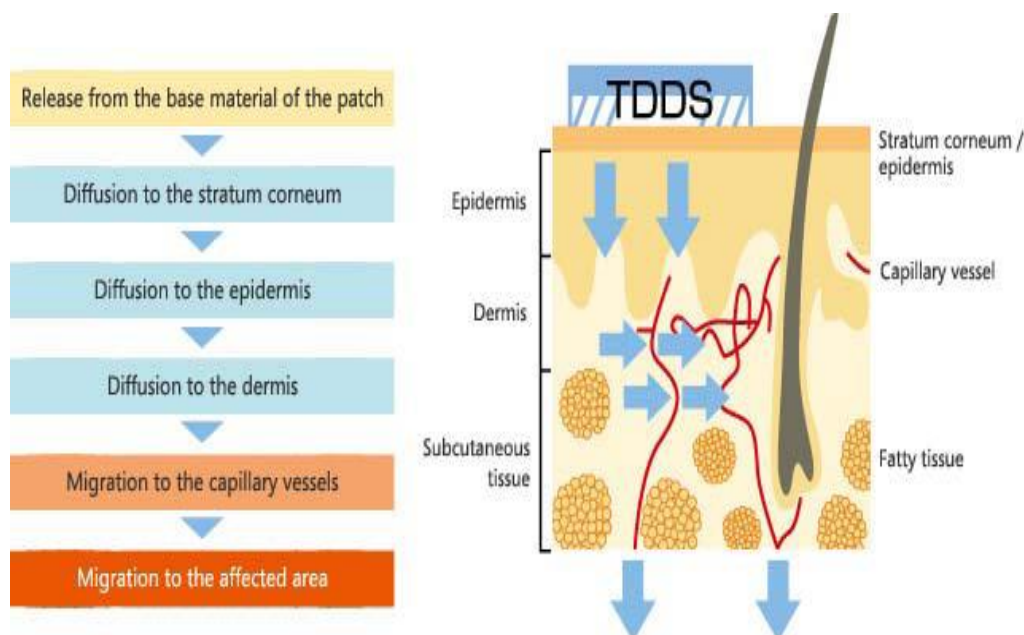


**Figure 2.36** TDDP release mechanism

Source: <http://www.hisamitsu.co.jp/english/company/operations/tdds.html>. Accessed on December 2, 2014

Designing transdermal patches is a three-step process. Step 1 involves finding the physicochemical compatibility between the active drug and polymers used in the films. Step 2 involves the film fabrication. Step 3 is the in-vitro active drug release evaluation where the cumulative release is then plotted against time as shown in Figure 2.34 where the diffusion coefficient is found from the slope. This is a trial and error method, which is time consuming. Although, with all the advantages that TDDs can offer, the methodology used has created several incidents in which the safety and design have been put to question as seen in the case of Fentanyl patches (Table 2.3).

A generally accepted set of selection rules, for materials, in TDD patches were suggested by Williams<sup>(19)</sup>. These can be summarized as follows:

1. Selection of a good drug candidate:
  - a. molecular size limit not to exceed between 300-500 Da.,
  - b. active release of drug in the range of 1 mg/cm<sup>2</sup>/day,
  - c.  $\log P_{(\text{octane} / \text{water})} = 1 - 3.5$ ,
  - d. aqueous solubility > 100 µg / ml,
  - e. daily dose  $\leq 10$  mg / day,
2. maintain optimum drug saturation, keeping in mind that the thermodynamic activity is the key driving force instead of concentration,
3. drug flux can be optimized by formulation design,
4. use of vehicles/solvents with good partition coefficients can increase dose delivery; and
5. Drug molecules will continue to move after penetrating the skin.

The most difficult part is to create a TDD patch that will lead to the desired dose delivery. In addition to Williams' rules, most research work involves an empirical trial and error process to identify the polymeric matrix that will release the drug at the desired therapeutic levels. Drug delivery is determined by the permeation rate in the patch; the critical factor in the permeation rate is the diffusion coefficient of the actives through the TDD matrix.

## CHAPTER 3

### DIFFUSION

#### 3.1 Definition

Diffusion is defined as the solute displacement in solids from high concentration to low concentration zones, ending with equal solute distribution. Diffusion can be considered as a process resulting not from a forced action, but more as a result of the random distribution of solute atoms (See Figure 3.1)<sup>(20, 21)</sup>.

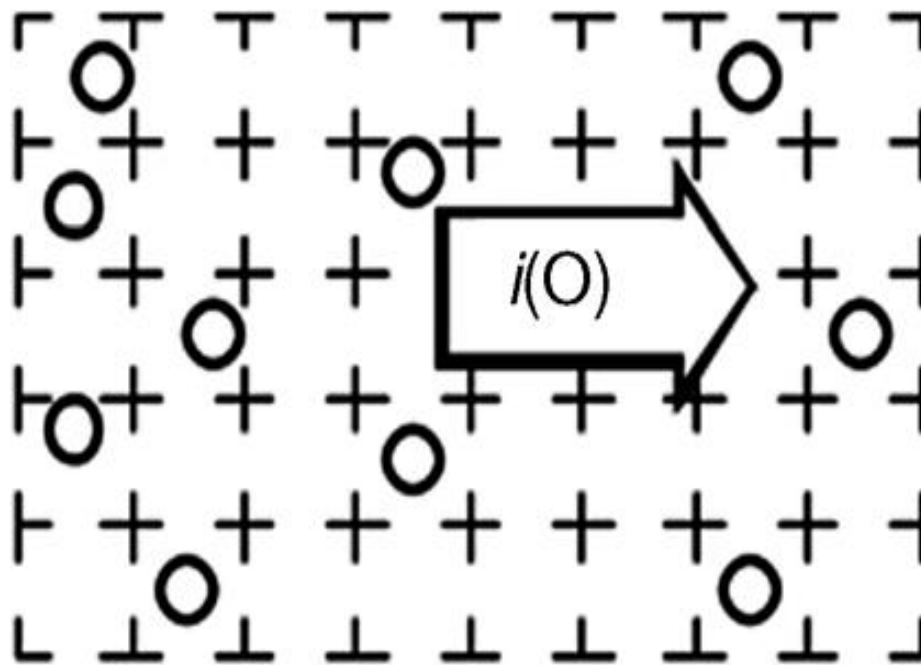


**Figure 3.1** Fick's self-diffusion

Source: Karger, J., Ruthven, D. M. and Theodorou, D. N., Diffusion in Nanoporous Materials, [http://www.wiley-vch.de/books/sample/352731024X\\_c01.pdf](http://www.wiley-vch.de/books/sample/352731024X_c01.pdf). Accessed on December 5, 2014.

This process was originally evaluated by Fick<sup>(22)</sup>, who described this phenomenon with equation (3.1):



$$\frac{\partial C}{\partial t} = D \frac{\partial^2 C}{\partial x^2} \quad (3.1)$$

where,

C = active concentration,

t = time,

x = traveling distance,

and D = diffusion coefficient.

Equation (3.1) is better known as Fick's Second Law, which takes into account the non-uniformity solubility of the diffusing solute into the matrix within which it is encased.

There are presently two models that describe the diffusion in solids and in polymeric matrices in particular. The molecular model analyzes how the diffusant or solute moves along the polymer chains with the correspondent molecular interactions or forces. The free volume model approximates the relationship between the diffusion coefficient and the free volume that is present in the polymeric matrix.

### **3.2 Definition of Molecular Models**

Molecular models assume that small voids or oscillating "cavities" are within the polymeric matrix. When the matrix is in equilibrium, these "cavities" could be defined as definite distribution centers inside the matrix. Solute diffusion is highly dependent on the number of available cavities that are large enough to allow the solute molecular movement throughout the matrix. A solute molecule could be in a cavity that is large enough for it to move (jumps) into the nearest available cavity as soon as it gathers the minimum amount of energy. This is shown in Figures 3.2 and 3.3.

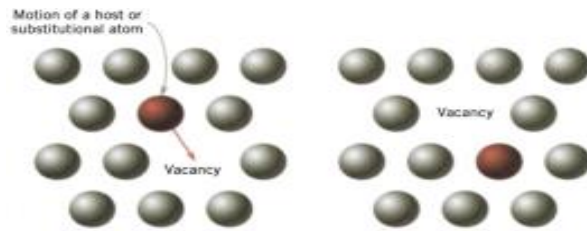


**Figure 3.2** Molecular mobility through voids / oscillating cavities

Source: Callister, W.D., Fundamentals of Materials Science and Engineering, 5th Edition, p. 149, NY, 2001

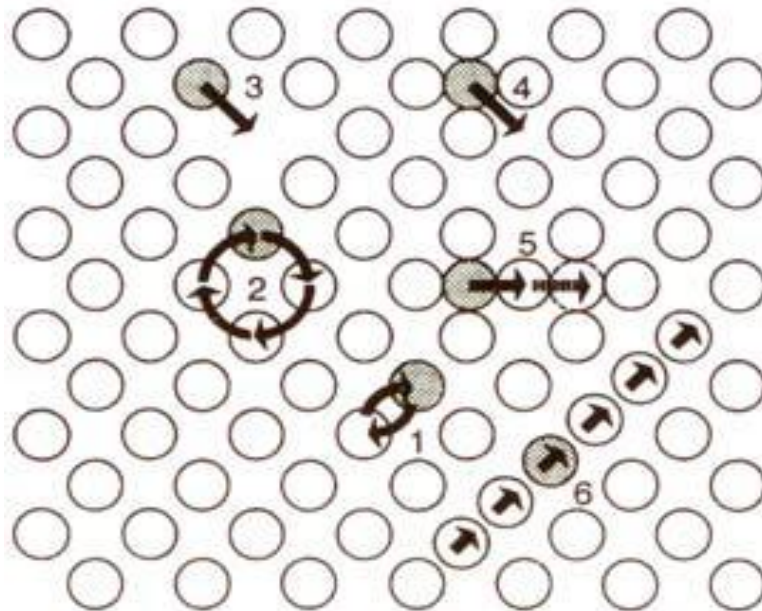


**Figure 3.3** Diffusion motion

Source: <http://amisca.chem.itb.ac.id/download/Fundamentals%20of%20Materials%20Science%20and%20Engineering%205th%20ed.pdf>. Accessed on December 6, 2014.

In Figure 3.3, the numbers represent the following:

1. Neighboring atoms exchange sites,
2. Ring mechanism,
3. Vacancy mechanism,
4. Direct interstitial mechanism, and
5. Indirect interstitial mechanism.

The minimum amount of energy is easily experimentally demonstrated by the modified Arrhenius seen for diffusion coefficients and shown in equation (3.2) <sup>(22)</sup> and Figure 3.4

$$D = D_0 \exp(-E_a/RT) \quad (3.2)$$

where,

$E_a$  = apparent activation energy of diffusion,

$D_0$  = a pre-exponential constant,

$R$  = the gas constant, and

$T$  = the absolute temperature.

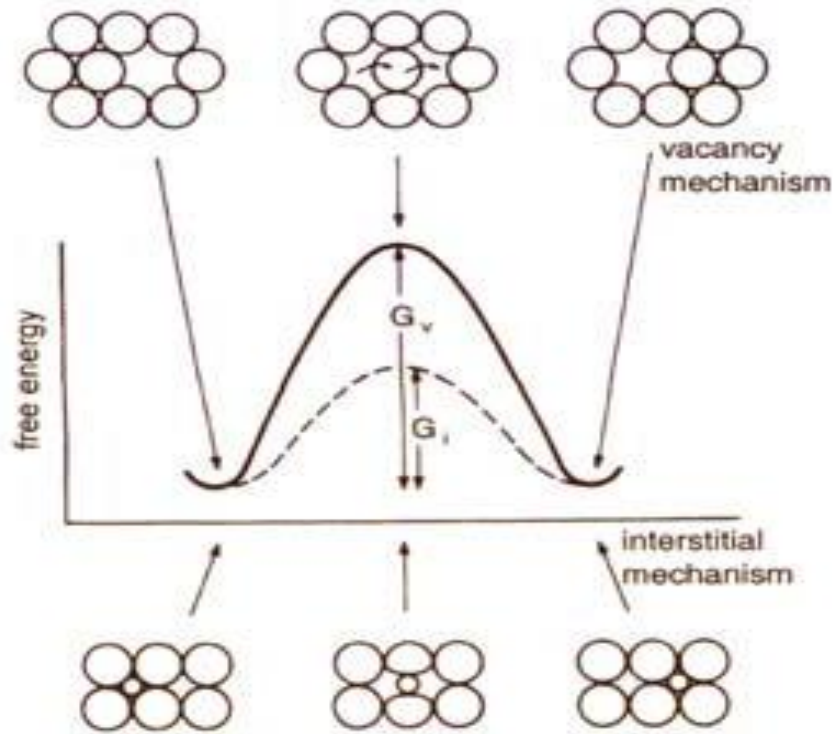


**Figure 3.4** Mechanism steps and activation energies

Source: Torres, L.L., Diffusion in Materials (PPT), <http://www.slideshare.net/luisobaya/diffusion-in-materials>. Accessed on December 6, 2014.

Meares <sup>(23, 24)</sup> suggested a molecular model for polymeric matrices in which the activation energy of diffusion was directly related to the square of the solute/diffusant diameter. Moreover, the initial diffusion step was related to the energy required to create a cylindrical path within the polymeric chains where the solute was able to move or jump from one position to the next. This was defined as:

$$E_d = (\pi/4) \sigma^2 N_A \lambda \text{ (CED)} \quad (3.3)$$

where,

$E_d$  is the activation energy of diffusion,

$\sigma$  is the collision diameter of the penetrant,

$N_A$  is the Avogadro number,

$\lambda$  is the diffusional jump length,

and CED is the cohesive energy density of the polymer.

It is relevant to indicate that Meares assumes the following:

1. The solute is solely spherical and that no other shapes are possible;
2. No polymer-solute interactions exist.

Brandt<sup>(25)</sup> suggested a different approach that employed a more succinct definition of the matrix structure to estimate  $E_d$ . The approximation is based on the assumption that diffusion is active when two or more polymer chains are symmetrically bent, thus, enabling direct routing for the solute. In turn, this promotes a synergistic process among neighboring polymer chains, which is deemed essential for solutes that unable movement within the existing inter-chain spaces.

The activation energy,  $E_d$ , is defined as the sum of an intermolecular contribution,  $E_i$ , and an intermolecular contribution,  $E_b$ .

$$E_d = E_b + E_i \quad (3.4)$$

$E_i$  is the result from the interaction between the internal resistance and the chain bending and  $E_b$  is defined as the repulsion of the bent chain segment due to its neighboring chains.

When applying this model to experimental results, it was found that  $E_d$  had a nonlinear dependence on the solute collision square diameter.

This is contradictory to the model of Meares, which shows a linear dependence of  $E_d$  on  $\sigma^2$ . Brandt's model also suggests that the activation energy is dependent on the molecular size. The smaller the molecule, the less relevant is the activation energy that is required to

diffuse throughout the existing free volume within the polymer chains. Brandt found that  $E_d$  was not proportional to the cohesive energy density of the polymer. The diffusion process could then be described in terms of polymer chain energy displacements where the matrix and solute interactions could be considered non-significant.

A different approach was proposed by DiBenedetto and Paul<sup>(26)</sup> in which the nonlinear interaction of  $E_d$  with  $\sigma^2$  was better predicted. Yet, it ignores any interactions that can exist between the matrix and the solute. In their approximation, the polymeric matrix can be assumed as a homogeneous continuous entity that consists of Avogadro's number of "principal components." A principal component is defined as a polymer repeat unit that comprises a cylindrically symmetric potential field formed by its four nearest-neighbors.

The activation energy is defined as the potential energy difference between the "normal" state in which the four neighboring components are at equilibrium positions, and the "activated" state in which they are separated by a cylindrical void. This implies that the activation energy can be described as the potential energy difference in the partial breaking of the bonds between the four principal components. This concept is very similar to the cohesive energy density as described by Meares.

A solute molecule is assumed to exist within a void or cell created by the four parallel polymer components. Coordinated rotations and vibrations of these components can result in another cylindrical void adjacent to the solute molecule. This is followed by the displacement of the solute molecule into the nearest newly created cylindrical void.

The energy required to compress the surrounding polymer is ignored. This approach does not take into account the complexity of the matrix and the molecular shape and size of the active. Thus, the free volume concept must be considered.

### 3.3 Free Volume

Free volume can be simply defined as the difference between the specific volume and the calculated molecular volume

$$V_f = V_s - V_{cm} \quad (3.5)$$

A graphical representation of the Free Volume concept is shown in Figure 3.5.

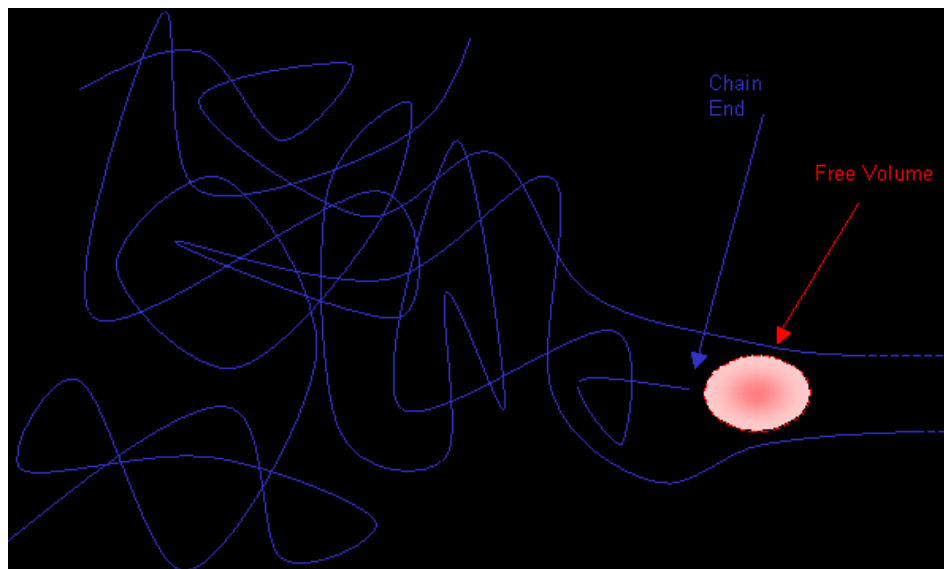


**Figure 3.5** Free Volume Model

Source: Free Volume, Cambridge University, <http://www.doitpoms.ac.uk/tlplib/glass-transition/free-volume.php>. Accessed on December 2, 2014.

Eyring<sup>(27)</sup> suggested that the molecular motion in any polymeric matrix is proportional to the presence of molecular cavities that are creating voids within the structure. In other words, when the solute molecule travels to a void, the void will trade places with the solute molecule as shown in Figure 3.6.

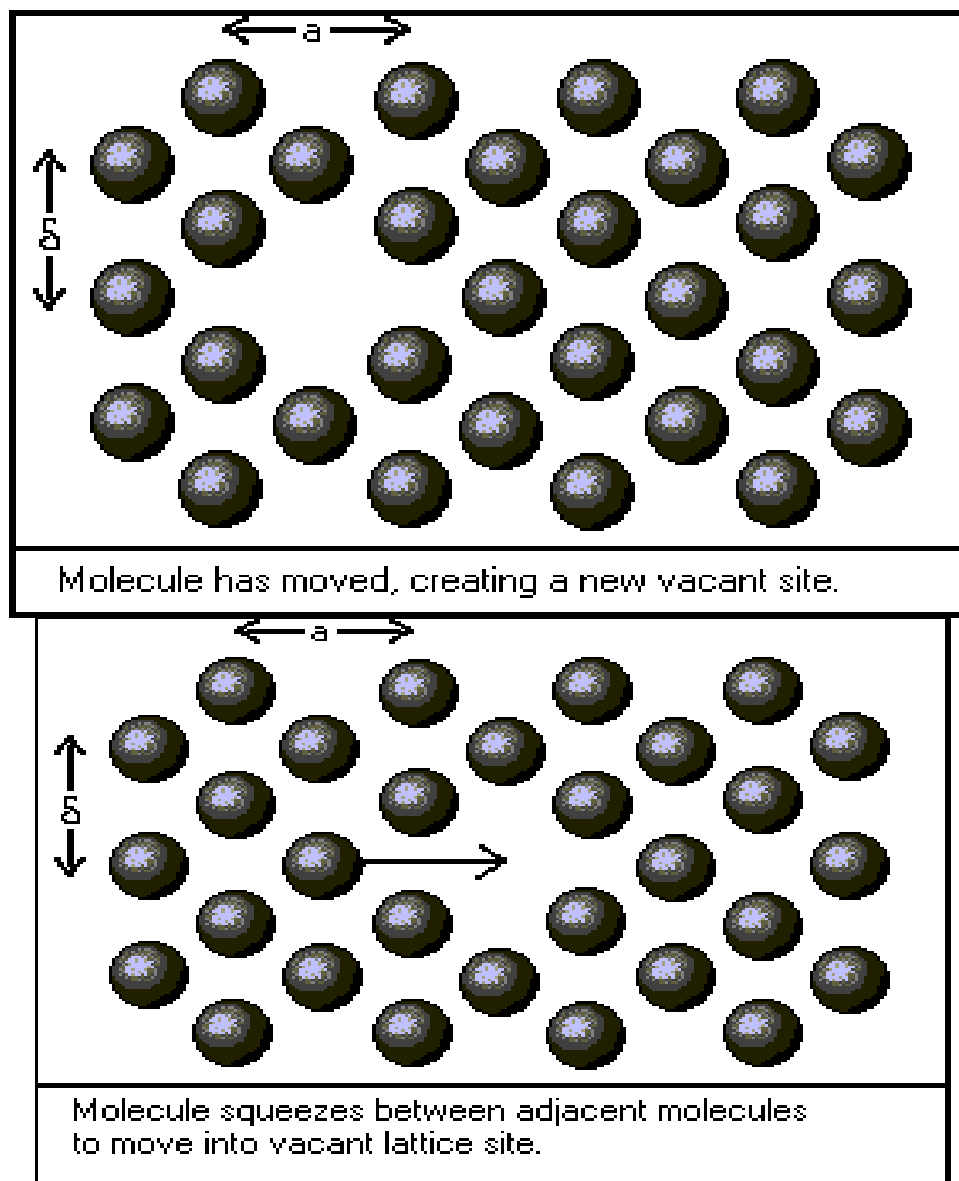


**Figure 3.6** Eyring Molecular Model

Source: <http://www.owl.net.rice.edu/~ceng402/proj02/beckys/>. Retrieved on December 16, 2014

For a solute molecule to move from one position to the next, a critical void volume must be in place before any changes or displacement can take place. This implies that solute motion will not take place if these voids are not present. These voids as a whole could be defined as the free volume. A 3-D representation of free volume is shown in Figure 3.7.



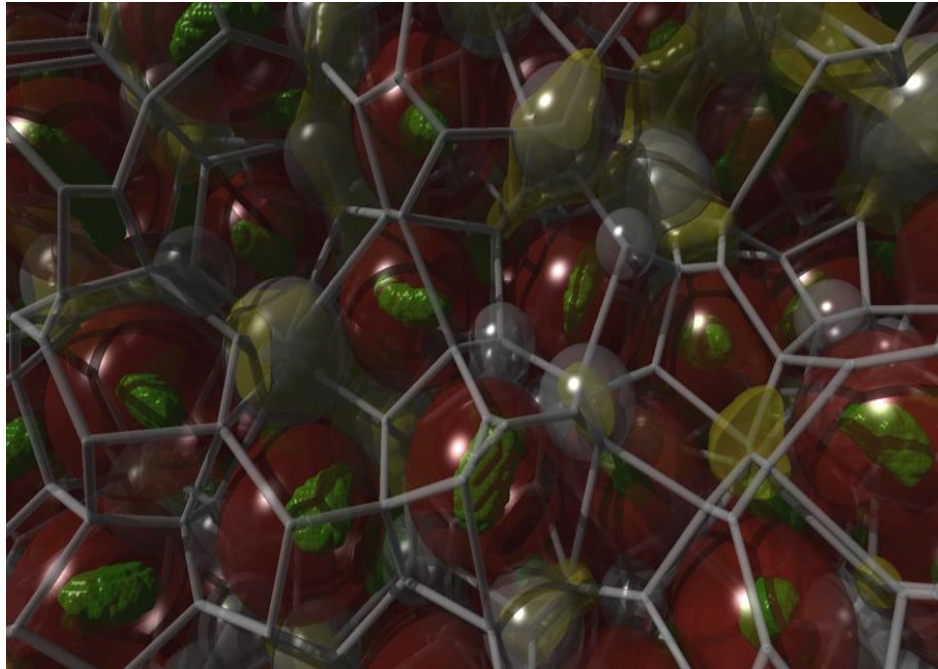


**Figure 3.7** Free volume 3D representation

Source: <https://www.xsede.org/documents/234989/378230/XSEDE12-willmore.pdf>. Retrieved on December 16, 2014.

In general terms, the free volume of a polymeric system can be stated as the volume of the one at a particular temperature of interest less the one of the same system that would exist at absolute zero.

Therefore, free volume can be seen as creating holes where solutes can diffuse and pass through. Free volume can be seen as the overall contribution of all the entities present in the matrix, solute and voids. Figure 3.8 shows the volume disposition in a rubbery matrix as a function of temperature.

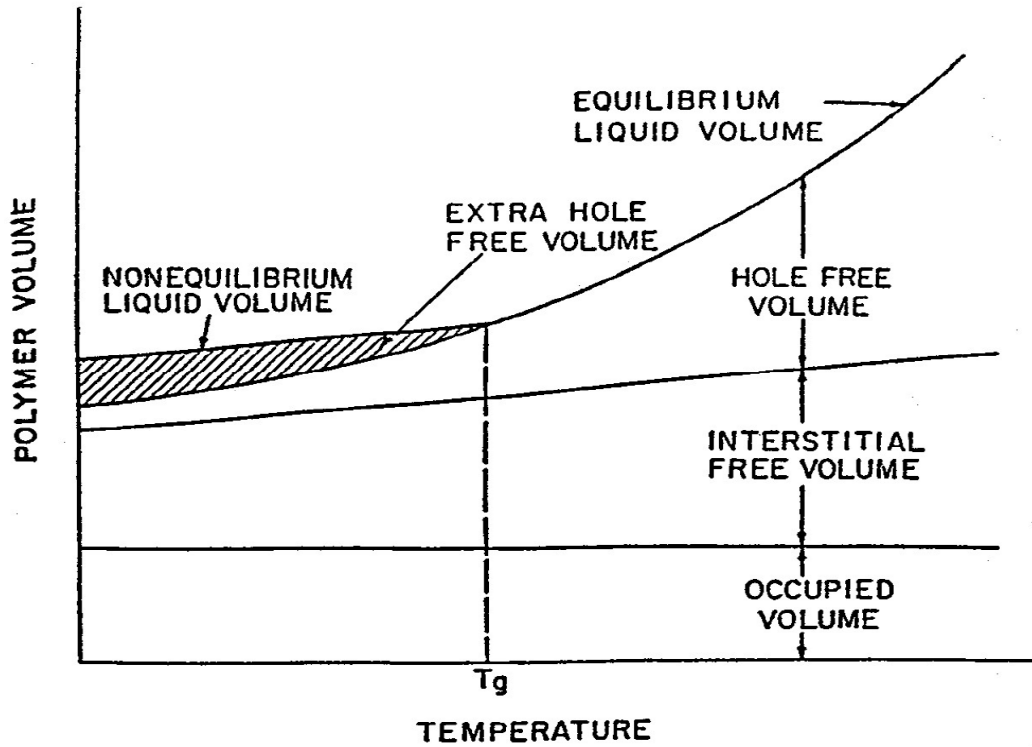


**Figure 3.8** Schematic representation of volume disposition in a rubbery matrix as a function of temperature

Source: Fig. 2 in J. L. Duda and J. M. and Zielinski, Ch. 3 in "Diffusion in Polymers", P. Neogi, ed., M. Dekker, N. Y., 1996. <https://www.uakron.edu/dotAsset/483661.pdf>. Accessed on December 2, 2014.

### 3.4 Free Volume Models

The difference between molecular and free volume (FV) models is that diffusion is not considered as a thermal dependent process in FV models. FV models assume diffusion as a random renormalization of free volume voids within the polymeric matrix.

This assumption was first suggested by Cohen and Turnbull.<sup>(27)</sup> They originally thought that this approach was only suited for liquids that could be visualized as the uniform aggregation of hard spheres. From the Cohen and Turnbull viewpoint, the hard sphere molecules would compose of an ideal liquid that exists in empty spaces created by the nearest neighbors. In other words, the total volume can be seen as two volumetric compartments, one occupied and the other free. Although the sphere does not have the ability to migrate within its space unless a thermal natural fluctuation would create a gap (vacancy) next to its enclosure, this gap must be sufficiently large enough that it would enable the displacement of a spherical molecular entity. The diffusion or molecular movement is deemed successful when the empty space left behind by a molecule is then filled by the adjacent molecule. Instead of creating gaps by the physical displacement of the nearest neighbors, this is a mechanical and not translational motion that does not need a set energy level to surmount an activation energy barrier. This is indicated in the activation energy approach of Pace and Daytner<sup>(28)</sup>. Molecular migration is solely based on the constant rearrangement of free volume entities inside the liquid. The mathematical description of the free volume entities could be better described as a probability function in which the diffusion coefficient can be assumed to be proportional to the probability of locating a gap of volume  $V^*$  or larger, and could be written as:

$$D = A \exp(\gamma V^*/V) \quad (3.6)$$

where the molecular self-diffusion coefficient,  $V^*$ , is the lowest gap size volume that a molecule can migrate,  $V$  is the specific volume and  $\gamma$  is a numerical factor between 0.5 and 1.0, to account for the overlap between free volume entities such as the free space (gap) shared by a neighboring molecule.  $A$  is defined as the proportionality constant that is associated with the gas kinetic energy. This clearly indicates that the molecular self-diffusion coefficient is an exponential function of the ratios of the molecular size of the diffusing solute to the free volume per molecule of the matrix. Considering the self-diffusion of a solute in a binary type matrix, equation (3.6) can be rewritten as follows:

$$D_1 = D_{01} \exp[-\gamma V_1^*/V_{FH}] \quad (3.7)$$

$V_1^*$  = critical molar free volume needed for any displaced singularity of species 1 to move,

$V_{FH}$  = free volume per mole of all individual moving solute units in the matrix,  
and  $D_{01}$  = temperature – independent constant.

While Cohen and Turnbull defined the moving solute unit as a single hard-sphere molecule that undergoes diffusion, this is not the case when dealing with polymeric systems where the matrix consists of a macromolecular mixture. Yet, an individual solute molecule can be made of several diffusing units that are united by covalent bonds. Free volume gaps that can easily accommodate whole polymeric entities will not readily form.

Rather, solute migration is seen as a series of continuous jumps of small parts along the matrix as shown in Figure 3.9.

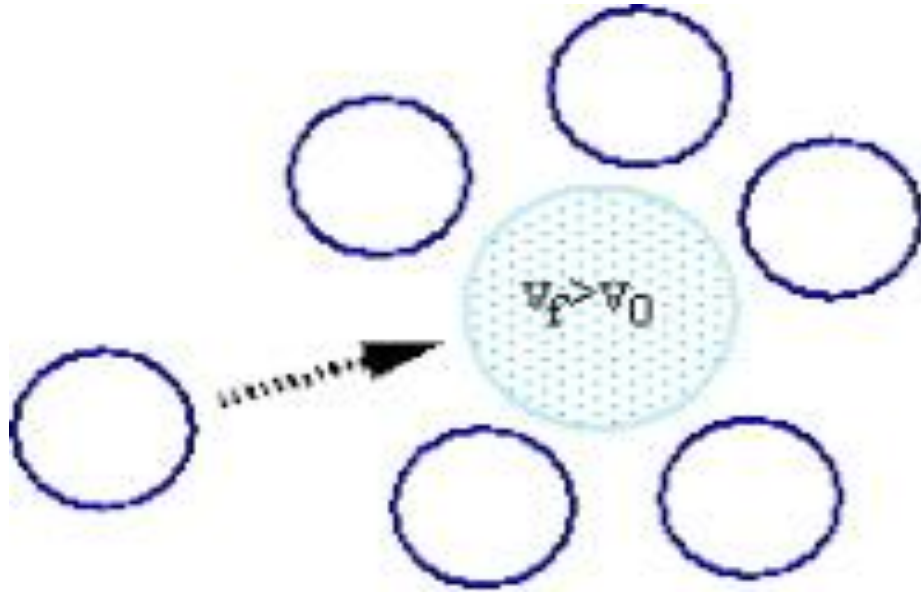


**Figure 3.9** Cohen and Turnbull graphical representation

Source: [http://www.scl.kyoto-u.ac.jp/~kanaya2/kanaya\\_lab~2009/e-g-j.htm](http://www.scl.kyoto-u.ac.jp/~kanaya2/kanaya_lab~2009/e-g-j.htm). Accessed on December 4, 2014

This could be further convoluted when low molecular weight solutes, having sufficient size and maneuverability, are able to move in a disposition similar to what is seen in polymeric systems that consist of the use of several components of the molecular chain<sup>(29,30)</sup>. Generalizing the Cohen and Turnbull theory to depict the motion in binary systems, where the molecular shape and size of the solute must be included, Vrentas and Duda<sup>(31)</sup> introduced the following relationships:

$$V_{FH} = \frac{V_{FH}}{\frac{\text{moles of diffusing units}}{g}} = \frac{V_{FH}}{\left( \frac{w_1}{M_{1j}} + \frac{w_2}{M_{2j}} \right)} \quad (3.8)$$

$V_{FH}$  = specific gap free volume of a solute with a weight fraction  $\omega_i$  of species  $i$ ,

$M_{ij}$  = molecular weight diffusing units ( $i = 1$  or  $2$ ).

Vrentas and Duda<sup>18</sup> further simplify this as:

$$D_{\infty} = D_0 \exp \left[ -\frac{E}{RT} \right] \exp \left[ -\frac{\zeta V}{V} \right] \quad (3.9)$$

where,

$D_{\infty}$  is the infinite dilution diffusion coefficient,

$D_0$  is a constant pre-exponential factor,

$E^*$  is the energy that a molecule must possess to overcome attractive forces from the surrounding neighboring entities,

$V^*$  is the specific free volume space of polymer needed for molecular jump,

$V_f$  is the space free volume provided by the polymer for solute to diffuse,

and  $\xi$  is the ratio of the solvent critical molar volume jumping unit to the polymer jumping unit.

Then, combining equations (3.7), (3.8), and (3.9), an expression is derived for the diffusion of a solute in a polymeric matrix that can be expressed as:

$$D_s = D_0 \exp \left\{ -\frac{E}{RT} \right\} \exp \left[ -\frac{\gamma(W_s V_s + W_p \xi V_p)}{V_{FH}} \right] \quad (3.10)$$

where,

$W_s$  is the weight percent of the solute – drug active present in the matrix,

$V_s$  is the volume of the solute or drug active in this case,

$W_p$  is the weight percent of the polymer – matrix component,

$V_p$  is the volume of the polymer matrix where the active drug is embedded,

$\xi$  is the ratio of the solvent critical molar volume jumping unit to the polymer jumping unit,

$V_{FH}$  is the free volume,

$E$  is the energy that a molecule must possess to overcome attractive

forces from the surrounding neighboring entities,

R is the Boltzmann's constant,

and T is the temperature at which the diffusion is taking place.

If  $\bar{V}_{FH}$  is defined as the specific hole free volume in a block copolymer and solute mixture, then, the available free volume for molecular diffusion/transport could be written as:

$$\bar{V}_{FH} = \frac{\hat{V}_{FH}}{\omega_1/M_{1j} + \omega_2 (W_{2a}/M_{2ja} + W_{2b}/M_{2jb})} \quad (3.11)$$

where,

$\omega_i$  is the weight fraction of component i ( $i=1$  or  $2$ ),

$W_{2a}$  and  $W_{2b}$  are the weight fractions of the blocks A and B within the copolymer,

$M_{1j}$ ,  $M_{2ja}$  and  $M_{2jb}$  are the molecular weights of the jumping unit for the solute, copolymers A and B respectively.

$$\xi_{12a} = M_{1j} \bar{V}_1^* / M_{2ja} \bar{V}_{2a}^* \quad (3.12)$$

$$\xi_{12b} = M_{1j} \bar{V}_1^* / M_{2jb} \bar{V}_{2b}^* \quad (3.13)$$

where,

$\xi_{ijk}$  is the ratio of solvent to polymer jumping units,

$M_{ij}$  is the molecular weight of the solute,

$M_{ijk}$  is the molecular weight of the block copolymer,

$V_i^*$  is the specific volume of the solute,

and  $V_{ik}^*$  is the specific volume of block k ( $k = a$  or  $b$ ) in the copolymer at 0 K.

Inserting equations (3.11), (3.12), and (3.13) into equation (3.10) gives,

$$D_1 = D_o \exp\left(-\frac{E}{RT}\right) \exp\left(-\frac{\gamma[W_1 \bar{V}_1 + W_2 (W_{2a} \xi_{12a} \bar{V}_{2a} + W_{2b} \xi_{12b} \bar{V}_{2b})]}{\bar{V}_{FH}}\right) \quad (3.14)$$

where,  $V_{2k}$  (k is for either a or b) is defined as the specific volume of block k in the copolymer at 0 K. In the event that the polymeric system is a homo-polymer, then  $W_{2a} = 0$  and  $W_{2b} = 1$  and equation (3.14) is reduced to the original system for solute self-diffusion in a homo-polymer in equation (3.10).

### 3.5 Effect of various physical effects on the Diffusion Coefficient

#### 3.5.1. Effect of Molecular Radius

Several researchers have shown the influence of molecular size on the diffusion coefficient. This was originally shown by Einstein and Stokes. They assumed an ideal solution, in which there is an inverse proportionality between diffusion and molecular size defined by the solute radius:

$$D_0 = \frac{k_B T}{6\pi\mu R_0} \quad (3.15)$$

where,

$K_B$  is the Boltzmann's constant,

$\mu$  is the solute viscosity,

and  $R_0$  is the solute molecular radius.

$R_0$  can be estimated from the volume  $V$ , which is defined as:

$$V = (4/3)\pi R_0^3 \quad (3.16)$$

and

$$(4/3)\pi R_0^3 = m/\rho \quad (3.17)$$



Defining  $m$  as solute mass and  $\rho$  as solute density,

$$M = M_w / N_A \quad (3.18)$$

where,

$M_w$  is the solute molecular weight,

and  $N_A$  is Avogadro number,

Substituting (3.18) in (3.16),

$$(4/3\pi R_0^3) = M_w/N_A\rho \quad (3.19)$$

Then,  $R_0$  can be defined as:

$$R_0 = \left( \frac{3M_w}{4\pi N_A \rho} \right)^{1/3} \quad (3.20)$$

$R_0$  is also known as hydrodynamic radius,  $R_h$ .  $R_g$  is defined as the mass weighted average distance from the core of a molecule to each mass element in the molecule. The radius of gyration of a molecule is the radius of a thin ring that has the same mass and moment of inertia as the molecule when centered at the same axis. Figure 3.10 shows the comparison between radius of rotation, hydrodynamic radius, radius of gyration and mass radius.

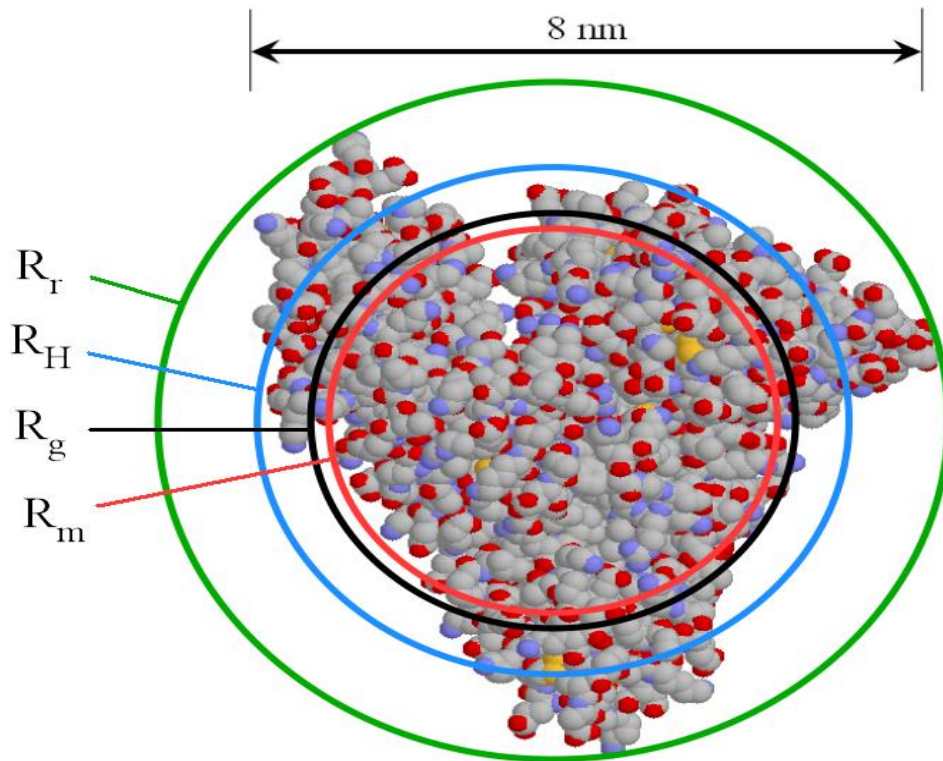


**Figure 3.10** Comparison between radius of rotation, hydrodynamic radius, radius of gyration, and mass radius

Source: [http://www.imbb.forth.gr/people/aeconomou/pdf/hydrodynamic\\_radius.pdf](http://www.imbb.forth.gr/people/aeconomou/pdf/hydrodynamic_radius.pdf). Retrieved on December 2, 2014.

There are different relationships for spheres, rods, and coils that can be expressed as <sup>(32)</sup>:

$$R_{\text{sphere}} = ksD / 2 \quad (3.21)$$

$$R_{\text{rod}} = ksL / 2 \quad (3.22)$$

$$R_{\text{coil}} = (k^2s^2r^2) / 2 \quad (3.23)$$

where,

D = diameter of sphere,

L = length of rod,

k and s = constants,

r = root mean square of the distance between the ends of the random coil.<sup>(32)</sup>

The radius of gyration ( $R_g$ ) is usually calculated from static scattering measurements and the hydrodynamic radius ( $R_h$ ) also known as the Einstein-Stokes radius or equivalent spherical radius. It can be determined by dynamic light scattering or other diffusion measurements.

For instance, a solid sphere can yield a value of:

$$R_g / R_h = \sqrt{3/5} \approx 0.77 \quad (3.24)$$

$$R_g = 0.77 R_h \quad (3.25)$$

$$D_{R_h} / D_{R_g} = (1/R_h) / (1/R_g) \quad (3.26)$$

$$D_{R_h} / D_{R_g} = R_g/R_h \quad (3.27)$$

$$D_{R_g} = D_{R_h} / 0.77 \quad (3.28) \text{ In}$$

this case, the  $R_g / R_h$  ratio could be estimated as:

$$R_g / R_h \sim 1.22 \ln (L/D) \quad (3.29)$$

where,  $L/D$  is the aspect ratio of the longitudinal and latitude axes of the molecule and this can be achieved by a slender rod geometry (Appendix E) and,

$$D_{R_g} = D_{R_h} / 1.22 \ln (L/D) \quad (3.30)$$

Tande et al noted that  $R_g$  and  $R_h$  can be determined in larger molecules as a power law relationship to the molecular weight. This is not the case with molecules having lower molecular weights.<sup>(32)</sup>

### 3.5.2 Effect of Molecular Shape

However, from 3D molecular modeling, not all molecules will have spherical shapes as seen for the nicotine molecule (Figure 3.11).



**Figure 3.3** 3D nicotine model

Source: <http://commons.wikimedia.org/wiki/File:Nicotine-3D-vdW.png>. Retrieved on November 23, 2014.

In the original work of Vrentas and Dudas,  $\xi$  is defined as the ratio of the molar volume of a solute jumping unit to the molar volume jumping unit. This is based on the assumption that the solute will jump in single units and flexible long chain solutes would exhibit segment-wise movement. A method for estimating  $\xi$  was developed by Vrentas et al. Moreover, this approach also assumes that the average hole free volumes within the polymer and solute jumping units would be different. Nobrega et al. suggested that, for solutes that can jump as single units,  $\xi$  could be defined as:

$$\xi = \frac{\xi_L}{1 + \xi_L \left(1 - \frac{\bar{A}}{\bar{B}}\right)} \quad (3.31)$$

### 3.6 Theoretical Background

The known solution for the equation of the diffusion coefficient, for a planar surface, a TDDP in this case, when the diffusion coefficient is constant, was shown by Crank<sup>(20, 21)</sup> to be:

$$C = \frac{M}{2(\pi Dt)^{1/2}} \exp\left(-\frac{x^2}{4Dt}\right) \quad (3.32)$$

In most cases, TDDP systems are designed to deliver, under non-steady state, where the following boundary conditions must be in place. Therefore, equation (3.32) can be further simplified as:

$$\frac{M_t}{M_\infty} = \frac{4}{l} \left(\frac{D}{\pi}\right)^{\frac{1}{2}} \frac{1}{t^{\frac{1}{2}}} \quad (4) \text{ when } \frac{M_t}{M_\infty} \leq 0.5 \quad (3.33)$$

where,  $M_t$  is the active released from the patch at time  $t$ ,  $M_\infty$  is the initial concentration of the active in the patch,  $D$  is the diffusion coefficient, and  $t$  is the time of release.

Diffusion phenomena in TDDS must be modeled as small molecule mobility in the macromolecular matrix. This along with the backbone chemistry are perhaps the main influential factors. Yet, in these types of systems, the mobility is considerably influenced by temperature and concentration. These conditions are mostly pronounced near the glass transition temperature ( $T_g$ ) where it has been shown that an increase of 1% of the solvent weight fraction in the matrix can effectively increase the diffusion ( $D$ ) by three orders of magnitude.

Therefore, significant experimentation is the key to obtaining satisfactory approximation, as well as optimization of results for this particular situation that is actually governed by molecular transport. However, this requires significant trial and error process in determining the right matrix that will provide the release rate of the solute into the skin to achieve the desired therapeutic effect.

This approach does not take into account the complexity of the matrix and the molecular shape and size of the active; thus, free volume concept must be considered in the polymer in the TDDS case. From this, it could then be assumed that free volume is the key factor that controls the diffusion of solutes through the polymeric matrix.

## CHAPTER 4

### EXPERIMENTAL RESULTS

#### 4.1 Experimental Methods

Nicotine patches were used for this evaluation for two key reasons:

1. Nicotine patches have been one of the most predominant and successful technologies used to control smoking cessation.
2. Nicotine patches are the most commercially sold TDD patches in the market.

The first step was to generate a nicotine ultraviolet absorption chart by means of setting a master curve. This master curve was determined from ultraviolet readings of different nicotine concentrations in a normal saline solution (0.90 % w/v of sodium chloride or about 300 mOsm/L or 9.0 g per liter).<sup>(33)</sup> The reason for using such a system is because the osmolarity of normal saline is a close approximation to the osmolarity of NaCl in blood. Different nicotine concentration solutions were made and ultraviolet absorption measurements were performed using a Genesys VI ultraviolet spectrophotometer.

An ultraviolet absorption versus nicotine concentration chart was generated in which the plots were fitted by means of regression, thus, resulting in a master curve having a linear characteristic with  $R^2 = 0.9778$ , which was deemed acceptable to use as a master calibration curve. This is shown in Figure 4.1. The nicotine was purchased as a 99% active pharmaceutical ingredient from Aceto Chemical.

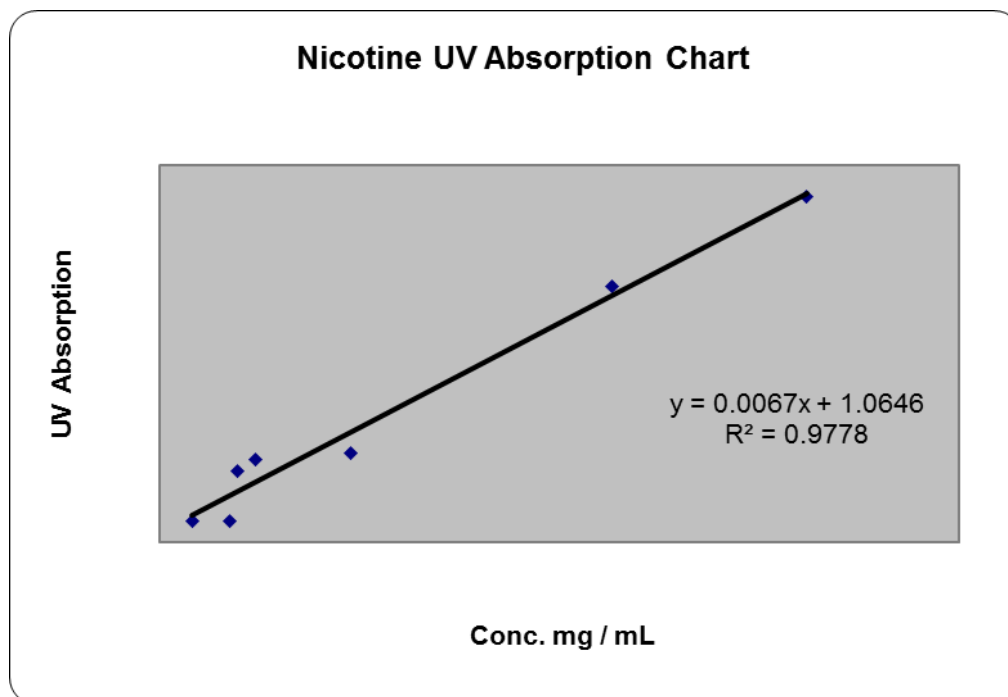


**Figure 4.1** Nicotine ultraviolet absorption chart

The next step was to determine the release from the nicotine patches. Samples were purchased from commercially available nicotine patches sold over the counter in the US. These patches consist of three layers: (a). backing to provide mechanical support as well as protection to the release layer from environmental conditions, (b). a nicotine reservoir containing a layer that includes the adhesive, and (c). the PET disposable piece that is removed when the patch is ready for positioning into the selected area (Figure 4.2)





**Figure 4.2** Diagram of a typical commercial nicotine patch <sup>[20]</sup>

Source: TRANSDERMAL A NOVEL DRUG DELIVERY SYSTEM  
<http://www.pharmatutor.org/articles/transdermal-novel-drug-delivery-system?page=0,1>. Retrieved on December 5, 2014.

The patch used in these experiments is the Nicoderm CQ, 7 mg daily dosage patch. The physical measurements of the patch is 1 inch square with a thickness of 0.229 cm. where the actual thickness of the diffusion layer is estimated to be approximately 0.0113 cm.

Patches from the same lot were assembled on top of vertical static Franz cells (Figure 4.3) and were placed in direct contact with the saline solution. These patches were secured in place by clamping the top onto the cell body as shown in Figure 4.3.

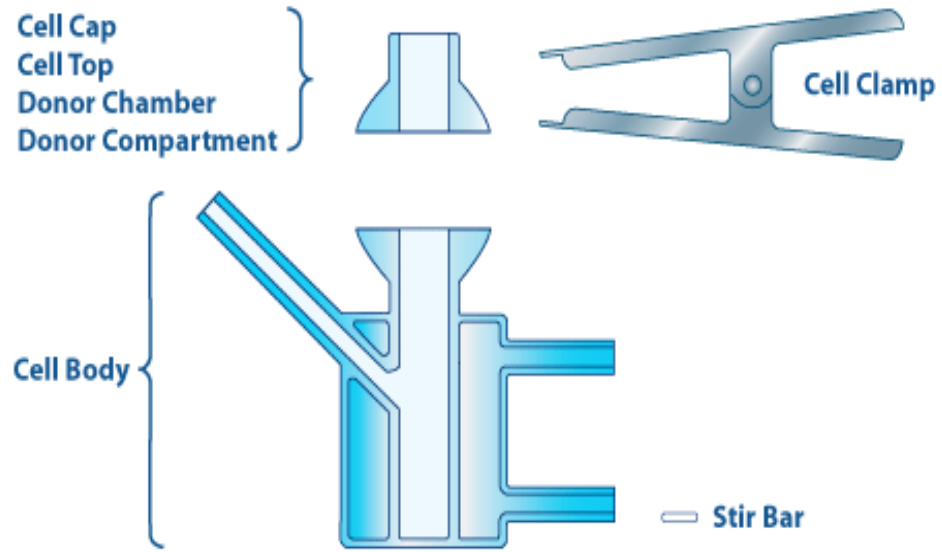


**Figure 4.3** Franz static cell components <sup>(34)</sup>

Source: <http://www.permegear.com/franzcellcomponents.gif>. Accessed on December 7, 2014.

The nicotine patch was placed between the top of the cell and the body of the cell (Figure 4.4) in contact with a normal saline solution which is kept at a constant temperature of  $37^{\circ}\text{C} \pm 3^{\circ}\text{C}$ .



**Figure 4.4** Fully assembled typical Franz static cell

Source: <http://www.permegear.com/6G01000520.jpg>. Accessed on December 7, 2014.

Measurements of the samples were taken at 1 hour intervals for the first 8 hours and then the last measurement after 24 hours. Then the amount released was estimated as a function of the measured concentration by ultraviolet spectrophotometry and the volume present in the vertical static Franz cell reservoir. This was done in accordance with the FDA SUPAC guidelines<sup>(35)</sup> as well those with Thakker and Chern,<sup>(36)</sup> Siewert, Dressman, Brown, and Shah,<sup>(37)</sup> Raney, Lehman, and Franz,<sup>(38)</sup> Marangon, Bock, and Haltner,<sup>(39)</sup> Lionberger<sup>(40)</sup>, Flynn,<sup>(41)</sup> Hauck, Shah, Shah, and Ueda,<sup>(42)</sup> and Addicks, Flynn, Weiner, and Chiang.<sup>(43)</sup>

Figure 4.5 shows the cumulative amount of nicotine released versus time.

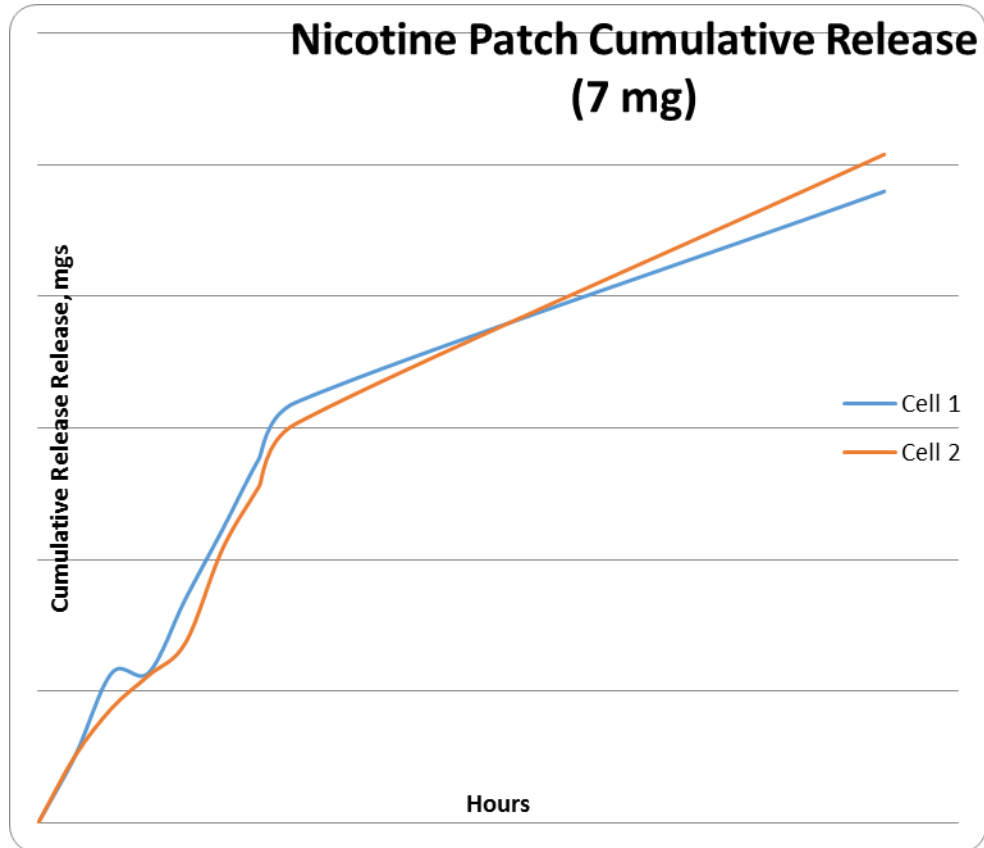


**Figure 4.5** Cumulative nicotine release.

The diffusion constant was estimated according to the methodology shown by Crank<sup>(21)</sup> and Miller, Oehler, and Kunz<sup>(44)</sup> as:

$$D = 1.467 \cdot 10^{-9} \text{ cm}^2/\text{sec}$$

#### 4.2 Theoretical Approach/Calculation of Diffusion Coefficient D

The next part of this section is the theoretical calculation of the diffusion coefficient by using the Duda and Zielinski equation (3.14):

$$D_1 = D_o \exp\left(-\frac{E}{RT}\right) \exp\left(-\frac{\gamma[W_1 \bar{V}_1^2 + W_2 (W_{2a} \xi_{12a} \bar{V}_{2a}^2 + W_{2b} \xi_{12b} \bar{V}_{2b}^2)]}{\bar{V}_{FH}}\right)$$

### 4.3 Estimation of Nicotine Values

$D_0$  was obtained from the Einstein-Stokes equation:

$$D_0 = \frac{k_B T}{6\pi\mu R_0} \quad (4.1)$$

$K_B$  is Boltzmann's constant,

$\mu$  is the solute viscosity,

and  $R_0$  is the solute molecular radius.

$R_0$  can be estimated from the volume  $V$  which is defined as  $(4/3) \pi R_0^3$ ,

$$(4/3\pi) R_0^3 = m/\rho \quad (4.2)$$

Defining  $m$  as  $(M_w / N_A)$  where,  $M_w$  is the molecular weight of nicotine,  $N_A$  is the Avogadro number, and  $\rho$  is the density of nicotine at 37°C, from the literature, the following properties are obtained and summarized in Table 4.1

**Table 4.1** Summary of Nicotine Properties

Property	Value
$\rho_{\text{Nicotine}}$	1.014 grams / cm <sup>3</sup> (45,46)
$M_w$	162 grams / mole (45,46)
$\mu_{\text{Nicotine}}$	2.9037 centipoises or 0.021 grams/cm*sec (45,46)

Rewriting equation (4.2) gives:

$$R_0 = 4.062 \cdot 10^{-8} \text{ cm}$$

Then, inserting the values for  $R_0$ ,  $\mu_{\text{Nicotine}}$  into equation (4.1) gives:

$$D_0 = 2.6685 \cdot 10^{-5} \text{ cm}^2 \text{ sec}^{-1}$$

To determine  $V_{\text{Nic}}$ , the Yamada and Gunn (47) (YG) equation was used to calculate:

$$V_s = V_c (0.29056 - 0.08775\omega) \left(1 - \frac{T}{T_c}\right)^{2/7} \quad (4.3)$$

The YG equation was chosen because it provided the closest value of  $V_s$  for molecules such as nicotine. To estimate the value of  $V_s$ , the critical volume ( $V_c$ ), acentric factor ( $\omega$ ),  $T$ , the temperature and critical temperature ( $T_c$ ) values are needed. Since these values are not available from the experimental data, they must be estimated.

The acentric factor is estimated from the Pitzer thermodynamic approximations<sup>(48-54)</sup>. The values of  $T_c$ ,  $P_c$ , and  $V_c$  for nicotine were required to be calculated using the group contribution method described by Joback<sup>(55, 56)</sup>. The reason for choosing this equation was because of the close approximation found in the estimation of pyridine cyclical structures such as nicotine as seen in Figure 4.6.

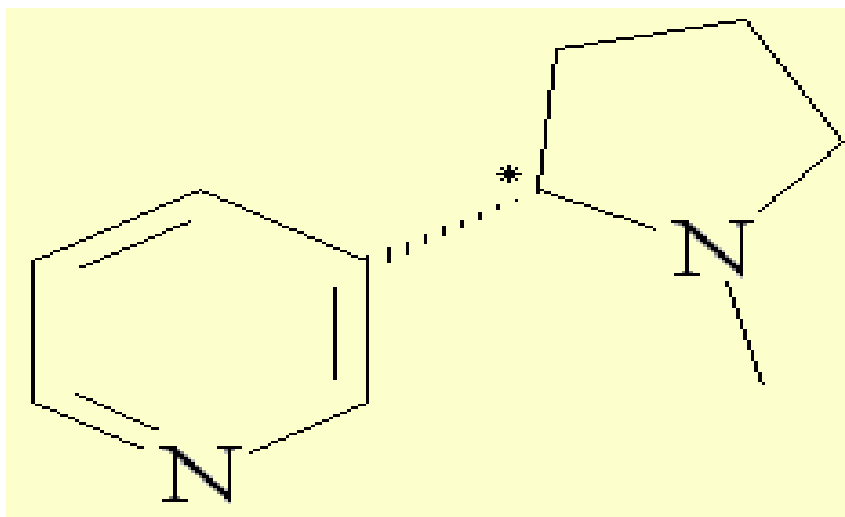


**Figure 4.6** Nicotine molecular structure

Source: <http://en.wikipedia.org/wiki/Nicotine>. Accessed on December 6, 2014

$$T_c = T_b [0.584 - 0.965 \sum G_i - (\sum G_i)^2]^{-1} \quad (4.4)$$

$$P_c = [0.113 + 0.0032 * N_A - \sum G_1]^2 \quad (4.5)$$

$$V_c = 17.5 + \sum G_1 \quad (4.6)$$

To obtain the value of  $T_c$  for nicotine, the boiling temperature was required and its experimental value was found to be 247°C or 520.15 K.<sup>[33]</sup> Table 3.2 presents a summary of the critical properties of nicotine found by using equations (4.4), (4.5), and (4.6).

**Table 4.2** Summary of Critical Properties of Nicotine

Property	Value
$T_c$	749.016 K
$P_c$	22.6365 atm
$V_c$	463.5 cm <sup>3</sup> /mole

The accentric factor for nicotine was found to be:

$$W_{pr}(\text{nicotine}) = 0.14316 \quad (4.7)$$

Using the YG equation, the values of  $V_s$  for nicotine, at 37°C (310.15 K) and 0 K (-273.15°C), were calculated and the results are summarized in Table 4.3.

**Table 4.3** Summary of Volumes of Nicotine @ 310 and 0 K

Temperature	$V_s$ (cm <sup>3</sup> /mole)	$V_s$ (cm <sup>3</sup> /gram)
310.15 °K (37 K)	154.606	0.954
0 K	94.002	0.580

Now, the corresponding values for nicotine must be estimated. By leveraging the modified version of the Doolittle equation for viscosity<sup>(56)</sup>

$$\ln \eta_2 = \ln A_2 + \frac{(\gamma V_2^* / K_{12})}{K_{22} + T + T g_2} \quad (4.8)$$

where,

$$\frac{(\gamma V_2^* / K_{12})}{K_{22} + T + T g_2}$$

and

$K_{22}+T$  are determined from a non-linear regression using viscosity and temperature data <sup>(56)</sup>

The results of these calculations are shown in Table 4.4.

**Table 4.4** Nicotine Values

Property	Value
$\frac{(\gamma V_2^* / K_{12})}{K_{22} + T + T g_2}$	57.32
$K_{11}/\gamma$	$3.41 \cdot 10^{-2}$
$K_{21}-T_{g1}$	-121.495
$\Xi$ (Nicotine/Ethylene)	0.797
$\Xi$ (Nicotine/Vinyl Acetate)	0.577

This gives the value for  $\frac{\hat{V}_{FH}}{\gamma}$

as 0.1465

#### 4.4 Estimation of the values of polymeric matrix components

As shown by Fierro et al., <sup>(57)</sup>

$$\begin{aligned} \frac{\hat{V}_{FH}}{\gamma} = & w_1 \left( \frac{K_{11}}{\gamma_1} \right) (K_{21} - T g_1 + T) + W_{2a} \left( \frac{K_{12a}}{\gamma_{2a}} \right) (K_{22a} - T g_{2a} + T) + W_{2b} \\ & \left( \frac{K_{2b}}{\gamma_{2b}} \right) (K_{22b} - T g_{2b} + T) \end{aligned} \quad (4.9)$$



where,  $w_1$ ,  $w_{2a}$ , and  $w_{2b}$  are the weight fractions for nicotine, ethylene, and vinyl acetate respectively.

The free volume parameters, used in this study, particularly for polymers, are related to the constants of the Williams-Landel-Ferry (WLF) <sup>(58)</sup> equation,  $C_{1p}$  and  $C_{2p}$ , by the following relationships:

$$K_{2p} = C_{2p} \quad (4.10)$$

$$\frac{\gamma V_p}{K_{1p}} = 2.303(C_{1p})(C_{2p}) \quad (4.11)$$

**Table 4. 5** Physical properties of ethylene and vinyl acetate units/blocks

Block Element	$C_1$	$C_2$	Tg	$W_a$
Ethylene	17.44 <sup>(59,60,61)</sup>	51.6 <sup>(59,60)</sup>	237 <sup>(59)</sup>	0.5989 <sup>(59,60)</sup>
Vinyl acetate	15.6 <sup>(59,61)</sup>	104.4 <sup>(59,61)</sup>	305 <sup>(59)</sup>	0.399 <sup>(59,60)</sup>

$$\hat{V}_{2j}^* (cm^3/mol) = 0.0925 Tg_{(2)}(K) + 69.47 \text{ if } T_g \leq 295 \text{ }^\circ\text{K} \quad (4.12)$$

$$\hat{V}_{2j}^* (cm^3/mol) = 0.6334 Tg_{(2)}(K) + 86.95 \text{ if } T_g \geq 295 \text{ }^\circ\text{K} \quad (4.13)$$

Then, taking the values from Table 4.5 and inserting them into equations (4.8), (4.9), and (4.11), the values for:

$$\frac{\gamma V_p}{K_{1p}} = 2.303(C_{1p})(C_{2p}), \hat{V}_{2j}^* (cm^3/mol) \text{ and } K_{li} - T_{gi} \quad (4.14)$$

are obtained and summarized in Table 4.6.

**Table 4.6 Results Summary**

Block Element	$\hat{V}_{2j}^* (cm^3/mol)$	$V_2$ (grams/cm <sup>3</sup> )	$K_{li}/\gamma$	$K_{li} - T_{gi}$
Polyethylene	91.392	1.005	$4.825 \cdot 10^{-4}$	-219.56
Polyvinyl acetate	102.882	0.728 <sup>(44)</sup>	$4.33 \cdot 10^{-4}$	-258.2

#### 4.5 Energy Calculations ( $E^*$ )

The energy component is calculated from the Tonge and Gilbert <sup>(62)</sup> equation:

$$\log_{10}(E^*) = 0.8988 \ln\{\log[(\delta_1 - \delta_2)^2 \hat{V}_s]\} + 2.8377 \quad (4.15)$$

$$\delta = (H-RT)^{0.5} / v^{0.5} \quad (4.16)$$

$$\delta_{(copolymer)} = \sqrt{\frac{E_{COH(copolymer)}}{V_{(copolymer)}}} \quad (4.17)$$

where,

$$E_{COH} = m_1 * E_{COH} (\text{homopolymer of repeat unit 1}) + m_2 * E_{COH} (\text{homopolymer of repeat unit 2}) \quad (4.18)$$

$$V_{copolymer} = m_1 * V (\text{homopolymer of repeat unit 1}) + m_2 * V (\text{homopolymer of repeat unit 2}) \quad (4.19)$$

and

$$m_i = \frac{\left(\frac{\omega_i}{M_i}\right)}{\sum_{j=1}^n \left(\frac{\omega_j}{M_j}\right)} \quad (4.20)$$

The values of energy for ethylene and vinyl acetate were estimated by Van Krevelen <sup>(64)</sup> and are presented in Table 4.7.

**Table 4.7** Hildebrand Coefficients for Ethylene and Vinyl Acetate

Property	Ethylene	Vinyl Acetate
$E_{COH}$ (J/mol)	9,500	25,300
$V_{copolymer}$ (cm <sup>3</sup> /mole)	32	72

Then, using the results from Table 4.7 and equations (4.15), (4.16), (4.17), and (4.18), the value of energy for the EVA copolymer is found to be 55.66 (cal/cm<sup>3</sup>).<sup>0.5</sup>

Because no values of Hildebrand Coefficients were found in the literature for nicotine, they had to be estimated by using the Fedor's equation/model <sup>(65)</sup>. This model uses the structure to calculate the approximate values of  $E_{COH}$  and volume and this, in turn, yields the Hildebrand coefficient. The results are summarized in Table 4.8.

**Table 4.8** Hildebrand Coefficients for Nicotine <sup>[54]</sup>

Property	Value
$E_{COH}$ (J/mol)	56,520
$V$ (cm <sup>3</sup> /mol)	139.7
$\delta_{NIC}$ (cal/cm <sup>3</sup> )	10.02697

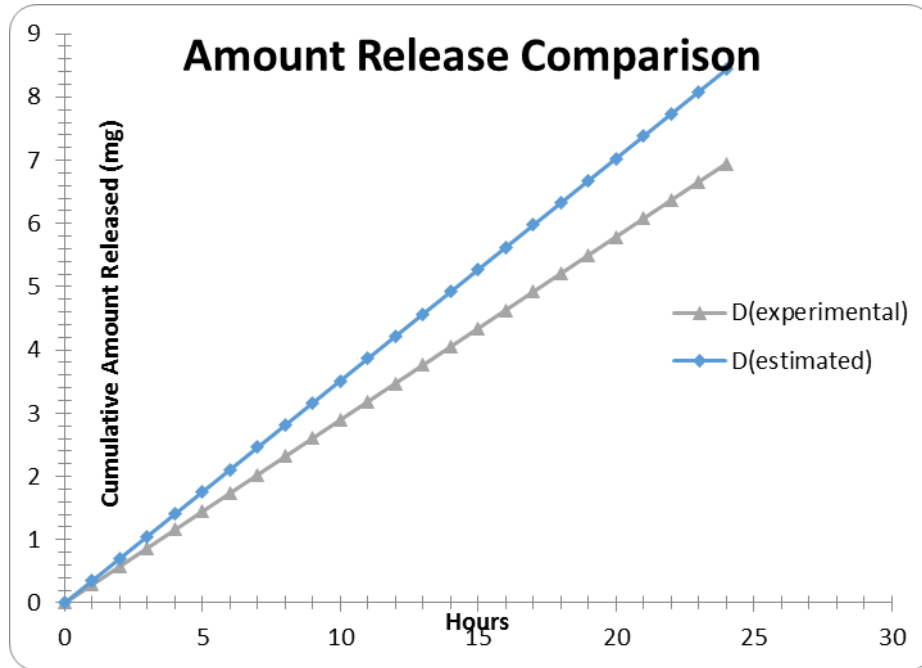
Then, inserting the values for  $\delta_{NIC}$  and  $\delta_{pol}$  into equation (4.15),  $E^*$  was found to be 8.0722 cal/mol.

Table 4.9 shows the summary of the calculated parameters used to calculate the Nicotine theoretical Diffusion Coefficient from an EVA polymeric matrix.

**Table 4.9** Parameters used to Estimate the Theoretical Diffusion Coefficient

Parameter	Nicotine	Vinyl Acetate	Ethylene
$W_s$	0.018	0.399	0.5989
$K_{11}/\gamma$	$3.41 \cdot 10^{-2}$	$4.33 \cdot 10^{-4}$	$4.825 \cdot 10^{-4}$
$K_{21}-T_{gl}$	-121.495	-258.2	-219.56
$\Xi$ (Nicotine/Ethylene)			0.577
$\Xi$ (Nicotine/Vinyl Acetate)		0.797	
$V_i$	0.954	0.728	1.005
$E^*$		8.0722	

Then, inserting all the values into (3.14), the diffusion was estimated to be  $1.781 \cdot 10^{-9}$  cm<sup>2</sup>/sec. Figure 4.7 shows the comparison between the theoretical and experimental values.



**Figure 4.7** Cumulative release comparison between  $D_{\text{exp.}}$  and  $D_{\text{calc.}}$ .

#### 4.6 Effect of Molecular Radius of Gyration

In the previous section, the radius of nicotine was estimated to be  $R_0 = 4.062 \cdot 10^{-8}$  cm. If assuming a spherical shape, the  $R_g$  and  $R_0$  are substituted into equation (3.14) where the following relationship between  $D_{R_g}$  and  $D_{R_0}$  (also known as  $D_c$ ) is:

$$D_{R_g} = D_{R_0} / 0.77 \quad (4.21)$$

where,  $D_{R_0}$  (calculated diffusion coefficient from section 1) was found to be  $1.781 \cdot 10^{-9}$   $\text{cm}^2/\text{sec}$ ; then equation (4.21) is:

$$D_{R_g} = 1.781 \cdot 10^{-9} \text{ cm}^2/\text{sec} / 0.77$$

and the diffusion coefficient is found to be:

$$D_{R_g} = 2.313 \cdot 10^{-9} \text{ cm}^2 / \text{sec}$$

If assuming a cylindrical shape, then using an analog to equation (4.21),

$$D_{R_g} = D_{R_0} / 1.732 \quad (4.22)$$

and the diffusion coefficient is found to be:

$$D_{Rg} = 1.028 \times 10^{-9} \text{ cm}^2/\text{sec}$$

**Table 4.10** Comparison of Experimental and Calculated Values of the Diffusion Coefficient using Different R<sub>g</sub> Values.

Property	Value
D <sub>(experimental)</sub>	1.467*10 <sup>-9</sup> cm <sup>2</sup> /sec
D <sub>Rg (Rg = 0.77 Rh)</sub>	2.313*10 <sup>-9</sup> cm <sup>2</sup> /sec
D <sub>Rg (Rg = 1.732 Rh)</sub>	1.028*10 <sup>-9</sup> cm <sup>2</sup> /sec

The calculated results of the diffusion coefficient, using different values of the radius of gyration, are shown in Figure 4.8.

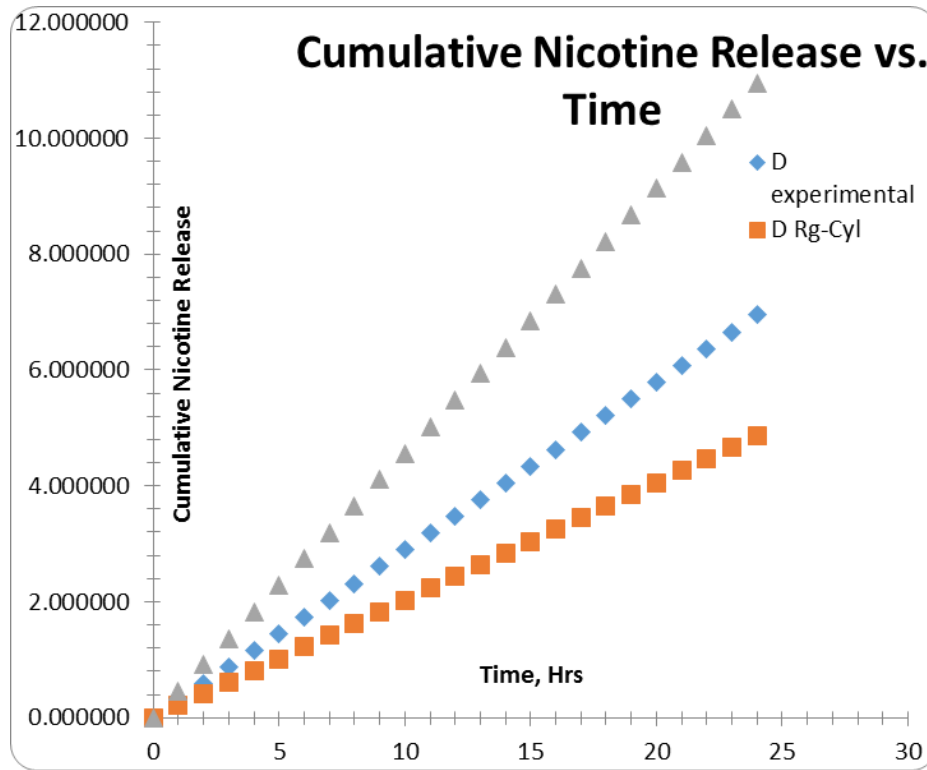


**Figure 4.8** Diffusion coefficient comparisons between R<sub>g</sub> and R<sub>h</sub>

## 4.7 Effect of Molecular Shape

In the previous section, the  $\xi_L$  values of nicotine and EVA were estimated to be as follows:

**Table 4.11**  $\xi_L$  Values

$\xi_L$ (Nicotine/Ethylene)	0.577
$\xi_L$ (Nicotine/Vinyl Acetate)	0.797

The molecular shape factor (A/B) of nicotine was estimated to be 1.450 (APPENDIX E). The  $\xi$  values can be estimated using equation (3.31) and APPENDIX E, and the results are summarized in Table 4.12.

**Table 4.12**  $\xi$  Values

$\xi$ (Nicotine/Ethylene)	0.7794
$\xi$ (Nicotine/Vinyl Acetate)	1.2427

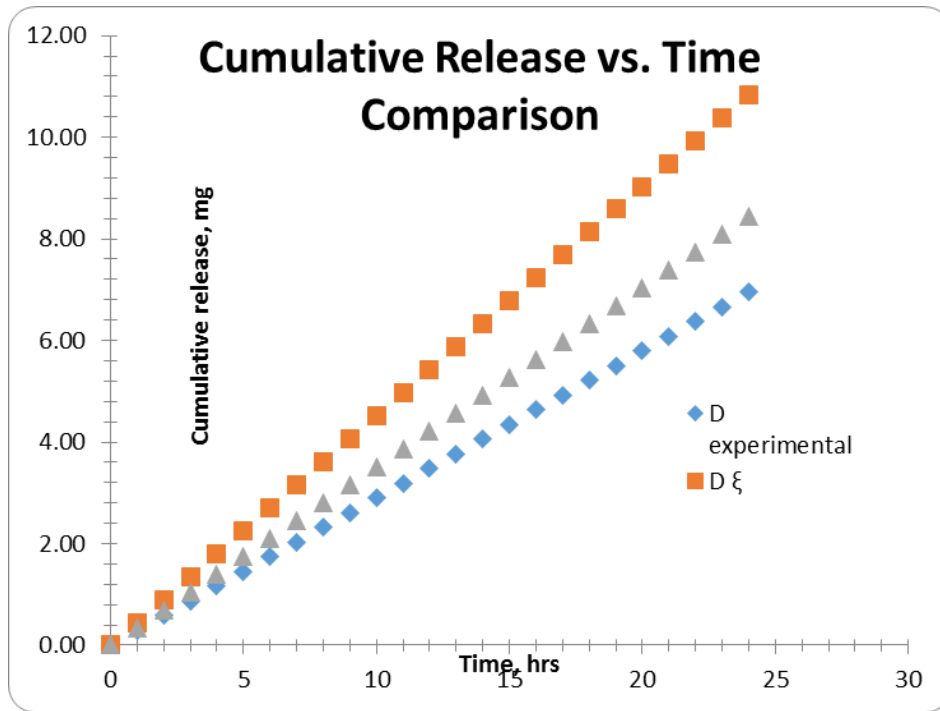
The diffusion coefficient  $D_\xi$  is estimated to be 2.2887E-09 cm<sup>2</sup>/sec.

**Table 4.13** Comparison of experimental and calculated values of the Diffusion

Coefficient using different  $R_g$  values.

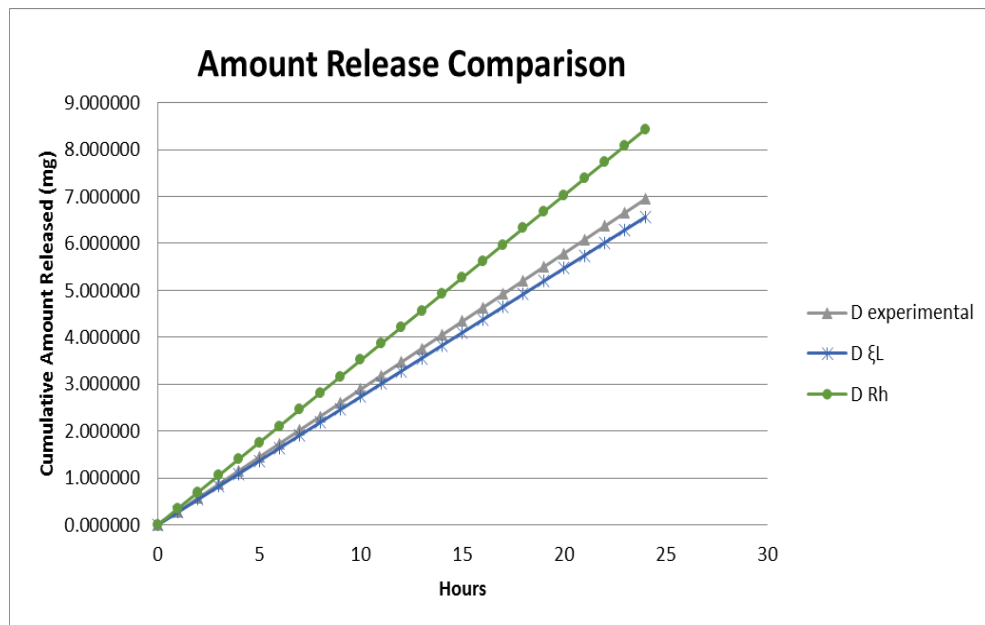
Property	Value
$D_{(\text{experimental})}$	$1.467 \cdot 10^{-9}$ cm <sup>2</sup> /sec
$D_{(\xi)}$	$2.2887 \cdot 10^{-9}$ cm <sup>2</sup> /sec
$D_{(\xi L)}$	$1.781 \cdot 10^{-9}$ cm <sup>2</sup> / sec

Figure 4.9 shows the comparison of the Diffusion Coefficients for different types of  $\xi$  values.



**Figure 4.9** Diffusion coefficient comparison between  $\xi$ ,  $\xi_L$  and experimental values

Figure 4.10 shows the effect of the different values of  $\xi$  on the results of the Diffusion Coefficient.



**Figure 4.10** Comparison between  $D_{\xi_L}$  and  $D_{R_h}$



#### 4.8 Effect of Combining Molecular Radius of Gyration and Shape Factors

Then, inserting the A/B values from Table 4.12 along with the different radii (hydrodynamic and gyration) from Table 4.13 into equation (3.14), the diffusion coefficients for different cases/conditions are estimated and the results are summarized in Table 4.14.

**Table 4.14** Diffusion Coefficients using Different Radius and  $\xi / \xi_L$  Values

Case	Diffusion Coefficient (cm <sup>2</sup> /sec)
$D_{Rg(0.77)+\xi+\xi_l(IIa)}$	1.7623E-09
$D_{Rg(1.732)+\xi+\xi_l(IIb)}$	3.964E-09
$D_{Rg(0.77)+\xi_L+\xi(IIIa)}$	1.7998E-09
$D_{Rg(1.732)+\xi_L+\xi(IIIb)}$	1.3214E-09
$D_{\text{experimental}}$	1.467E-09

The comparison of cumulative release curves of  $D_{\text{experimental}}$  and  $D_{Rg(0.77) + \xi + \xi_l(IIa)}$  is shown in Figure 4.11.

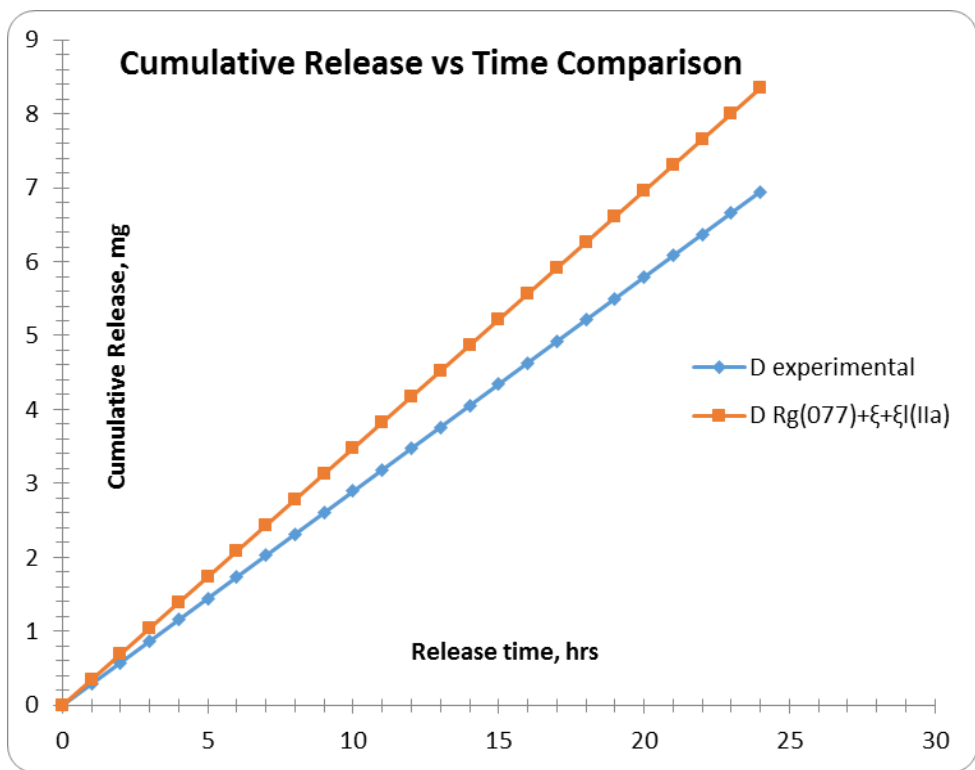


**Figure 4.11** Diffusion coefficient comparison between experimental and  $D_{Rg(0.77)+\xi+\xi l(IIa)}$

The comparison of cumulative release curve of  $D_{\text{experimental}}$  and  $D_{Rg(1.732)+\xi+\xi l(IIb)}$  is shown in Figure 4.12.

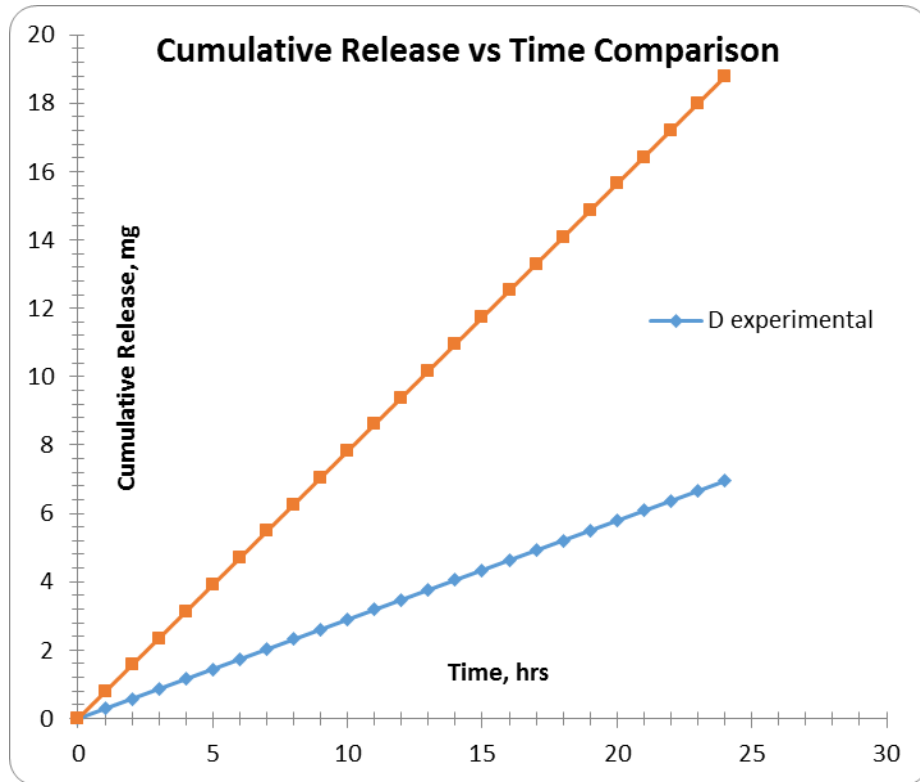


**Figure 4.12** Comparison of Diffusion coefficient of experimental and  $D_{Rg(1.732)+\xi+\xi l(IIIb)}$ .

The comparison of cumulative release curve of  $D_{\text{experimental}}$  and  $D_{Rg(0.77)+\xi L+\xi(IIIa)}$  is shown in Figure 4.13.

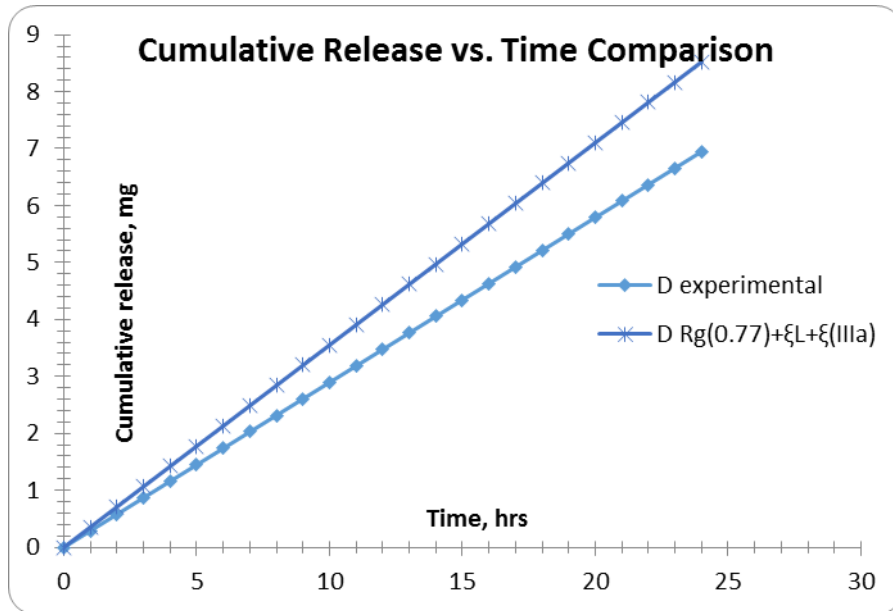


**Figure 4.13** Comparison of Diffusion coefficient of experimental and  $D_{Rg(0.77)+\xi L+\xi(IIIa)}$  The comparison of cumulative release curve of  $D_{\text{experimental}}$  and  $D_{Rg(1.732)+\xi L+\xi(IIIb)}$  is shown in Figure 4.14.

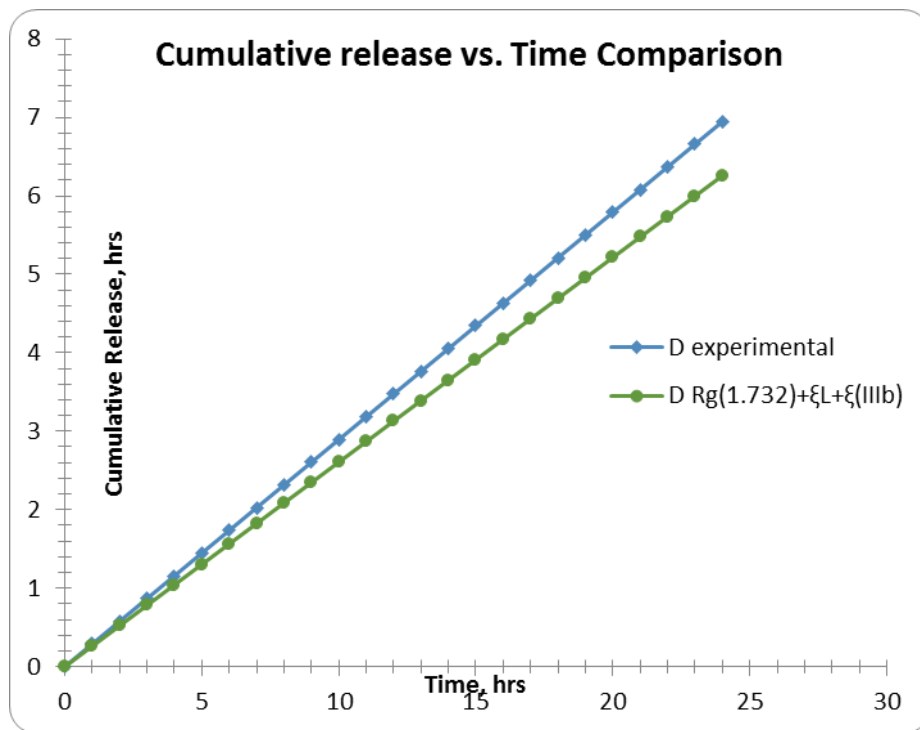


**Figure 4.14** Comparison of Diffusion coefficient of experimental and  $D_{Rg(1.732)+\xi L+\xi(IIIb)}$ .

## CHAPTER 5

### DISCUSSION

The DZE equation shows that Diffusion Coefficient can easily be estimated without the need of experimental work and still provide a very good approximation. The DZE demonstrates the effect of molecular shape as seen in Figure 5.1.

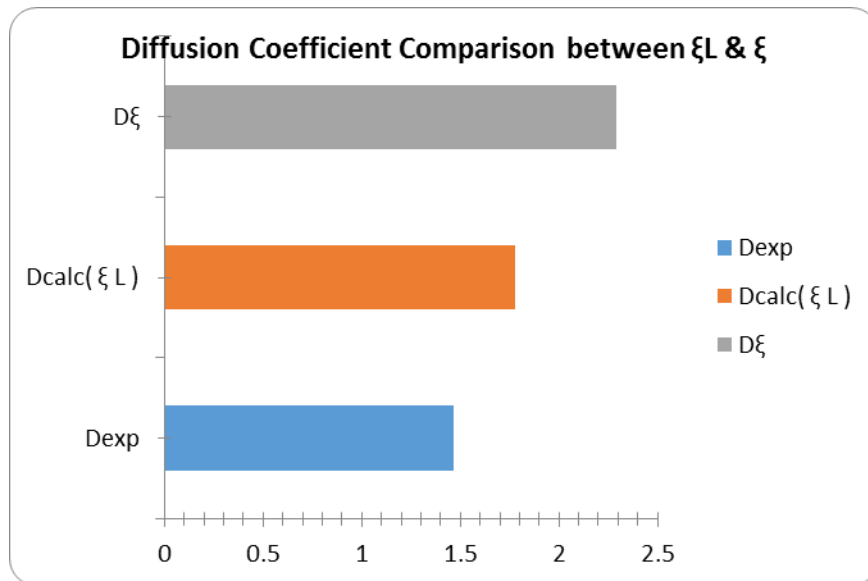


**Figure 5.1** Comparison of Diffusion Coefficient using shape factors

The effect of the radius on the diffusion coefficient is as follows – 30% ( $R_g = 1.732 R_0$ ) to + 58% ( $R_g = 0.77 R_0$ ) difference when compared with the experimental value as seen in Figure 5.2.

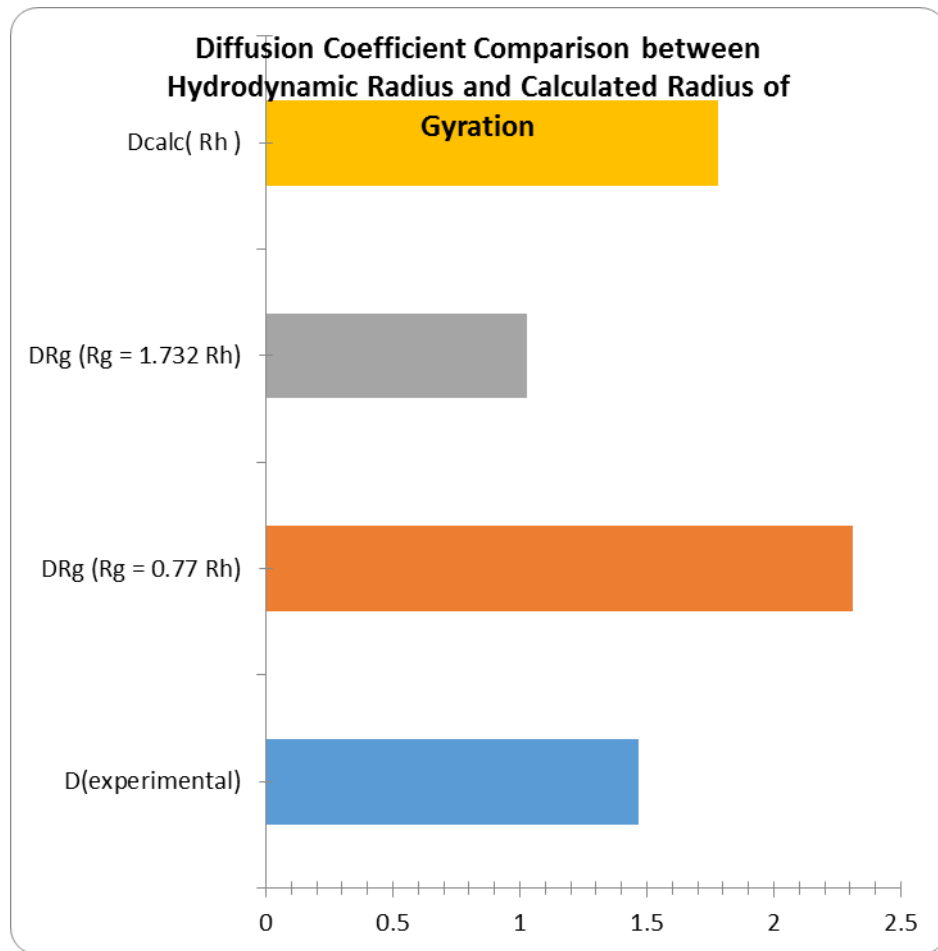


**Figure 5.2** Comparison of Diffusion Coefficient

The effect of the integration of molecular shape and radius of gyration, used in the diffusion coefficient, affected the results from 90% to 270% when compared with the experimental value.

A combination of parameters such as  $D_{Rg} (1.732) + \xi L + \xi$  (IIIb)) has a 90% accuracy against the experimental value as seen in Figure 5.3.

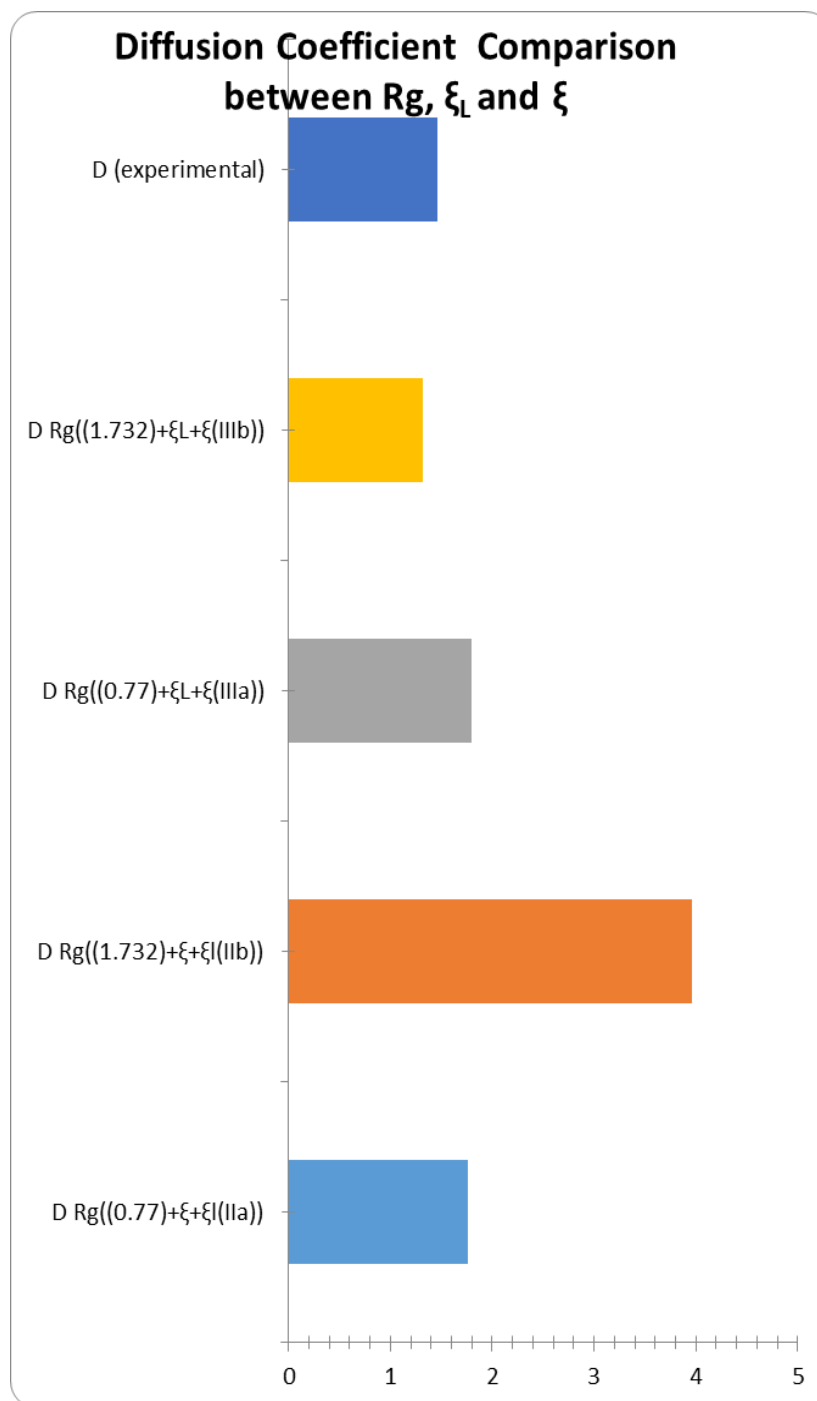


**Figure 5. 3** Comparison of Diffusion Coefficient using different molecular shape and radius combinations



However, when combining the effect of the hydrodynamic radius,  $R_h$ , with the modified shape factor,  $\xi_L$ , then a very close approximation to the experimental value is achieved as seen in figure 5.4.

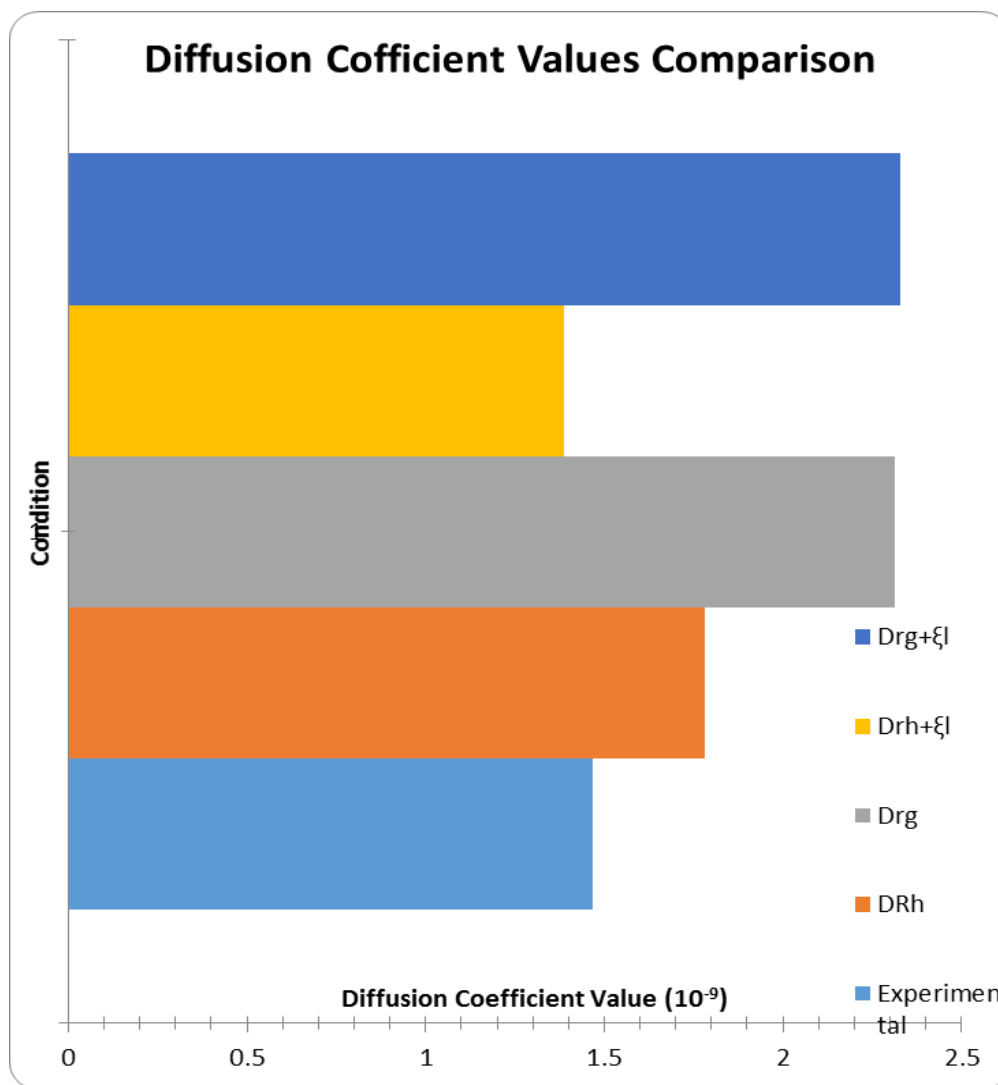


**Figure 5.4** Overall Comparison of Diffusion Coefficients

Although the DZE can be considered as an empirical approach, it still uses molecular descriptors that relate to the morphology and chemical parameters of the diffusing solute and the surrounding matrix.

One of the key aspects of this model is the use of group contribution and thermodynamic methods such as Joback, Yamada and Gunn, Pitzer and Williams and Landel.

The energy component,  $E^*$ , is not particularly large which is in agreement to the findings of Vrentas and Vrentas<sup>(66)</sup> which contradicts the findings seen by HU<sup>(67)</sup>. This could perhaps be due to the lack of a chemical affinity between the solute and the polymeric matrix. Nevertheless, DZE shows a very close approximation of the experimental values.

## CHAPTER 6

### CONCLUSIONS

In US patent 5603947 [1], Wong et al. reported typical diffusion coefficient values of Nicotine patches that were experimentally determined to be between  $10^{-8}$  to  $10^{-9}$  cm<sup>2</sup>/sec. This is in agreement with the experimental and theoretical values obtained in this research.

The DZE modified equation (DZME) shows a small influence of the interaction between the solute and the polymeric structure which was indicated by Wang, Wu and Wang<sup>(68)</sup>. DZME shows that molecular shape has a greater impact on the Diffusion Coefficient and this is in agreement with the findings of Reyner et al<sup>(69)</sup>.

The combination of molecular size, defined as hydrodynamic and Gyration radius,  $R_h$  and  $R_g$ , along with molecular shape of the diffusing molecule, can influence the Diffusion Coefficient as reported by Zhimin<sup>(70)</sup> and De Kee et al<sup>(71)</sup> work.

The DZME shows a slight deviation from Chandler's<sup>(72)</sup> Self Diffusion Coefficient models based on hard spheres and this should be expected since solute molecules should not be seen as hard spheres but more as small to large flexible coils as described by De Gennes<sup>(73)</sup> (Figure 6.1)

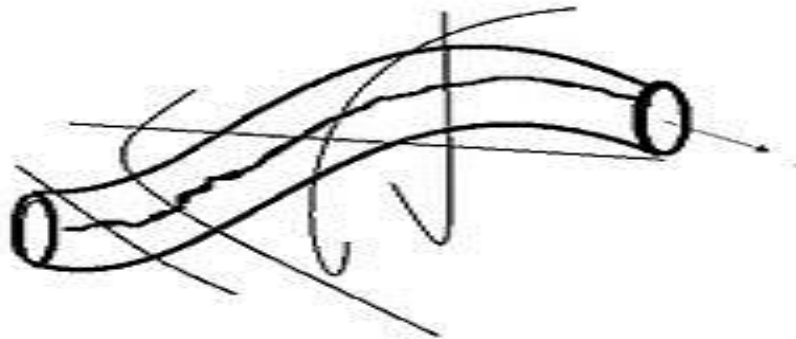


**Figure 6.1** De Gennes Molecular Representation

Source: Reptation, <http://en.wikipedia.org/wiki/Reptation>. Accessed on December 7, 2014

where solute molecules will diffuse through a polymeric matrix on a reptation pattern  
(74, 75) as shown in Figure 6.2.

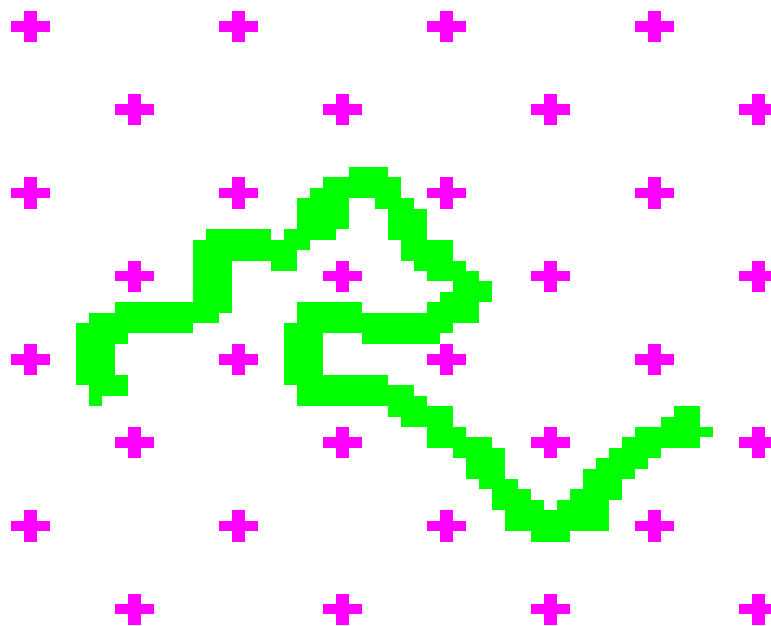


**Figure 6.2** De Gennes Molecular Reptation Pattern

Source: Polymer Reptation, [http://euler.phys.cmu.edu/widom/images/polymer\\_icon.gif](http://euler.phys.cmu.edu/widom/images/polymer_icon.gif). Retrieved on December 7, 2014.

Examining the results obtained when considering hydrodynamic radius,  $R_h$ , compared to the gyration radius,  $R_g$ , the results are close to the experimental values. This particular model shows that the Diffusion Coefficient can be influenced by the molecular shape and size, type of radius used.

The DZE proves that mathematical models can help and demonstrate key processes that can influence drug delivery<sup>(76)</sup>.

Therefore, this work shows that the modified Duda Zelinsky equation can be used not only to obtain diffusion coefficients that are closer to the experimental value, but more importantly, it can be used as a screening methodology to help select the most suitable polymeric matrix for a particular solute that will provide the right Diffusion Coefficient that will achieve the most desired therapeutic level at a quickest pace.

## CHAPTER 7

### FUTURE WORK

Although this work shows that DZE is a good screening methodology, the following aspects could enhance this methodology:

1. Physical properties selection protocol (PPSP) -

The use of group contribution methods for the estimation of physical properties when the experimental data is missing or not readily available; this should be based on Aliphatic and Aromatic chemical structures.

2. Expand from a singularity to a general model -

Compare DZE with different solutes and polymeric matrices with experimental/literature data.

3. Reptation Model evaluation -

Evaluate the effect of DeGennes scaling reptation concept<sup>(74)</sup>

$$D \sim M^{-2} c^{(2-\nu)/(1-3\nu)}$$

4. Skin Penetration Effect -

Evaluate the effect of incorporating DZE into the Guy-Potts skin penetration equation

$$\log K_P = -2.71 - 0.0061 * M_W + 0.74 * \log P \quad (75-78)$$

5. Permeation in Textiles -

Evaluate the effect of incorporating the DZE into the modified Darcy's equation proposed by Verleye et al.<sup>(79)</sup>

## APPENDIX A

Table A.1 shows the transdermal delivery systems that are presently available in the global market (up to 2014).

<b>Table A.1. Commercially Available Transdermal Delivery Systems</b>						
Active ingredient	Molecular weight (Da)	Trade name(s)	Manufacturer	Daily dose	Frequency of application	Type of system
Clonidine	230	Catapres-TTS®	ALZA Corporation, Mountain View, CA, USA	The 3.5, 7.0, and 10.5 cm <sup>2</sup> systems deliver 0.1, 0.2, and 0.3 mg of clonidine per day, respectively	Weekly	A drug reservoir of clonidine, mineral oil, polyisobutylene, and colloidal silicon dioxide
Estradiol	272	Esclim®	Laboratories Fournier SA, Dijon, France	0.025–0.1 mg	Weekly	Drug-in-adhesive
		Vivelle® Vivelle-Dot®	Noven Pharmaceuticals Inc., Miami, FL, USA	Nominal <i>in vivo</i> delivery rates of 0.025, 0.0375, 0.05, 0.075, or 0.1 mg of estradiol per day	Twice weekly	Adhesive formulation containing estradiol
		Climara®	3 M Drug Delivery Systems, Northridge, CA, USA Copyright © 2007, Bayer HealthCare Pharmaceuticals Inc.	Menostar (estradiol transdermal system), 14µg/day. Each 3.25 cm <sup>2</sup> system contains 1 mg of estradiol USP	Only one system should be worn at any one time during the 7-day dosing interval	Adhesive matrix containing estradiol

**Table A.1. Commercially Available Transdermal Delivery Systems (Cont'd.)**

Active ingredient	Molecular weight (Da)	Trade name(s)	Manufacturer	Daily dose	Frequency of application	Type of system
Ethinyl Estradiol w/ Norelgestromin	296/328	Ortho-Evra®	Ortho-McNeil Pharmaceutical, Inc., Raritan, NJ, USA	0.15 mg/0.02 mg Each systems contains 6 mg norelgestromin and 0.75 mg ethinyl estradiol	This system uses a 28-day (four-week) cycle. A new patch is applied each week for three weeks (21 total days). Week four is patch-free	Adhesive layer contains norelgestromin and ethinyl estradiol polyisobutylene/polybutene adhesive, crospovidone, non-woven polyester fabric and lauryl lactate as inactive components
Fentanyl	337	Duragesic	Manufactured by: ALZA Corporation, Mountain View, CA, USA. Manufactured for: Janssen, division of Ortho-McNeil-Janssen Pharmaceuticals, Inc., Titusville, NJ, USA	0.6 mg	Once every three days	Reservoir
Lidocaine	234	Lidoderm®	Endo Pharmaceuticals Inc., Chadds Ford, PA, USA	Lidoderm (lidocaine patch 5%)	Apply lidoderm to intact skin to cover the most painful area. Apply up to three patches, only once for up to 12 hours within a 24-hour period	Drug-in-adhesive
Nicotine	162	Nicoderm CQ®	GlaxoSmithKline Consumer Healthcare, L.P, Philadelphia, PA, USA	7-21 mg	Daily	No information available



**Table A.1. Commercially Available Transdermal Delivery Systems (Cont'd.)**

Active ingredient	Molecular weight (Da)	Trade name(s)	Manufacturer	Daily dose	Frequency of application	Type of system
Nitroglycerin	227	Nitro-Dur®	Schering-Plough Pty Ltd, Baulkham Hills, NSW, Australia. Copyright © 1987, 2002, Key Pharmaceuticals, Inc.	Each cm <sup>2</sup> of applied system delivers approximately 0.02 mg of nitroglycerin per hour	Daily	Nitroglycerin in acrylic-based polymer adhesives with a resinous cross-linking agent to provide a continuous source of active ingredient
		Nitrodisc®	GD Searie, Chicago, IL, USA	Nitrodisc, release rate 0.2/0.3/0.4 mg of nitroglycerin per hour	Daily	Reservoir
Scopolamine	303	Transderm-Scop®	ALZA Corporation, Palo Alto, CA, USA	0.33 mg programmed to deliver in vivo approximately 1.0 mg of scopolamine over 3 days	Once every three days	Reservoir of scopolamine, light mineral oil, and polyisobutylene
Testosterone	288	Androderm®	Watson Pharma, Inc. A subsidiary of Watson Pharmaceuticals, Inc., Corona, CA, USA	2.5-5 mg	Androderm 5 mg system or two androderm 2.5 mg systems applied nightly for 24 hours, providing a total dose of 5 mg/day	Reservoir of testosterone USP, alcohol USP, glycerin USP, glycerol monooleate, methyl laurate, sodium hydroxide NF, to adjust pH, and purified water USP, gelled with carbomer copolymer Type B NF

Ref.: Tanner, T. and Marks, R., Delivering drugs by the transdermal route: review and comment, *Skin Research & Technology*, [Volume 14, Issue 3](#), pages 249–260, 2008 – Accessed on December 1, 2014

## APPENDIX B

### TYPES OF TRANSDERMAL PATCHES

Table A.2 shows the types of patches commercially available in the US and EU

**Table B.1** Types of Transdermal Patches globally sold

<b>Marketed Products of Transdermal Drug Delivery System</b>	<b>Product</b>	<b>Active drug</b>	<b>Type of transdermal patch</b>	<b>Purpose</b>
1.	Estraderm	Estradiol	Membrane	Postmenstrual syndrome
2.	Duragesic	Fentanyl	Reservoir	Pain relief patch
3.	Transderm-Scop	(Scopolamine)	Reservoir	Motion sickness
4.	Alora	Estradiol	Matrix	Postmenstrual Syndrome
5.	Climara	Estradiol	Matrix	Postmenstrual Syndrome
6.	Androderm	Testosterone	Membrane	Hypogonadism in males
7.	Captopress TTS	Clonidine	Membrane	Hypertension
8.	Combipatch	Estradiol	Matrix	Postmenstrual Syndrome
9.	Esclim	Estradiol	Matrix	Hormone replacement therapy
10.	Deponit	Nitroglycerine	Drug in adhesive	Angina Pectoris
11.	FemPatch	Estradiol	Matrix	Postmenstrual syndrome
12.	Lidoderm	Lidocaine	Drug in adhesive	Anesthetic
13.	Ortho Evra	Estradiol	Drug in adhesive	Postmenstrual Syndrome
14.	Testoderm TTS	Testosterone	Reservoir	Hypogonadism in males
15.	Habitrol	Nicotine	Drug in adhesive	Smoking Cessation

**Table B.1** Types of Transdermal Patches globally sold  
(Continued)

<b>Marketed Products of Transdermal Drug Delivery System</b>	<b>Product</b>	<b>Active drug</b>	<b>Type of transdermal patch</b>	<b>Purpose</b>
16.	Prostep	Nicotine	Reservoir	Smoking Cessation
17.	Nicotrol	Nicotine	Drug in adhesive	Smoking Cessation
18.	Vivelle	Estradiol	Reservoir	Postmenstrual syndrome
19.	MatrifenR	Fentanyl	Reservoir	Pain relief patch
20.	NuPatch 100	Diclofenac diethylamine	Drug in adhesive	Anti Inflammatory
21.	Nicoderm CQ	Nicotine	Drug in adhesive	Smoking Cessation
22.	Vivelle-Dot	Estradiol	Reservoir	Postmenstrual syndrome
23.	Minitran	Nitroglycerine	Drug in adhesive	Angina Pectoris
24.	Nitrodisc	Nitroglycerine	Micro reservoir	Angina Pectoris
25.	Nitrodur	Nitroglycerine	Matrix	Angina Pectoris
26.	TransdermNitro	Nitroglycerine	Reservoir	Angina Pectoris
27.	OxytrolR	oxybutynin	Matrix	Overactive bladder
28.	Nuvelle TS	Estradiol	Drug in adhesive	Harmone replacement therapy
29.	Fematrix	Estrogen	Matrix	Postmenstrual syndrome
30.	Climaderm	Estradiol	Matrix	Postmenstrual syndrome

Ref: TRANSDERMAL PATCHES: A RECENT APPROCH TO NEW DRUG DELIVERY SYSTEM, SONIA DHIMAN\*, THAKUR GURJEET SINGH AND ASHISH KUMAR REHNI, International Journal of Pharmacy and Pharmaceutical Sciences, Vol 3, Suppl 5, 2011

## APPENDIX C

### Summary of Release Kinetics

Table C.1 shows a summary of the release kinetics and transport mechanisms of all commercially sold transdermal patches.

**Table C.1** - Summary of release kinetics and transport mechanisms of nondegradable polymer based delivery devices

Type of material	Type of device	Loaded drug	Burst release	Release kinetics	Transport mechanism
Segmented PU (Cardiomat 610)	Drug-eluting stent	1,3-Dipropyl-8-cyclopentyl xanthine	1 d	Near linear release (~ 20 d)	Non-Fickian diffusion
Elast-Eon™	Drug-eluting stent	Dexamethasone acetate	w/	Biphasic pattern	Fickian diffusion
Polyurethane (Walopur®)	Disk-shaped matrices	Flucloxacillin-Na Fosfomycin Gentamicin-base	1 d	Near linear (2 ~ 5 d)	Matrix-controlled
Poly(urea-urethane)	Microcapsule	Auramine (Oil-soluble dye)	w/o	Near linear (~20 min)	Non-Fickian Diffusion
PEG modified polyurethane	Dermal patch	Thiamazole, diclofenac sodium, ibuprofen	12 h	Biphasic pattern (~ 48 h)	-
PDMS	Rod (matrix vs. reservoir)	Ivermectin	w/o	Matrix: first order, 50 d; Reservoir: zero order, 84 d	Matrix: diffusion Reservoir: case II transport

Table C.1 - Summary of release kinetics and transport mechanisms of nondegradable polymer based delivery devices (Cont'd.)

Type of material	Type of device	Loaded drug	Burst release	Release kinetics	Transport mechanism
PDMS	Intravaginal ring (reservoir)	TMC120	1–2 d	Biphasic; near zero order release for 30 d	Case II transport
PDMS	Intravaginal ring (core-type)	TMC120	w/o	Zero order, 71 d	Case II transport
PDMS	Strip (10x20 mm)	Metronidazole	w/	Higuchi (linear vs. $t^{1/2}$ )	Fickian diffusion
PEVA (VA content, 40%)	Membrane	Quinupramine	w/	Higuchi (linear vs. $t^{1/2}$ )	Fickian diffusion
PEVA	Thin film	Acyclovir Chlorhexidine diacetate	w/o	Near zero-order (~ 8 d)	Non-Fickian diffusion
PEVA	Drug-eluting stent coating	5-Fluorouracil	w/	Biphasic pattern (~20 d)	Fickian diffusion
PEVA (VA content, 40%)	Disk-shape Film	Chlorhexidine diacetate	w/	Near-zero order (~ 7 d)	Non-Fickian diffusion
PEVA (VA content, 40%)	Membrane	Furosemide	w/	Higuchi (linear vs. $t^{1/2}$ )	Fickian diffusion

Table C.1 - Summary of release kinetics and transport mechanisms of nondegradable polymer based delivery devices (Cont'd.)

Type of material	Type of device	Loaded drug	Burst release	Release kinetics	Transport mechanism
Dextran sulfate	Microcapsule	Insulin	w/	Biphasic pattern (~12 h)	Fickian diffusion
Methacrylated dextran	Hydrogel	Vitamin E	~3 h	Biphasic	Swelling
HPMC with $\beta$ -CD	Tablet	Difunisal	w/o	Zero-order for nonsoluble $\beta$ -CD First-order for soluble $\beta$ -CD	Non-Fickian diffusion

## APPENDIX D

### Experimental Data Analysis

This appendix the statistical analysis done for the validation of the data generated during the experimental phase. Experimental data for testing Transdermal Patches in Vitro by means of Franz Cells utilizing the procedures outlined by the United States Pharmacopeia (USP)<sup>(1 -2)</sup> and the FDA<sup>(3)</sup>. (See Tables D.1 and D.3).

#### Cell Bank D.1 – Raw Data

Cum Release									
Mt / Minf									
Cell Bank 1									
Time, hrs. →	0	1	2	3	4	5	6	7	23
Cell # ↓									
1	0	0.51	1.14	1.42	1.70	2.23	2.77	3.19	4.80
2	0	0.48	1.21	1.52	1.84	2.14	2.85	3.13	4.61
3	0	0.47	1.11	1.49	1.74	2.11	2.96	3.07	4.94
4	0	0.55	1.08	1.38	1.57	2.34	2.69	3.39	4.42
5	0	0.48	1.12	1.34	1.75	2.43	2.71	3.42	4.90



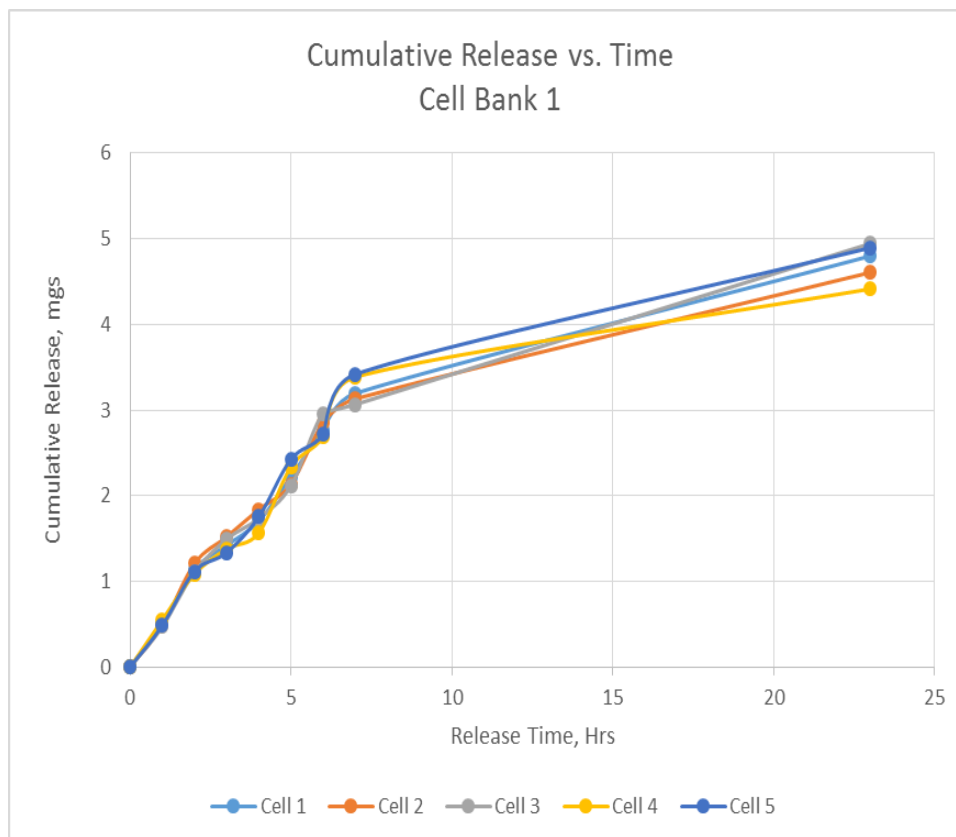


**Figure D.1.** Cell Bank 1 - Cumulative Release vs. Time

**Table D.2.** Cell Bank 1 – Statistical Analysis

Cell #	R <sup>2</sup> (Polynomial Fit)	R <sup>2</sup> (Linear Fit)
1	0.9953	0.8656
2	0.9898	0.8589
3	0.9845	0.8844
4	0.9832	0.7592
5	0.994	0.8338

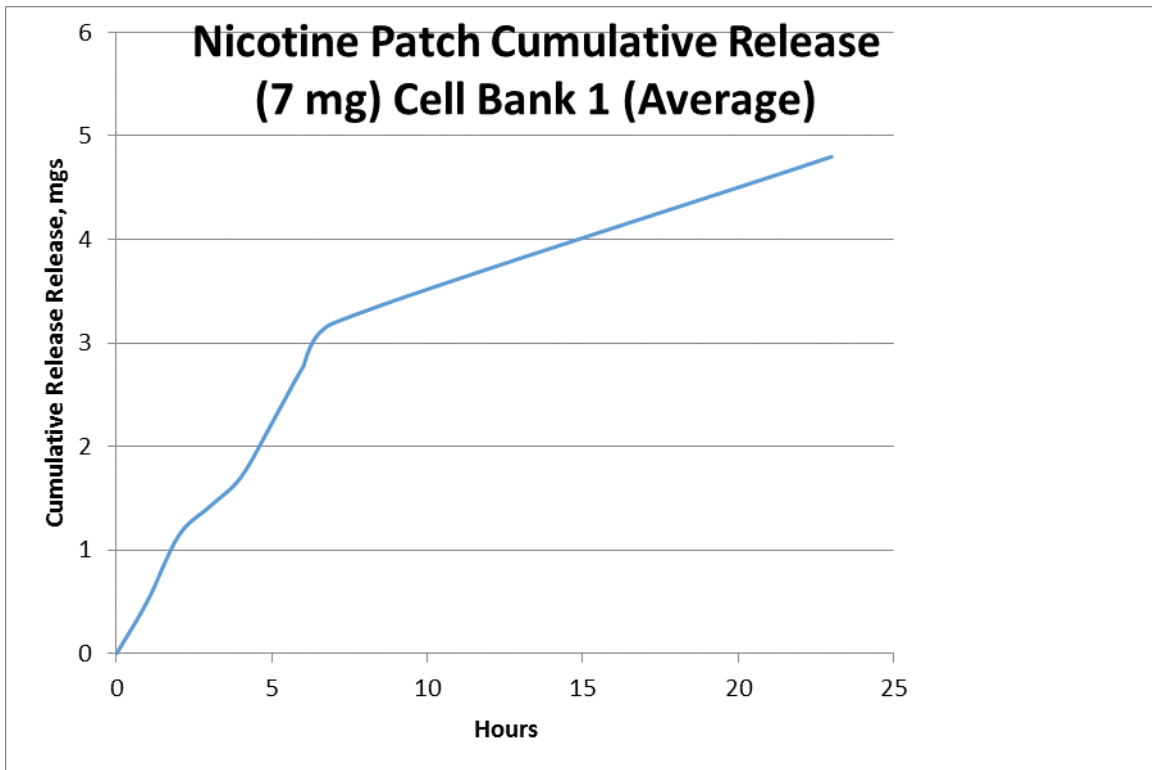


**Figure D.2.** Cell Bank 1 - Cumulative Release vs. Time – Average Curve / Response  
Statistical Analysis:  $R^2$  (Polynomial Fit) = 0.9944 /  $R^2$  (Linear Fit) = 0.8271

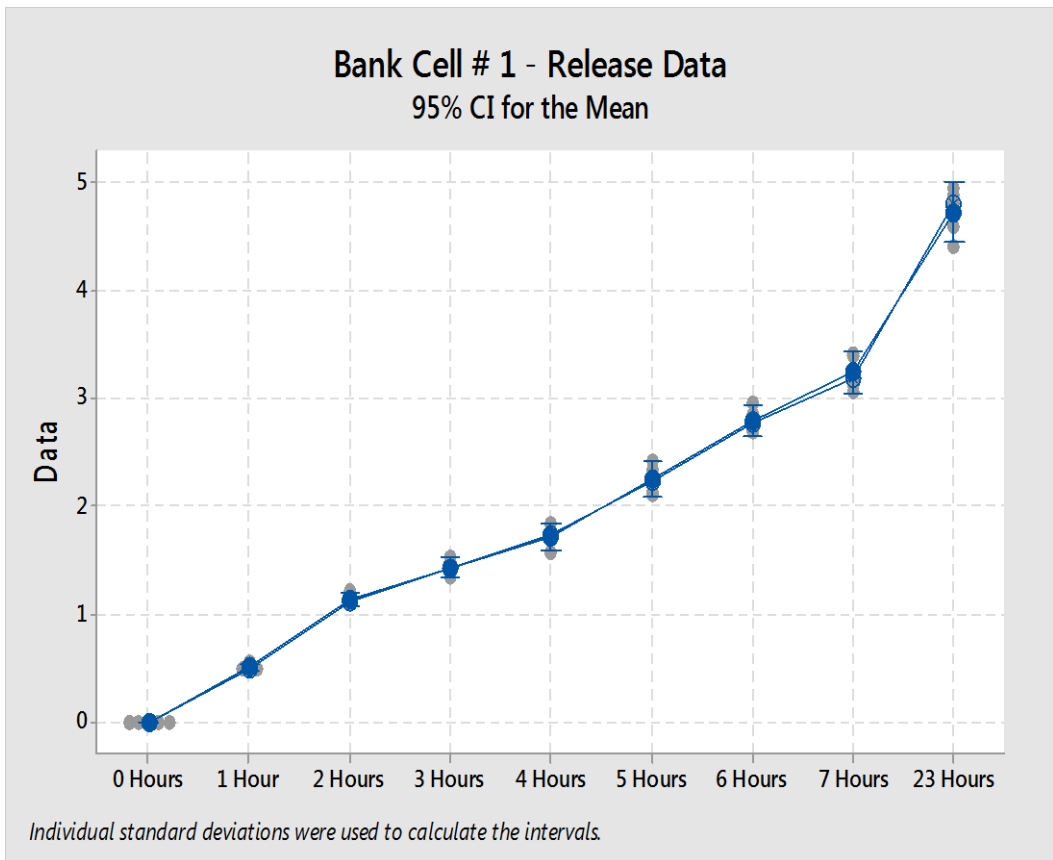


**Figure D.3.** Cell Bank 1 –Confidence Interval Level Analysis (Individual and Sum Plots)

The 95 % Confidence Interval Level Analysis for the experimental data from Cell Bank 1 is uniform and with a narrow difference between data points indicating a robust statistical data set. (See Figure D.4)

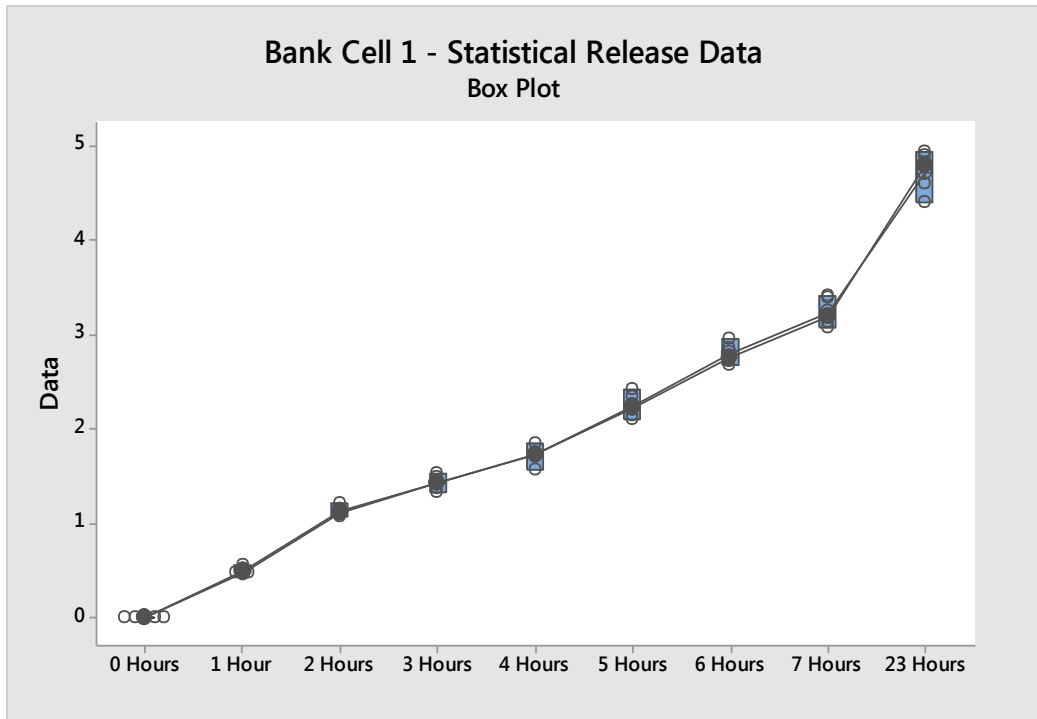


**Figure D.4.** Cell Bank 1 –Box Plot Analysis (Individual and Sum Plots)

The box plot analysis for the experimental data from Cell Bank 1 is uniform and with a narrow difference between data points indicating a robust statistical data set.

**Table D.3.** Cell Bank 2 – Raw Data

Cum Release									
Mt / Minf									
Cell Bank 2									
Time, hrs. →	0	1	2	3	4	5	6	7	23
Cell # ↓									
1	0	0.50	0.87	1.12	1.37	2.08	2.56	3.03	5.08
2	0	0.54	0.85	1.06	1.46	1.95	2.66	3.11	4.88
3	0	0.57	0.81	1.10	1.43	2.03	2.61	3.33	4.63
4	0	0.53	0.85	1.12	1.48	2.11	2.53	3.49	4.91
5	0	0.56	0.78	1.15	1.40	2.24	2.33	3.28	4.67

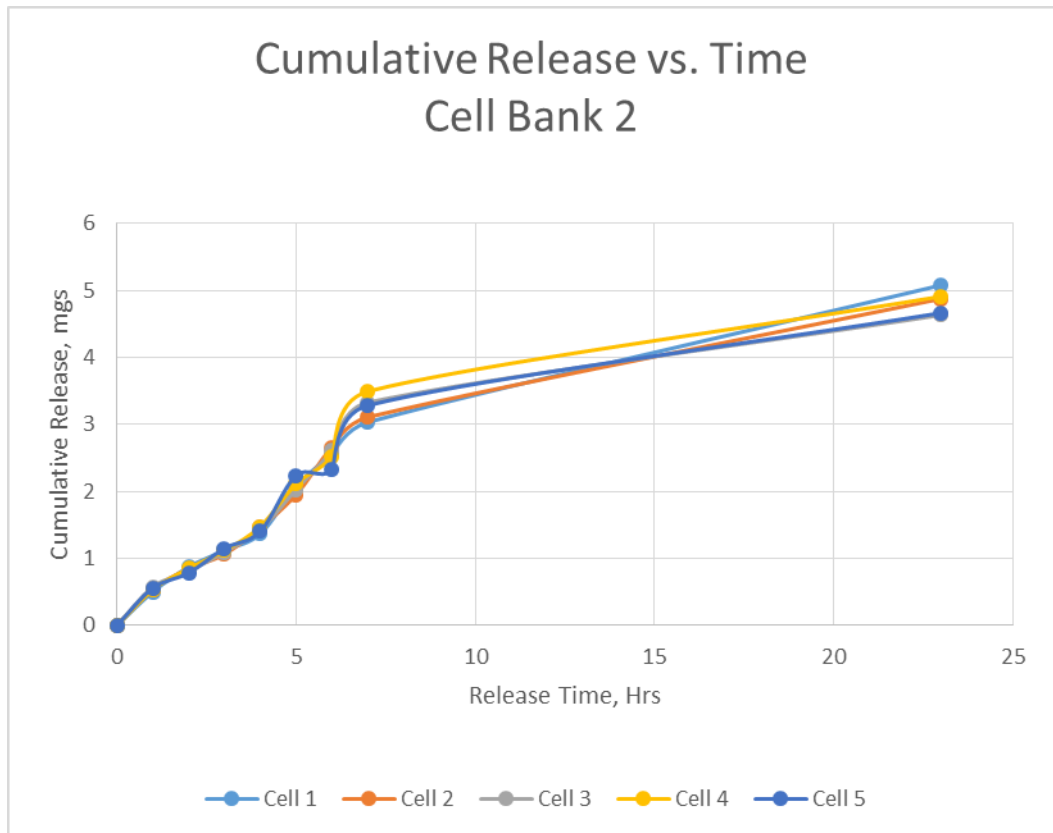


**Figure D.5.** Cell Bank 2 - Cumulative Release vs. Time

**Table D.4.** Cell Bank 2 – Statistical Analysis

Cell #	R <sup>2</sup> (Polynomial Fit)	R <sup>2</sup> (Linear Fit)
1	0.9884	0.8872
2	0.984	0.8596
3	0.9752	0.8124
4	0.9743	0.8283
5	0.9756	0.8265

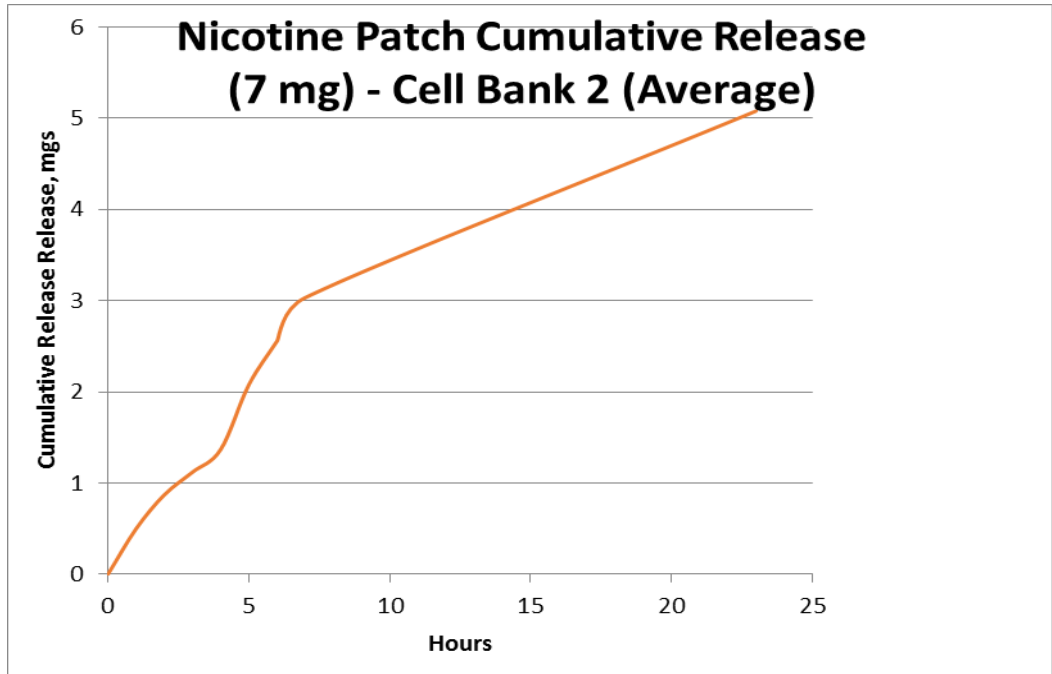


**Figure D.6.** Cell Bank 2 - Cumulative Release vs. Time – Average Curve / Response

Statistical Analysis:  $R^2$  (Polynomial Fit) = 0.9882 /  $R^2$  (Linear Fit) = 0.8872

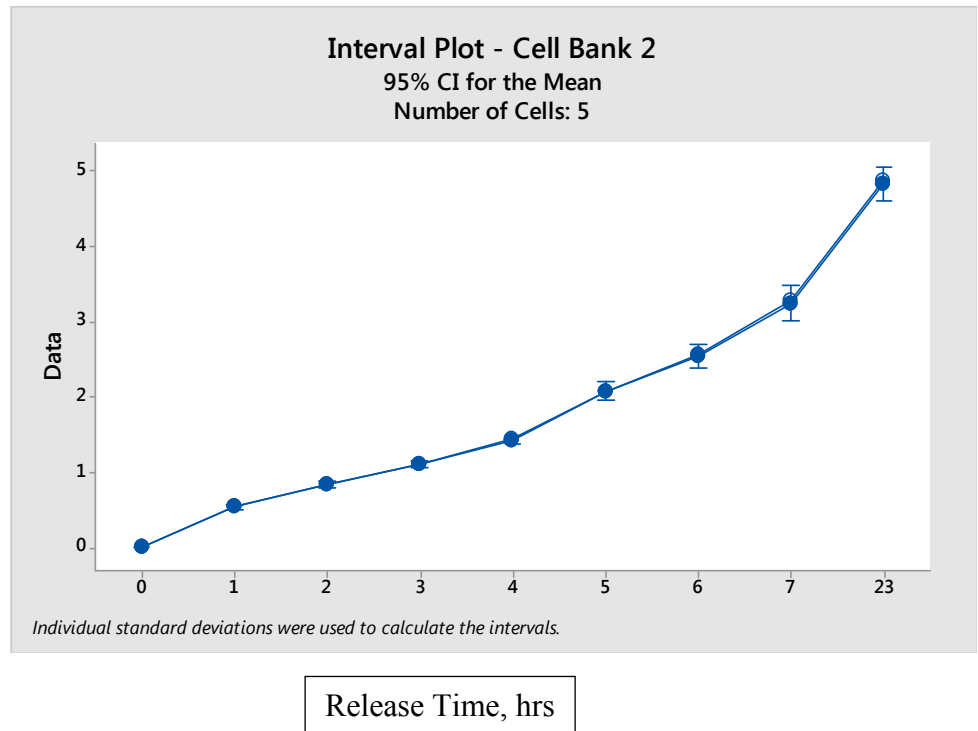


**Figure D.7.** Cell Bank 2 –Confidence Interval Level Analysis (Individual and Sum Plots)

The 95 % Confidence Interval Level Analysis for the experimental data from Cell Bank 2 is uniform and with a narrow difference between data points indicating a robust statistical data set.

The box plot analysis for the experimental data from Cell Bank 2 is uniform and with a narrow difference between data points indicating a robust statistical data set. (See Figure D.8)

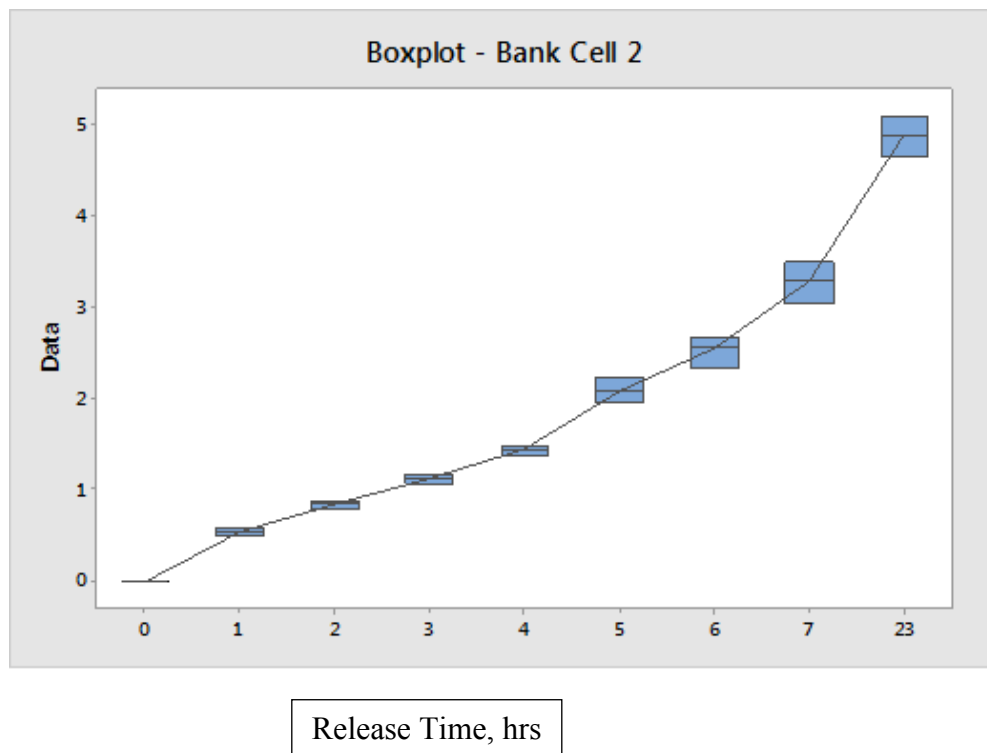


**Figure D.8.** Cell Bank 2 –Box Plot Analysis (Individual and Sum Plots)

In order to assess the statistical validity / cohesiveness of the data from the readings, one preferred option is using the Coefficient of Variation that can help determine the frequencies of the magnitudes of differences amongst the experimental values. The lower the value, the more accurate the testing procedures are <sup>(5)</sup>.

## “Coefficient of variation”

In probability theory and statistics, the **coefficient of variation (CV)** is a standardized measure of dispersion of a probability distribution or frequency distribution. It is defined as the ratio of the standard deviation  $\sigma$  to the mean  $\mu$ . It is also known as **unitized risk** or the **variation coefficient**. The absolute value of the CV is sometimes known as relative standard deviation (RSD), which is expressed as a percentage.

### Definition

The coefficient of variation (CV) is defined as the ratio of the standard deviation  $\sigma$  to the mean  $\mu$ :

$$c_v = \frac{\sigma}{\mu}$$

It shows the extent of variability in relation to mean of the population.

The coefficient of variation should be computed only for data measured on a ratio scale, as these are measurements that can only take non-negative values. The coefficient of variation may not have any meaning for data on an interval scale. Measurements that are log-normally distributed exhibit stationary CV; in contrast, SD would vary depending on the expected value of measurements.<sup>(6)</sup>



### Statistical Data Summary

The Coefficient of Variance for Bank Cell 1 shows a very narrow distribution of 4.022 to 6.413 which indicates results are substantive and valid with no major statistical deviations amongst all results. (See Table 5)

**Table D.5.** Bank Cell 1 Statistical Review

Time (hours) →	1	2	3	4	5	6	7	23
Average	0.499	1.130	1.430	1.720	2.248	2.796	3.240	4.732
Standard Deviation	0.032	0.048	0.077	0.099	0.133	0.112	0.156	0.219
Coefficient of Variation	6.413	4.241	5.381	5.773	5.899	4.022	4.811	4.625

Number of Cells: 5

The Coefficient of Variance for Bank Cell 1 shows a very narrow distribution of 2.915 to 5.610 which indicates results are substantive and valid with no major statistical deviations amongst all results. (See Table 6)

**Table D.6.** Bank Cell 2 Statistical Review

Time (hours) →	1	2	3	4	5	6	7	23
Average	0.540	0.833	1.109	1.429	2.083	2.535	3.249	4.834
Standard Deviation	0.028	0.035	0.032	0.045	0.106	0.127	0.182	0.185
Coefficient of Variation	5.119	4.188	2.915	3.120	5.084	5.022	5.610	3.831

Number of Cells: 5

## SUMMARY

The experimental data and statistical analysis from Cell Banks 1 and 2 show a good consistent response with a very narrow deviation and close Coefficient of Variation values indicating a very robust data set. (See Figure D.9 and Table D.7).

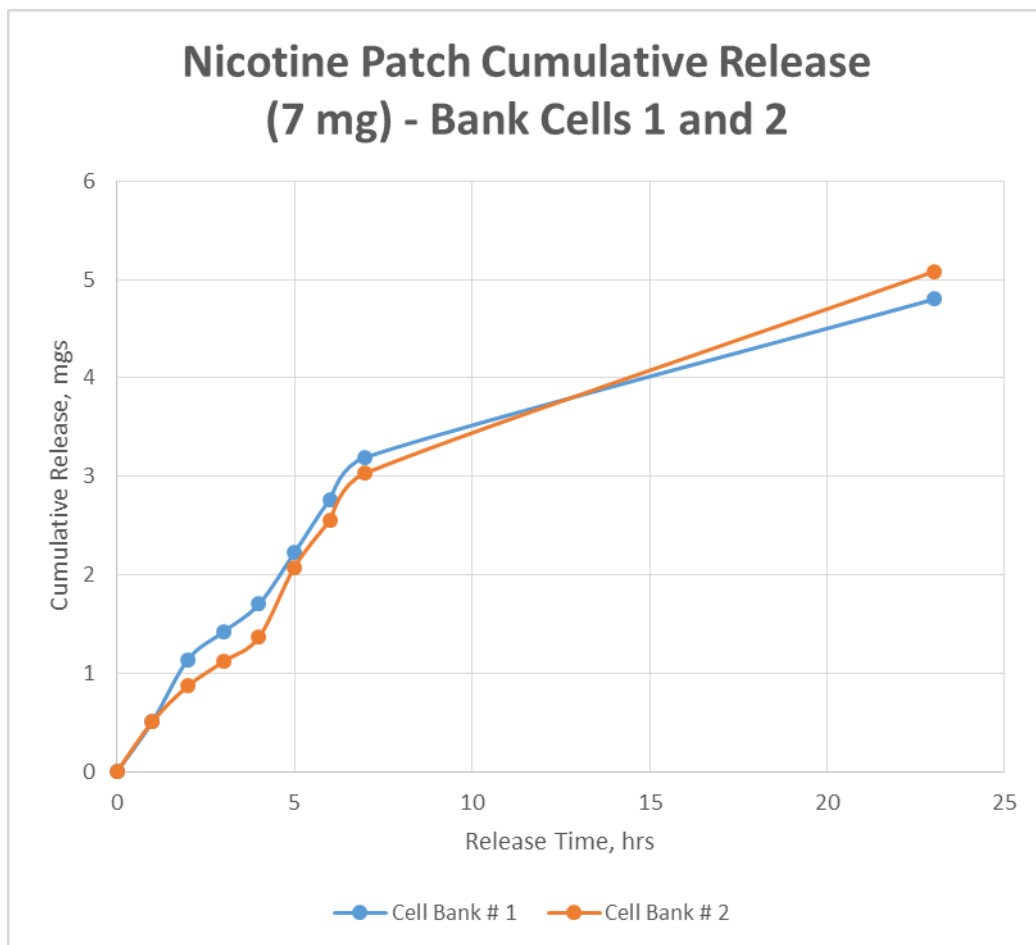


**Figure D.9.** Cell Banks 1 and 2 – Cumulative Release vs. Time – Average Curve / Response Comparison

The statistical results from both Bank Cells are consistently equivalent to each other. (See Table D.7)

**Table D.7.** Cell Banks 1 and 2 – Summary Statistical Analysis

Bank Cell ID	R <sup>2</sup> (Polynomial Fit)	R <sup>2</sup> (Linear Fit)
1	0.9944	0.8271
2	0.9882	0.8872

References:

1. DeStefano, A.J., USP Workshop on Topical and Transdermal Drug Products, Presentation made on September 14 – 15, 2009.  
[http://www.usp.org/sites/default/files/usp\\_pdf/EN/meetings/workshops/2009topicaltransdermalday1.pdf](http://www.usp.org/sites/default/files/usp_pdf/EN/meetings/workshops/2009topicaltransdermalday1.pdf). Accessed on December 31, 2014.
2. Topical and Transdermal Drug Products, USP Protocols, Pharmacopeia Forum, Vo. 35 (3), [May – June 2009].  
[http://www.usp.org/sites/default/files/usp\\_pdf/EN/USPNF/transdermalStimArticle.pdf](http://www.usp.org/sites/default/files/usp_pdf/EN/USPNF/transdermalStimArticle.pdf). Accessed on December 31, 2014
3. Ghosh, T., Biorelevant In-Vitro Release Testing of Non Oral Dosage Forms- FDA Perspectives, FDA Presentation, 2013 AAPS Annual Meeting, San Antonio Texas, November 11, 2013.  
<http://www.fda.gov/downloads/AboutFDA/CentersOffices/OfficeofMedicalProductsandTobacco/CDER/UCM406888.pdf>. Accessed on December 31, 2014
4. Software Used:
  - a. Plot and Basic Analysis (Figures 1, 2, 5, 6 and 9) – Excel 2010 and 2013
  - b. Statistical Plots and Analysis (Figures 3, 4, 7 and 8) – Minitab 17
5. Direct quotation from Wikipedia.  
[http://en.wikipedia.org/wiki/Coefficient\\_of\\_variation](http://en.wikipedia.org/wiki/Coefficient_of_variation). Retrieved on January 7, 2015.
6. Reed, G.F., Lynn, F. and Meade, B.D., Use of Coefficient of Variation in Assessing Variability of Quantitative Assays, Clin Diagn Lab Immunol. Nov 2002; 9(6): 1235–1239. Retrieved on January 7, 2015.

## APPENDIX E

### Molecular Shape Factor Calculations

In order to evaluate the effect of the molecular shape, a series of calculations had to be performed based on the work of Dr. Jurs' group at Pennsylvania State University in late 1970's to late 1980's. They developed a software package named ADAPT that was capable to determine the molecular radius, among other parameters. However, trying to obtain and use the software became a challenge and with the assistance of Dr. C.M. Vrentas, who became one of the main users / adaptors for the work done in diffusion modelling, was able to locate one of its members, Dr. David T. Stanton. The author approached Dr. Stanton and explained the need to obtain access to the software. Dr. Stanton not only offered to assist but also performed all the necessary calculations that enable to complete the DZE model and research. The following pages are the summary of the results and the theoretical background of the ADAPT software done by Dr. David T. Stanton to whom the author is highly indebted for his generosity and willingness to assist a total stranger.

Table E.1

ADAPT Size/Shape Descriptors											
D.T. Stanton, 19-Jan-2010											
ADAPT Worklist	ADAPT Structure ID	Full Structure ID	Ionization State	MAX-L/B	MIN-L/B	SHDW-1	SHDW-2	SHDW-3	SHDW-4	SHDW-5	SHDW-6
1	2-phenoxyethanol	2-phenoxyethanol	Neutral	1.580	1.580	51.72	38	24.04	0.5224	0.5352	0.4906
2	Fentanyl	Fentanyl	Neutral	1.817	1.724	106.8	82	50.04	0.4748	0.5093	0.5267
3	Glycidate	Glycidate (AM1)	Anion	1.442	1.399	32.92	28.56	20.44	0.5144	0.476	0.4443
4	Glycidate2	Glycidate2 (DFT)	Anion	1.452	1.306	32.88	28.04	19.8	0.5138	0.4673	0.44
5	N-hydroxymethyl-gly	N-(hydroxymethyl)-glycine	Neutral	1.510	1.507	36.08	31.48	20.32	0.5229	0.5161	0.4417
6	Nicotine	Nicotine	Neutral	1.452	1.313	49.6	51.12	34.96	0.4769	0.5112	0.4856
7	Scopolamine	Scopolamine	Neutral	1.570	1.570	76.08	70.04	49.04	0.5005	0.5559	0.5389
<p>Note: The structures were first oriented to align the first two principal moments of inertia to the X and Y axes, respectively, before any of the shape calculations were performed.</p> <p>MAX-L/B = the L/B ratio for the structure orientation that maximizes this ratio            MIN-L/B = the L/B ratio for the structure orientation that minimizes this ratio            SHDW-1 = area projected onto the X-Y plane            SHDW-2 = area projected onto the X-Z plane            SHDW-3 = area projected onto the Y-Z plane            SHDW-4 = Standardized SHDW-1            SHDW-5 = Standardized SHDW-2            SHDW-6 = Standardized SHDW-3</p> <p>The Standardized shadow areas (SHDW-4, SHDW-5, and SHDW-6) minimize the the size dependence of the shadow areas by dividing the shadow area by the area of the box that encompasses the shadow for a given plane. In other words, the 1st standardized shadow area (SHDW-4) is the first shadow area (SHDW-1) divided by the area of the box defined by the maximum X and Y dimensions for that shadow.</p>											

# Lab Notes: 18-Jan-2010

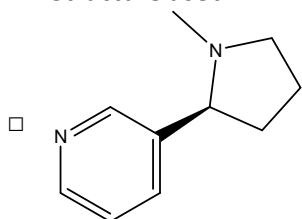
Monday, January 18, 2010  
9:20 PM

- The original Rohrbaugh and Jurs paper used molecular mechanics to obtain the 3D atomic coordinates for the shadow areas. The papers by Vrentras and Vrentras do not specify how the 3D coordinates were generated. It's expected that as long as all the calculations are done using the same methods, the results will be consistent. With that in mind, I've chosen to use semi-empirical quantum mechanical optimization (AM1) as is available in Spartan '08 (Wavefunction, Inc., ver. 1.1.0, Build 131)
- Began data entry

- Nicotine

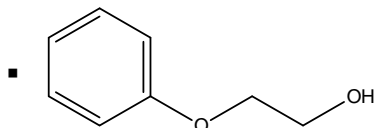
- Information received was ambiguous with regard to the position of the pyridine nitrogen. Decided to use SciFinder as the primary reference

- Nicotine: CAS-Number = 54-11-5, Name = 3-[(2S)-1-methyl-2-pyrrolidinyl]-pyridine
- Structure used:



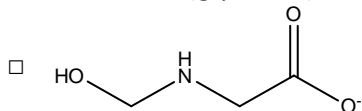
- Phenoxyethanol

- SciFinder: Name = 2-phenoxyethanol, CAS-Number = 122-99-6
- Structure used:



- Hydroxymethylglycinate (Sodium salt)

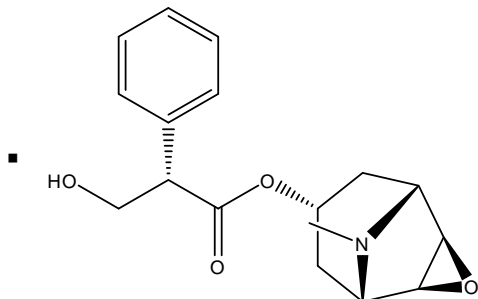
- SciFinder: Name = N-hydroxymethyl glycine sodium salt, CAS-Number 70161-44-3
- The ionized form (glycinate) is an anion as shown:



- Both the anion and the neutral form (glycine) will be used (just in case)

- Scopolamine

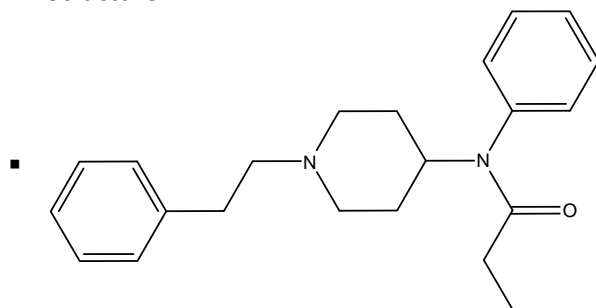
- SciFinder: Name = Benzeneacetic acid, .alpha.-(hydroxymethyl)-, (1.alpha.,2.beta.,4.beta.,5.alpha.,7.beta.)-9-methyl-3-oxa-9-azatricyclo[3.3.1.0<sup>2,4</sup>]non-7-yl ester, (.alpha.S)-
- CAS-Number = 51-34-3
- Structure:



- Fentanyl

- SciFinder: Name = N-phenyl-N-[1-(2-phenylethyl)-4-piperidinyl]-propanamide

- CAS-Number = 437-38-7
- Structure:



- Spartan calculation sequence:
  - Compute equilibrium conformer
    - Molecular mechanics, MMFF force field
    - Total charge = Neutral (used Anion for glycidate)
  - Compute equilibrium geometry
    - Semi-empirical, AM1
    - Total charge = 0 (used Anion for glycidate)
  - The geometry obtained for glycidate was folded, with the hydroxyl hydrogen being strongly attracted to the anion. In water this might not be a proper geometry, but I am not certain about the case of glycidate in the polymer if it exists as the anion in the polymer.
- Decided to run a copy of the final glycidate AM1 structure at the ab initio level to see if the geometry changes at all
  - Copies the Glycidate structure to a new file named Glycidate2
  - Spartan conditions: Equilibrium geometry, DFT, B3LYP, 6-31G\*, in water
- Exported all seven of the structures from Spartan as individual Sybyl MOL2 files
  - See Data Files Section
- Imported the MOL2 files into Sybyl
  - Added appropriate file names (Spartan did not put proper structure file name in the exported MOL2 File).
  - Stored the files in a single Sybyl database
  - Working directory: ~/dat/Falcone/Polymer-diffusion/
- Exported the Sybyl database as a single multi-structure MOL (Sybyl MOL) format file
- Moved the MOL file to the Linux computer
- Created a new ADAPT data area
  - Working directory: ~/dat/Falcone/Polymer-diffusion/adapt1
- Stored the structures in the ADAPT files
  - Created a worklist including the seven structures
- Computed the SHADOW descriptors
  - SHADOW parameters:

```
CURRENT OPERATING PARAMETERS
```

```
USE MAIN DESCRIPTOR AREA
```

```
USE WORKLIST
```

```
GRID DENSITY:      5
```

```
ORIENT WITH MOMENTS OF INERTIA
```

```
FIRST AREA WILL BE STORED IN LAN      1
```

```
SECOND AREA WILL BE STORED IN LAN     2
```

```
THIRD AREA WILL BE STORED IN LAN      3
```

```
AREA ONE STD. WILL BE STORED IN LAN    4
```


```
AREA TWO STD. WILL BE STORED IN LAN    5
```

```
AREA THREE STD. WILL BE STORED IN LAN  6
```

```
OUTPUT TO OUTPUT FILE
```

STRUCTURES WILL BE STORED IN INITIAL ORIENTATION

- Note that the structures were stored in the initial orientation (oriented the first two principal moments on the X-Y axes).
- Computed the LOVERB ("L/B") descriptors
  - LOVERB parameters:

```
CURRENT OPERATING PARAMETERS:  
USE MAIN DESCRIPTOR AREA  
USE WORKLIST  
ANGLE FOR ROTATION: 1.0  
MAXIMUM L/B RATIO IS SET FOR STORAGE  
MIN. AREA L/B IS SET FOR STORAGE  
DESCRIPTORS WILL BE STORED IN LANS :  
7  
8  
OUTPUT TO OUTPUT FILE
```
- Exported the computed descriptors to a text file. Moved the text file back to the PC and created an Excel spreadsheet
  -  Polymer diffusion ...
- Forwarded the results and the Rohrbaugh and Jurs paper to R. Falcone by Email (19-Jan-2010)

**END**



## REFERENCES

1. Drug Development and Delivery, (<http://drug-dev.com/Main/Back-issues/SPECIAL-FEATURE-Transdermal-Topical-Subcutaneous-D-607.aspx>), 2013, Retrieved on May 26, 2014
2. Market Research News, (<http://www.salisonline.org/market-research/advances-in-the-transdermal-drug-delivery-market-market-size-leading-players-therapeutic-focus-and-innovative-technologies/>). Retrieved March 11, 2011
3. Advanced Drug Delivery Systems: New Developments, New Technologies, (<http://www.bccresearch.com/market-research/pharmaceuticals/drug-delivery-systems-phm006g.html>), Retrieved on October 28, 2014
4. Wright, P., Transdermal drug delivery looks for new frontiers, ([http://pharmaceuticalcommerce.com/manufacturing\\_and\\_packaging?articleid=2677](http://pharmaceuticalcommerce.com/manufacturing_and_packaging?articleid=2677)) . Retrieved on October 28, 2014
5. Rachakonda, V.K., Effective Screening of Chemical Penetration Enhancers for Drug Delivery, Master Thesis, Oklahoma State University, p. 2, 2006
6. Prausnitz, M.R., Mitragotri, S. and Langer, R., Current status and future potential of transdermal drug delivery, *Nature Reviews Drug Discovery* **3**, 115-124, 2004
7. Prausnitz, M.R. and Langer, R., Transdermal drug delivery, *Nature Biotechnology*, **26** (11), 1261 – 1268, 2008
8. Michniak, B. B., Transdermal delivery systems. Presentation to the FDA Advisory Committee for Pharmaceutical Science and Clinical Pharmacology, FDA Document # UCM 178989, 2009 Research
9. Gannu, R., Vishnu, Y. V. Kishan, V., and Rao, M., Development of nitrendipine transdermal patches: In vitro and ex vivo characterization, *Current Drug Delivery*, **4**, 69-76, 2007
10. [FDA alert \(2005, July\). Narcotic overdose and death. Food and Drug Administration. http://web.archive.org/web/20070220083526/http://www.fda.gov/cder/drug/InfoSheets/HCP/fentanylHCP.htm](http://web.archive.org/web/20070220083526/http://www.fda.gov/cder/drug/InfoSheets/HCP/fentanylHCP.htm), Retrieved on June 5, 2011

## REFERENCES

(Continued)

11. Bath-Hextall, F.; Riley, F. *Understanding First Pass Metabolism*. Nottingham: © 2004 School of Nursing, Midwifery and Physiotherapy, University of Nottingham. <http://www.nottingham.ac.uk/nmp/sonet/rlos/bioproc/metabolism/default.html> (accessed 12/11/2010).
12. Page, N.; Perkins, M.; Howard, J. *Toxicology Tutor II: Influence of Route of Exposure*. Bethesda: US National Library of Medicine. <http://sis.nlm.nih.gov/enviro/toxtutor/Tox2/a32.htm> (accessed 22/12/2009).
13. Human Skin Tissues. PPT  
<http://www.google.com/url?sa=t&rct=j&q=&esrc=s&source=web&cd=11&ved=0CB0QFjAAOAO&url=http%3A%2F%2Fwww.tamdistrict.org%2Fsite%2Fhandlers%2Ffiledownload.ashx%3Fmoduleinstanceid%3D7776%26dataid%3D14305%26FileName%3DHumanSkinTissuesLecture.ppt&ei=ysF7VJ3NIobesAT-jIH4AQ&usq=AFQjCNE66ihbnqoftxh5XtVXRul3ywueDg&bvm=bv.80642063,d.cWc>. Accessed on November 30, 2014
14. Falcone, R., Jaffe, M. and Ravindra, N.M., New screening methodology for selection of polymeric matrices for transdermal drug delivery devices, *Bioinspired, Biomimetic and Nanobiomaterials*, Volume 2 Issue BBN2, p. 65 – 75, 2013
15. <http://en.wikipedia.org/wiki/Collagen>. Accessed on November 30, 2014
16. <http://pharmaxchange.info/press/wp-content/uploads/2011/03/Figure-6-Layers-of-epidermis.jpg>. Accessed on November 30, 2014
17. [http://biomed.brown.edu/Courses/BI108/BI108\\_2003\\_Groups/Transdermal/Skin/SkinPerm.htm](http://biomed.brown.edu/Courses/BI108/BI108_2003_Groups/Transdermal/Skin/SkinPerm.htm). Accessed on December 1, 2014.
18. [http://biomed.brown.edu/Courses/BI108/BI108\\_2003\\_Groups/Transdermal/Skin/SkinPerm.htm](http://biomed.brown.edu/Courses/BI108/BI108_2003_Groups/Transdermal/Skin/SkinPerm.htm). Accessed on December 1, 2014.
19. Sachan, R. and Bajpai, M., TRANSDERMAL DRUG DELIVERY SYSTEM: A REVIEW, *International Journal of Research and Development in Pharmacy and Life Sciences*, Vol.3, No.1, pp 748-765, 2013 Accessed on December 2, 2014
20. Korus, W. J., *Barrier polymers and structures*. Washington, DC, ACS Publications. 1990
21. Crank, J., *The mathematics of diffusion* (2<sup>nd</sup> Ed.). 2-12, 46-47, 1975
22. Fick, A., *Annals of Physics*, 59, 170. 1855

## REFERENCES

(Continued)

23. Meares, P., Polymers: Structure and bulk properties. London, UK, D. Van Nostrand Co. LTD, 1965
24. Chapter 2 Background of Diffusion Models.  
[http://scholar.lib.vt.edu/theses/available/etd-71498-94026/unrestricted/etd\\_Chapt\\_2.pdf](http://scholar.lib.vt.edu/theses/available/etd-71498-94026/unrestricted/etd_Chapt_2.pdf) . Retrieved on April 7, 2015
25. Brandt, W. W., Journal of Physical Chemistry, 63, 1080. 1959
26. Benedetto, A. T. and Paul, D. R., Journal of Polymer Science, Part A, 2, 1001, 1964
27. Cohen, M. H. and Turnbull, D., Journal of Chemical Physics, 31, 1164, 1959
28. Benedetto, A. T., Journal of Polymer Science A, 1, 3477, 1963
29. Brandt, W., Physics Review, 98, 243, 1955
30. Arnold, D. and Laurence, R. L., Industrial Engineering Chemistry, 31, 218, 1992
31. Vrentas, J. S., Duda, J. L. and Hou, A. C., Journal of Applied Polymer Science, 31, 739, 1985
32. [http://www.imbb.forth.gr/people/aeconomou/pdf/hydrodynamic\\_radius.pdf](http://www.imbb.forth.gr/people/aeconomou/pdf/hydrodynamic_radius.pdf). Retrieved on December 2, 2014.
33. Willits, C. O., Swain, M. L., Connelly, J. A. and Brice, B. A., Spectrophotometric determination of nicotine, US Department of Agriculture, Eastern Regional Research Laboratory, Analytic Chemistry, 22(3), 430-433, 1950
34. Franz Cell description. Retrieved from  
<http://www.permeagear.com/franzatfaqs.htm> on February 21, 2012
35. FDA guidelines for scale up and post-approval changes (SUPAC) for in vitro release testing and in vivo, UCM 070930, 23-28, 1997
36. Thakker, K. D. and Chern, W. H., Dissolution technologies, 10-15, 2003
37. Siewert, M., Dressman, J., Brown, C. and Shah, V., Dissolution technologies, 6-15, 2003

## REFERENCES

(Continued)

38. Raney, S. G., Lehman, P. A. and Franz, T. J., In vitro in vivo correlation (IVIVC) of percutaneous absorption through human skin. Cetero Research AAPS 2010 Poster Presentation.
39. Marangon, A, Bock, U. and Haltner, E.,  
([http://www.acrossbarriers.de/uploads/media/FCT08\\_SUPAC\\_SS.pdf](http://www.acrossbarriers.de/uploads/media/FCT08_SUPAC_SS.pdf).) Retrieved on December 11, 2013
40. Lionberger, FDA pharmaceutical equivalence of topical dosage forms presentation, QbD Series., 2005
41. Flynn et al., Assessment of value and applications of in vitro testing of topical dermatological drug products, *Pharmaceutical Research*, 16(9), 1325-1330, 1999
42. Hauck, W. W., Shah, V. P., Shah, S. W. and Ueda, C. T., *Pharmaceutical research*, 24(11), 2018-2024, 2007
43. Miller, J. A., Oehler, D. D. and Kunz, S. E., *Journal of Economic Entomology*, 76(6), 1335-1340.
44. Addicks, W. J., Flynn, G. L., Weiner, N. and Chiang, C. M., *Pharmaceutical Research*, 5(6), 377-382., 1988
45. Retrieved from <http://cameochemicals.noaa.gov/chris/NIC.pdf> on December, 23, 2009.
46. Retrieved from <http://www.inchem.org/documents/pims/chemical/nicotine.htm> on December, 23, 2009.
47. Yamada T. and Gunn, R. D., *Journal of Chemical Engineering Data*, 18, 234, 1973
48. Pitzer, K. S. *Journal of Chemical Physics*, 7, 583, 1939
49. Pitzer, K. S., *Thermodynamics*, (3<sup>rd</sup> ed.). New York, NY: McGraw Hill, 521, 1995
50. Pitzer, K. S. and Curl, R. F., *Journal of American Chemical Society*, 77, 3427, 1955
51. Pitzer, K. S. and Curl, R. F., *Journal of American Chemical Society*, 79, 2369, 1057a, 1957a

## REFERENCES

(Continued)

52. Pitzer, K. S. and Curl, R. F., The thermodynamic properties of fluids. Inst. Mechanical Engineering. London, UK, 1957b
53. Pitzer, K. S., Lippmann, D. Z., Curl, R. F., Huggins, C. M. and Petersen D. E., Journal of American Chemical Society, 77, 3433, 1955
54. Pitzer, K. S. and Scheiber, D. R., Fluid Phase Equilibrium, 41, 1, 1988
55. Joback, K. G. and Reid, R. C., Chemical Engineering Comm., 57, 233, 1987
56. Poling, B. E, Prausnitz, J. M. and O'Connell, J. P., The properties of liquids and gases (5<sup>th</sup> ed.), McGraw Hill. New York, NY, 2007
57. Fierro, D., Scharnagl N., Emmler, T., Boschetti de Fierro, A. and Abetz, V., Journal of Mem. Science, 2011
58. Ferry, J. D., Viscoelastic properties of polymers (2<sup>nd</sup> ed.). John Wiley and Sons, Hoboken, NJ, 1969
59. Mark, J. E., Polymer data handbook, Oxford University Press, Oxford, UK, 1999
60. Hong, S. U., Prediction of polymer/solvent diffusion behavior using free volume theory, Industrial Engineering Chemical Res., 34, 2536-2544, 1995
61. Sanditov, D. S. & Bartenev, G. M., Refinement of the Williams-Landel-Ferry Equation, Vysokomolekulyarnye Soyedineniya Seriya B. Kratkiye Soobshcheniya, 14(12), 882-885. Paper translated by John A. Miller, Foreign Technology Division, Wright Patterson Air Force Base, (Doc. # FTD-HT-23-831-73), 1973
62. Tonge, M. P., & Gilbert, R. G., Testing models for penetrant diffusion in glassy polymers, Polymer, 42, 501-513., 2001
63. Bicerano, J., Prediction of polymer properties (3<sup>rd</sup> ed.). Marcel Dekker, Inc., 614-617, 2002
64. Van Krevelen, D. W. and Nijenhuis, K. T., Properties of polymers (4<sup>th</sup> ed.). Elsevier, 2009
65. Fedor's parameter calculation, <http://www.pirika.com/ENG/TCPE/SP-Fed-JAVA.html>, Retrieved on December 29, 2011.

## REFERENCES

(Continued)

66. Vrentas, J.S. and Vrentas, C.M., Energy Effects for Solvent Self- Diffusion in Polymer-Solvent Systems, *Macromolecules*, 1993, 26, 1277-1281.
67. HU, H., Jiang, W. and Han, S., Influence of Energy on Solvent Diffusion in Polymer / Solvent Systems, *Chinese J. Chem. Eng.*, 10 (4) 459 – 463, 2002
68. Wang, C.Y., Wu, Y.H. and Wang, D.M., Effect of Drug-Polymer Interaction on Drug Diffusion through Polymeric Membranes, *Journal of Medical and Biological Engineering*, 27 (1): 35 – 40, 2007
69. Reyner, A., Dole, P., Humbel, S. and Feigenbaum, A., Diffusion Coefficients of Additives in Polymers. I. Correlation with Geometric Parameters, *J. Appl. Polym. Sci.*, 82, 2422 – 2433, 2001
70. Zhimin, H., Theoretical Effects of Molecular Dimension and Configuration on Effective Diffusion Coefficient of Macromolecules in Microporous Membranes, *Transaction of Tianjin University*, Vol. 1, No. 1, p. 42 – 47, 1995
71. De Kee, D., Liu, Q. and Hinestroze, J., Viscoelastic (Non-Fickian) Diffusion, *The Canadian Journal of Chemical Engineering*, Vol. 83, 913, 2005
72. Chandler, D., Rough hard sphere theory of the self-diffusion constant for molecular liquids, *Journal of Chemical Physics*, Vol. 62, No. 4, p. 1358 – 1363, 1975.
73. Harris, R., Polymers: Their Movement and the Transition to Reptation Motion as a Function of Polymer Length, <http://www.physics.fsu.edu/users/Dobrosavljevic/Phase%20Transitions/reptationpaper.pdf>. Published on October 2010. Retrieved on December 7, 2014.
74. Barkema, G.T. and Krenzlin, H.M., Long Time Dynamics of De Gennes 'model for reptation, *J. Chem. Phys.* 109, 6486, 1998
75. Khan, M.A. and T.S., Role of Mathematical Modeling in Controlled Drug Delivery, *J. Sci. Res.* 1 (3), 539-550, 2009.
76. Masaro, L. and Zhu, X.X., Physical models of Diffusion for polymer solutions, gels and solids, *Prog. Polym. Sci.*, 24, 731-775, 1999.
77. Potts, R. O., and Guy, R. H., Predicting skin permeability. *Pharm. Res.* 9, 663-669, 1992

## REFERENCES

(Continued)

78. Gregoire, S, Ribaud, F., Benech, J.R., Meunier, A., Garrigues-Mazert and Guy, R.H., Prediction of chemical absorption into and through the skin from cosmetic and dermatological formulations, *British Journal of Dermatology*, 160, pp. 80 – 91, 2009
79. Verleye, B., Klitz, M., Croce. R., Roose, D., Lomov, S. and, Verpoest, I. Computation of permeability of textile reinforcements, <http://wissrech.ins.uni-bonn.de/research/pub/croce/imacs200507.pdf>. Retrieved on April 7, 2015